W-Pos50 ***DATA ACQUISITION AND MANIPULATION ON THE IBM PC FOR ESR SPECTROSCOPY***

Philip D. Morse, II University of Illinois College of Medicine and Illinois ESR Research Center, Urbana, IL 61801

The Illinois ESR Research Center has developed software which will allow data acquisition from both Varian and IBM Instruments ESR spectrometers. The software runs on an IBM PC and currently uses analog/digital boards manufactured by Metrabyte and IBM although other A/D boards could be used with minimal changes. The program permits collection of data from the spectrometers either during a sweep of the magnetic field, or, for observation of transient phenomena, independently of the magnetic field sweep. Data are collected as rapidly as 50 µsec/point (although faster speeds are possible) and stored in 1024 point arrays. During collection in field sweep mode, the A/D converter acts as a boxcar integrator and collects data at each magnetic field for the time determined by the sweep speed of the spectrometer. Data so collected are divided by the number of collections so all data scale directly to height independently of the length of time of the scan. Marker data from a field frequency lock and gauss meters can also be collected independently.

Once collected, data can be plotted to the spectrometer plotter, the spectrometer oscilloscope, the computer monitor, or a digital plotter such as the Houston HI-PLOT. Data are stored on disk as ASCII-readable files and can be retrieved by FORTRAN, BASIC, FORTH, and PASCAL programs. Some simple manipulation of the data is permitted as well. This includes double integration, baseline correction, scaling, "glitch" correction, spectral subtraction, and smoothing. The current version of the program is written in 8086 assembly and compiled BASIC. Program listings, operational software, and hardware suggestions are available from the author at the University of Illinois ESR Research Center.

Supported by NIH RR 01811.

W-Pos51 MANAGEMENT OF THE DATA ASSOCIATED WITH LARGE-SCALE SEQUENCING AND MAPPING.

James W. Fickett, Michael J. Cinkosky, Christian Burks, Walter B. Goad, Santosh K. Mishra, and Chang-Shung Tung. Theoretical Biology and Biophysics Group, Los Alamos National Laboratory, Los Alamos, NM 87545.

Technical breakthroughs in experimental methods during the last decade have greatly accelerated the accumulation of genetic data including, for example, nucleotide sequences (and the amino acid sequences derived from them) and gene map positions. It appears that in coming years we will see at least as great if not a greater growth rate in these data (there is now serious discussion of mapping and sequencing the complete human genome).

In order to optimally serve those scientists relying on up-to-date awareness of the progress of various data collection efforts as well as those scientists wanting to analyze the data, it will be necessary to develop alternatives to the current approaches to collecting, organizing, maintaining, and distributing genetic data. The solutions to the problem of managing these data should allow for: a high degree of automation of the data input, merging, and error-checking process; continuous and up-to-date responses to questions about the data; and responses to sophisticated questions involving many aspects of one kind of data or several kinds of data.

We have begun to assess the requirements for managing the expected volume and variety of genetic data and to to implement trial systems meeting these requirements.

W-Pos52 **MOLECULAR DYNAMICS OF A LIPID BILAYER USING NOVEL MONOTONIC LOGICAL GRID (MLG) AND MULTIPLE CONSTRAINT RELAXATION (MCR) ALGORITHMS**

S. Lambrakos[1], M. Nagumo[2], J. Boris[1], E. Oran[1] and B. Gaber[2]

[1]Laboratory for Computational Physics, Code 4040, Naval Research Laboratory, Washington, DC 20375-5000, USA
[2]Bio/Molecular Engineering Branch, Code 6190, Naval Research Laboratory, Washington, DC 20375-5000, USA

We present results of an application of two novel algorithms to the study of the molecular dynamics of lipid bilayers. These algorithms attack two computational problems that limit the size and duration of molecular dynamic simulations of biological molecules. The first is the determination of near neighbors, used to calculate interaction forces. Our approach to the near neighbors problem is the Monotonic Logical Grid (MLG)[3], which results in a substantial gain in computational efficiency. The second algorithm is the application of constraints, typically rigid bonds, which increases the allowed timestep. We introduce a new noniterative constraint algorithm based on a two body solution for the constraint forces that permits small deviations from constrained values. Our bilayer model consists of an array of 12x12x2 decane molecules with infinitely heavy heads. The application of these new algorithms has demonstrated their stability and speed, and shows great promise for large scale simulations of biological molecules.

[3]J. Boris (1986) J. Comput. Phys. 66, 1.

W-Pos53 IMPLICIT CONSTRAINTS IN THE MATHEMATICAL MODELING OF HETEROGENEOUS ASSOCIATING SYSTEMS IN THE ANALYTICAL ULTRACENTRIFUGE. Marc S. Lewis, Biomedical Engineering and Instrumentation Branch, Division of Research Services, National Institutes of Health, Bethesda, MD 20892.

Analytical ultracentrifugation is a very effective technique for studying the thermodynamics of reversible macromolecular associations of the type $A + nB \rightleftharpoons AB_n$; mathematical modeling is the most effective means of analyzing data from such experiments. A model suitable for fitting is given by $C_r = C_{A,b}\exp(A_A M_A(r^2 - r_b^2)) + C_{B,b}\exp(A_B M_B(r^2 - r_b^2)) + K\, C_{A,b}^n C_{B,b}\exp(A_{AB_n} M_{AB_n}(r^2 - r_b^2))$, where the terms have their usual meanings and the concentrations and the equilibrium constant are molar quantities. The values of n, A_i and M_i are known or determined in separate experiments and the values of $C_{A,b}$, $C_{B,b}$ and K are fitting parameters to be determined. These can be constrained to positive values by using the logarithms of their values as fitting parameters (M. Johnson, et al (1981) Biophys. J. 36: 575 and M. S. Lewis, et al (1984) Biochemistry 23: 3874). It has been shown that conservation of mass in the ultracentrifuge cell can provide a further constraint in the case of equimolar 1:1 stoichiometries (M. S. Lewis and R. J. Youle (1986) J. Biol. Chem. 261: 11571). This approach has been extended to other stoichiometries and other molar ratios but does require that the initial concentration (C_0) of each component must be known. Defining $X_i = A_i M_i(r_b^2 - r_m^2)$, the molar concentration of component B at the cell bottom is then given by the equation $C_{B,b} = nC_{A,b}(X_B/X_A)(1 - \exp(-X_A))/(1 - \exp(-X_B)) + (C_{0,B} - nC_{0,A})(X_B/(1 - \exp(-X_B)))$. Substituting this in the fitting equation implicitly constrains the value of $C_{B,b}$ to a value defined by the initial concentrations and the value of $C_{A,b}$. Similar equations can be derived to describe multi-step equilibria. Computational efficiency is significantly enhanced by this approach.

W-Pos54 NEURAL COMPUTATION OF VISUAL IMAGES. P. Mueller, P. Spiro and R.E. Furman*. Depts. of Biochemistry & Biophysics and Neurology*, Univ. of Pennsylvania, Philadelphia, PA.

Recently there has been a resurgence of interest in neural computation. The large scale parallel and analog computing methods used by neural circuits are ideally suited for real world computation, e.g., visual or acoustical pattern recognition, and rapid advances in microelectronics have made it possible to implement electronic analogs of neural circuits.

As a first step in the design and construction of a neural network for visual image analysis, a computer model for neural computation of static visual pattern primitives has been developed. Based on the computations perfomed by the retina and primary visual cortex, the model consists of a 60x60 array of receptor cells connected in an antagonistic center-surround manner to two arrays of neurons similar to the "on center" and "off center" retinal or geniculate neurons. Through appropriate inhibitory and excitatory connections and synaptic gains from outputs of both on and off center units, the neurons in each array are tuned to different features such as the light-dark direction and orientation of an edge, the orientation of a line, line width (spatial frequency), endpoints and length of lines and edges (corner and curvature detection). In all 144 different arrays of neurons are represented for each orientation angle computed.

There is a good correspondence between the performance of the units in this system and the feature specific simple and hypercomplex cells in the visual cortex, including receptor field shape (similar to a Gabor function), orientation specificity, contrast detection, and spatial frequency tuning.

W-Pos55 VIDEO DISPLAY OF SPREAD OF CARDIAC EXCITATION MEASURED WITH POTENTIOMETRIC DYES. Lars Cleemann, Alan Kadish, J. Michael Carstensen and Martin Morad. University of Pennsylvania, Philadelphia, PA 19104.

Potentiometric dyes have been widely used for recording of action potentials in multiple sites. The development of a computer based system which uses acousto-optical deflectors to scan the excitation of cardiac preparations with a beam from a He-Ne laser previously has been reported (Dillon and Morad, 1981, Science 214:453). This system has been expanded in 4 different ways: 1) A pulse code modulator (Sony PCM-701) and a videocassette recorder (Sony SL-2700) have been incorporated to make it possible to record, in digital form, information (10 gicabytes) sampled continuously during hours of experimentation. 2) 4 megabytes of memory has been made available for detailed analysis of sequences of excitation lasting up to 40 sec. 3) Computer programs have been developed for fast automatic analysis of the spread of excitation. 4) A graphics interface has made it possible to show the spread of excitation in slow motion and record it on video cassette (NTSC standard) for later display on a normal TV. This system has been used to study normal and abnormal patterns of spread of excitation in ventricular myocardium stained with the flourescent potentiometric dye WW781.

W-Pos56 EFFECT OF CULTURE CONDITIONS ON CELL COMPETENCE IN DNA-MEDIATED GENE TRANSFER. M. Mitas and J. J. Gargus, Department of Physiology, Emory University School of Medicine, Atlanta, GA 30322.

DNA-mediated gene transfer (DMGT) has been extensively used to study and characterize genes of known and unknown function in eukaryotic cells. Since implementation of the $CaPO_4$ method of transfection by Graham and Van der Eb in 1973, numerous attempts have been undertaken to enhance the efficiency of the DMGT process. Among the repertoire of agents that have met with demonstrable success in augmenting transfection are DMSO, glycerol, some polyene antibiotics, DEAE dextran, and inhibitors of autophagic lysosomal function. The factors responsible for conferring competence on a cell, including environmental effects, have yet to be defined. In most cases competence appears not to reflect genetic variation, though some examples of stable, highly transformable variants have been reported. We have undertaken a study of some of the environmental factors which may influence cell competence using $LMTK^-$, a murine fibroblastic cell line, transfected with plasmid pTKx1, a pBR322 construct carrying the HSV TK^+ gene, and high molecular weight carrier DNA. A dramatic effect of the cells' state of growth on cell competence was observed. Optimal transformation frequencies occurred when cells were plated 5 days prior to the day of transfection. A significant reduction in frequency was obtained if the cells were plated for either a longer or shorter period of time. Factors relating to this observation such as cell density, serum concentration, conditioning of the medium, and frequency of feeding were also explored. (Supported by NIH R01 GM34939 and GM34436.)

W-Pos57 HPLC HIGHLY SENSITIVE ENZYMIC ASSAY FOR THE QUANTITATIVE DETECTION OF DNA. T. Goldkorn, A. Crickard, L. Hecker, D.J. Prockop and R. Goldkorn (Intr. by John Lenard). Department of Biochemistry, UMDNJ-Robert Wood Johnson Medical School, Piscataway, NJ 08854

Existing methods for DNA detection use radionucleotides or colorimetric assays. Our goal was to develop a non-radioactive probe which is more sensitive than current probes and can quantitatively detect single copy genes. This probe consists of an enzyme which is linked to DNA and has a high turnover number, making it possible to benefit from the amplification generated by its catalytic activity. The assay developed is based on HPLC separation and UV detection of the hydrolysis products obtained by the enzymic activity. 3×10^{-19} moles of the enzyme probe could be analyzed. Therefore, when linked to DNA about 0.1 pg of a 1 kb fragment of DNA could be detected. Since current probes have the potential to detect only about 5 pg of DNA (average length 1 kb), our newly developed system is about 50 times more sensitive.

W-Pos58 HPLC-BASED SIZE-EXCLUSION CHROMATOGRAPHY FOR THE DETECTION OF INTERACTIONS BETWEEN NUCLEIC ACIDS AND PROTEINS. William E. Boernke and Fred J. Stevens. Nebraska Wesleyan University, Lincoln, NE and Argonne National Laboratory, Argonne, IL.

Formation of a complex by two interacting macromolecules results in an aggregate with Stokes radius larger than that of either of the constituent molecules. Therefore, size-exclusion chromatography may, in principle, be used to evaluate interactions between molecules; a number of analytical techniques have been developed in several laboratories. We are examining the suitability of this approach to study protein:DNA association. Several distinctions between protein:nucleic acid interactions and typical protein:protein interactions apply with respect to gel chromatography behavior, specifically, differences in the dependence of elution position upon molecular weight as a result of conformational differences. We have used HPLC to demonstrate interactions between DNA and various proteins, such as ribonuclease A, recA, SSB and G5BP. Binding of SSB and G5BP leads to a decrease in the apparent molecular weight of the DNA, perhaps because of an amplification of weak protein:matrix interactions resulting from polymerization. The chromatography system is sufficiently sensitive to visualize samples on the order of 10 ng, suggesting that this approach may be applied to a broad range of protein:nucleic acid studies.

W-Pos59 STOPPED-FLOW CALORIMETRIC METHODS

R. L. Berger*, C. P. Mudd+, W.A. Schuette+ Laboratory of Technical Development, NHLBI*, Biomedical Engineering and Instrumentation Branch, DRS+, National Institutes of Health, Bethesda, MD 20892.

A new system of microcalorimetry has been developed which brings microcalorimetry into the same time domain and sensitivity as spectrophotometry. Two systems will be presented. System one is a polypropylene, black diamond like coated flow cell which can be retrofitted to any heat conduction batch calorimeter of the Evans or Wadso type. The second system is an all new tantalum flow system. This system has flow artifacts of less than four microjoules, reaction repeatability of every three minutes, true adiabatic kinetic response by data correction to approximately one second, and long term drift and noise of 0.1 microjoule/second. Both systems use only 50 microliters of each reactant per experiment. Operational details of both systems will be presented along with several examples of enzyme kinetic and enthalpic determinations.

W-Pos60 **DYNAMIC ANALYSIS OF DIFFERENTIAL SCANNING CALORIMETRY DATA.** Obdulio Lopez Mayorga and Ernesto Freire. Department of Biology, The Johns Hopkins University, Baltimore, MD 21218.

The measurement of the heat capacity function by differential scanning calorimetry requires a continuous temperature scan as a function of time. As such, the measured data contains dynamic components arising from two different sources: (1) An intrinsic component due to the finite instrument time response; and, (2) A sample component arising from the kinetics of the thermal transition. The intrinsic component is always present and its magnitude depends on the charac-teristic of each instrumental design; usually, high sensitivity instruments exhibit characteristic time responses varying from 10 to 50 seconds. The effects of this instrumental component is usually seen as a progressive distortion in the shape of the heat capacity function as the scanning rate is increased. On the other hand, the magnitude of the sample component depends on the characteristic relaxation time of the transition and its contribution becomes more prominent at faster scanning rates. The purpose of this communication is to present a dynamic deconvolution technique directed to recover the true shape of the heat capacity function at any scanning rate, and to obtain a kinetic characterization of a thermally induced transition. The kinetic characterization obtained by this method allows the researcher to obtain transition relaxation times as a function of temperature. We have applied these techniques to the study of the phase transitions of DPPC. It is shown that for the main phospholipid transition undistorted heat capacity profiles can be obtained at scanning rates as fast as 90 deg/hour. In the case of the kinetically slow pretransition, the dynamic deconvolution technique allowed estimation of the transition relaxation time as a continuous function of temperature. (Supported by NIH grant GM-37911.)

W-Pos61 MINIMUM SIZE OF THE MOLECULAR ELECTRONIC DEVISES. Y. Shinagawa and M. Kikuchi*, Department of Physiology, Nippon Medical School, Tokyo 113 JAPAN, *Systems Research and Development Institute, Tokyo 105 JAPAN.

Current issue of the future computer development is to search the minimum size and low energy computer such as biocomputer. The information theory shows that one bit of information content requires energy, $E=kT\ln 2 \doteqdot 2.8\times10^{-14}$ erg at 300K. The theoretical limit of size of the information processing devises is given by the uncertainty principle; $\Delta x \cdot \Delta p > \hbar/2$ or $\Delta x > \hbar/\sqrt{8mE}$. This value is calculated as 0.17Å(1.7×10^{-11}m) for H-atom at 300K, which is coincident with size of hydrogen atom. For carbon atom $\Delta x \sim 0.05$Å, which is smaller than atomic size. Thence, the size of atom is limiting factor of dimension of the information processing elements. Size of an electron is much smaller than atom. However, Δx is order of 7Å at 300K. To obtain the dimension of 0.2Å, we need higher energy around 26.5eV. This value is in range of the bound energy of the electron in molecule. We can use the electron in molecule as element of the electronic device. In this case, size of the device is that of the molecule. In consideration of a "photon computer", the dimension of the computing element, Δx, is order of wave length, of which value at 300K is around 5μm. The wave length of 0.2Å corresponds to X-ray range. This range is also the energy of the electron in molecule or atom. In order to obtain low energy computer, low temperature of 1K is applied, Δx being 3Å for hydrogen atom. The limit of the computing time, Δt, is given by the uncertainty principle, $E \cdot \Delta t > \hbar/2$. This value at 1K is 5.3 nsec. If we had a technique to control the high energy of mega eV (gamma ray or radiation from atomic nuclei), the minimum size of the computing element could be in range of 1pm(10^{-12}m). In conclusion, the size of the molecular electronic device is limited by the size of hydrogen atom, 0.2Å.

W-Pos62 A TEMPERATURE GRADIENT METHOD FOR LIPID MESOMORPHIC PHASE DIAGRAM CONSTRUCTION USING TIME-RESOLVED X-RAY DIFFRACTION.

Martin Caffrey and Frederick S. Hing, Section of Biochemistry, Molecular and Cell Biology, Clark Hall, Cornell University, Ithaca, New York 14853.

A method which enables temperature-composition phase diagram construction at unprecedented rates is described. The method involves establishing a known temperature gradient along the length of a metal rod. Samples of different compositions contained in long, thin-walled capillaries are positioned lengthwise on the rod and "equilibrated" such that the temperature gradient is communicated into the sample. The sample is then moved through a focused, monochromatic synchrotron-derived x-ray beam and the image-intensified diffraction pattern from the sample is recorded on video tape continuously in live-time as a function of position and, thus, temperature. The temperature at which the diffraction pattern changes corresponds to a phase boundary, and the phase(s) existing (coexisting) on either side of the boundary can be identified on the basis of the diffraction pattern. Repeating the measurement on samples covering the entire composition range completes the phase diagram. These additional samples can be conveniently placed at different locations around the perimeter of the cylindrical rod and rotated into position for diffraction measurement. Temperature-composition phase diagrams for the fully hydrated binary mixtures, DMPC/DPPC and DPPE/DPPC, have been constructed using the new temperature-gradient method. They agree well with and extend the results obtained by other techniques. In the DPPE/DPPC system structural parameters as a function of temperature in the various phases including the subgel phase are reported.

W-Pos63 A LYOTROPE GRADIENT METHOD FOR LIPID MESOMORPHIC PHASE DIAGRAM CONSTRUCTION USING TIME-RESOLVED X-RAY DIFFRACTION: APPLICATION TO THE MONOOLEIN/WATER SYSTEM.

Martin Caffrey, Section of Biochemistry, Molecular and Cell Biology, Cornell University, Ithaca, NY 14853

A new method for rapidly constructing isobaric temperature-composition (T-C) phase diagrams is described. The method involves establishing a concentration gradient of one component in another lengthwise in an x-ray capillary tube. At a fixed temperature such a sample corresponds to an isotherm in the corresponding isobaric phase diagram. The concentration gradient is conveniently established by bringing the two components into contact in the capillary and allowing limited diffusion of one component into the other. Phase boundaries are located and phases are identified and structurally characterized continuously along the length of the capillary using time-resolved x-ray diffraction. This involves moving the sample capillary through a focused, monochromatic synchrotron-derived x-ray beam and recording the image-intensified 2-D diffraction pattern on videotape continuously in live-time along the direction of the concentration gradient. Repeating the measurements on the same sample at a series of temperatures in the range of interest completes the phase diagram. The method relies upon slow macroscopic diffusion rates on the time-scale of the diffraction measurement and is limited by the fact that the exact concentration along the gradient is not known and must be established by independent means. The method has been used to construct the T-C phase diagram for monoolein/water in the 30°C to 110°C range. It agrees well with and extends the results obtained by conventional methods.

W-Pos64 A SCANNING TUNNELING MICROSCOPE FOR BIOLOGY. S.M. Lindsay and B. Barris, Department of Physics, Arizona State University, Tempe, Arizona 85287.

We describe the construction of a particularly simple scanning tunneling microscope (STM) in which biopolymers are deposited onto a substrate using electrophoresis and imaged with the tunneling tip and substrate submerged in water. The microscope has yielded atomic resolution images of metal and graphite surfaces in air. The performance of this STM in water appears to be limited by movement of the target molecule under the scanning tip. Nonetheless, we appear to be able to manipulate charged polymers onto the surface with the appropriate electric field and remove them by reversal of the field. (Work supported by NSF PCM8215433, ONR N00014-84-C-0487, EPA 68-02-4105 and the vice president for research and the physics department, Arizona State University.)

W-Pos65 THREE-DIMENSIONAL IMAGING USING TSRLM CONFOCAL MICROSCOPY.

E.L. Buhle, Jr., B. Himpens, A.V. Somlyo, H. Shuman, and A.P. Somlyo, Penn. Muscle Inst., Univ. Penn. Med. Sch., Philadelphia, PA.

Tandem scanning reflected light (TSRLM) confocal microscopy permits the imaging of optical sections through translucent material in real time. We are currently using a TSRLM microscope (1,2) to examine the morphological components of living frog muscle and Golgi stained fish muscle(3). Optical sections of the biological specimens can be rapidly obtained by a through focus series of a dynamically changing structure. Unstained living frog muscle fibers were imaged with sufficient contrast to obtain 20 optical sections traversing a total distance of approximately 80u. Computed Fourier transforms were obtained from these sections and suggest that this method is suitable for assessing the contribution of local sarcomere domains(4) to the global diffraction patterns. Golgi impregnation of fish muscle sarcoplasmic reticulum produced high contrast optical sections that we are currently quantitating for three dimensional reconstruction. (Supported by NIH HL15835 to Penn. Muscle. Inst. HL07499, NSF DMB8519677 and by an educational grant from Gould Inc.)

(1) M. Petran et al. (1968) J. Optical Soc. of Am. 58:661-664.
(2) A. Boyde (1985) Science 230:1270-1273.
(3) C. Franzini-Armstrong et al. (1982) J. Histo. Cyto. 30:99-105.
(4) C. Sundell et al. (1986) J. Biophys. Soc. 49:521-530.

W-Pos66 SIMULTANEOUS NOMARSKI IMAGING WITHOUT FLUORESCENCE LIGHT LOSS DURING DIGITAL MICROSCOPY OF Ca IN SINGLE CELLS. J. Kevin Foskett (Intr. by. P. Gunter-Smith). Physiology Department, Armed Forces Radiobiology Research Institute, Bethesda, MD 20814-5145.

Video imaging of fluorescence in living cells is a powerful tool in cell biology. To minimize possible adverse effects of fluorescent probes and their illumination, the amount of probe and illumination are minimized, necessitating use of intensified cameras and elimination of optical elements, e.g., phase rings, polarizers which reduce fluorscence intensity. Low light-level sensitive cameras are inherently unsatisfactory for high resolution transmitted-light imaging. Combined with elimination of contrast-enhancing optical elements, low light level fluorescence is associated with poor transmitted-light imaging, making correlations of fluorescence with simultaneous cell structure difficult. I have developed a system to make quantitative fluorescence measurements of Ca and pH in single cells while they are simultaneously imaged with high contrast and resolution in Nomarski optics, without the light losses (60-70%) normally associated with this contrast enhancement technique. Cells loaded with the Ca-sensitive dye, Fura-2, are observed on the stage of an inverted microscope. Fluorescence excitation wavelength (epi-illumination) is selected under computer control of a bank of solenoid-controlled filter holders. Switching between two wavelengths (350, 380 nm) takes < 50 msec. Transmitted light is 620 nm and passes through a 1/4λ-plate, polarizer and Wollastin prism before the preparation. Transmitted light and fluorescence emission (~500 nm) pass through a second Wollastin prism. Light loss due to this prism is ~2%. The system uses 2 video cameras. A dichroic mirror (DM; long pass 580 nm) reflects fluorescence emission out a side port through a 500 nm filter to an intensified camera. Transmitted light continues through the DM to the second camera through a polarizer, completing the Nomarski optical path. Both cameras are interfaced to an image processing computer for image storage and analysis.

W-Pos67 SCANNING TUNNELING/OPTICAL MICROSCOPY-AN INTEGRATED SYSTEM FOR BIOMOLECULAR INTERFACING, MANIPULATION AND ANALYSIS, SR Hameroff, CW Schneiker, RC Watt, Advanced Biotechnology Lab, Optical Sciences Center, University of Arizona, Tucson, Arizona.

Scanning Tunneling Microscopes (STMs) nondestructively probe atomic level properties of metals, semiconductors, and biomolecules. An electronic servo system driving a piezoceramic positioner controls highly localized electron tunneling between ultrasharp electrode tips and chosen materials. Tip movement which maintains constant tunneling during surface scanning translates to a surface map with atomic level resolution under optimal conditions. By holding constant different combinations of voltage, current, and tunneling distance, different types of information and material effects occur. Such versatility permits imaging and manipulation of molecules and organelles and endows STMs with molecular interfacing,manipulation and machining capabilities.

Biomolecules, cells, and tissues are not conductors and electron tunneling through these materials is limited. Nevertheless biomaterials have been imaged. The tunneling is thought to occur from tip onto biomolecular surface followed by transport to the conducting substrate. By insulating STM probes to very near their tips, biomaterials in physiological buffer may be studied. We are developing a system which includes an optical microscope, multi-tip STMs, fiber optic waveguides and nanoapertures. This combination of STM and optical microscopy should be synergistic: optical microscopy can provide a coarse approach mode for the "near sighted" STM, and STM can provide a nanomanipulative cursor mode for optical microscopy. Potential biophysical applications of optical/STM include structure mapping, manipulation and modification of organelles, detection of dynamics (phonons, conformation changes, solitons, etc.), molecular identification, biochemical effects of toxins, drugs, medicinal chemistry, interfacing and regulation of cell processes.

W-Pos68 RAPID-FREEZE EXAFS METHOD: APPLICATION TO THE ANALYSIS OF INTERMEDIATES OF HEME PROTEINS
S. Saigo, A. Naqui, L. Powers*, G. Zhang, & B. Chance. Dept. Biochem/Biophys, Univ. of Penna; Inst.Struc.& Funct.Studies, Univ.City Sci.Ctr, Phila., PA; *AT&T Bell Labs, Murray Hill, NJ

A rapid-freeze apparatus for EXAFS measurement with a quenching time of 5 ms has been developed (1) and applied to the analysis of the intermediates of cytochrome c (cyt.c) and horseradish peroxidase (HRP). Rapid-freezing was accomplished by ejecting a reacting solution from a nozzle into isopentane kept at -140° C (Bray's method). The ejected solution forms fine ice particles, which are then packed into an observation cell by extracting isopentane through a filter. A conformational intermediate with a lifetime of 400 ms appears during isomerization of cyt.c after reduction of its ferric form by dithionite at pH 10.6. The intermediate was trapped by this method and its X-ray absorption spectrum was measured at SSRL (Beamline II-2). Analysis showed that the 1st shell EXAFS of the intermediate can be fitted with a model of 6 N atoms ligated to the iron, while the EXAFS of the neutral ferric form can be fitted with a model of 5 N and 1 S atoms and that of the alkaline ferric form with a model of 6 N atoms. This is consistent with the mechanism proposed previously (2). Two intermediates appear during catalytic action of HRP. Compound II of HRP in turnover was trapped by this method and its X-ray absorption spectrum was measured. The features of the spectrum were almost the same with those reported previously (3). These results demonstrate the feasibility of rapid-freeze EXAFS method for characterization of intermediates in fast enzymatic reactions.
(1) Saigo S et al (1986) Proc.Int.Conf.Biophys.Sync.Rad. submitted; (2) Lambeth DO et al (1973) J.Biol.Chem. 248:8130; (3) Chance B et al (1984) Arch.Biochem.Biophys. 235:596. SUPPORT: NIH grants GM 31992, GM 33165, HL 18708, HL 31909, RR 01366; & SSRL PROJECT 961B.

W-Pos69 CRYOSECTIONS FROM UNTREATED COLLAGEN USING A RELIABLE AND VERSATILE FAST-FREEZING METHOD.
M.W.K. Chew, J.M. Squire & J. Hill. Biophysics Section, Blackett Laboratory, Imperial College, London SW7 2BZ.

The methods conventionally used to produce ultrathin sections for transmission electron microscopy require the use of chemical fixatives, dehydrating agents and resins which may introduce artefacts into the specimen. Modern high resolution electron microscopy, where preservation of native structure and antigenicity has become increasingly important, has initiated the advances in low temperature techniques that are widely used today. By employing the techniques of cryosectioning, in which much of the chemical processes are avoided, good structural preservation and resolution can be obtained (Chew and Squire, 1986, Int.J.Biol.Macromol. 8, 27-36). The milder treatment is not only more favourable for tissue preservation but is also safer and less time-consuming. An improvement on the technique has recently been successfully tried on tendon collagen. Without prior fixation and cryoprotection the tissue is frozen by clamping with a pair of copper-jawed pliars cooled to LN2 temperature, and 1000A-thick cryosections are obtained at about -110C. Negatively stained longitudinal sections show fibrils with regular periodicities which can then be analysed by optical diffraction and computer-based image analysis. Lateral periodicities within collagen fibrils are distributed into two distinct groups: most are in the range of 55-80A, and a smaller distribution in the 95-105A range. The results are comparable with previous studies with cryosectioned collagen, and are discussed in the context of current models of collagen I molecular packing. The practicalities and advantages of the method are discussed in detail; in summary, this fast-freezing technique is easy and inexpensive to use, efficient, reliable and versatile.
Supported by Arthritis & Rheumatism Council (U.K.).

W-Pos70 IMPROVING PATCH CLAMP PERFORMANCE WITH SUPERCHARGING. C.M. Armstrong and R.H. Chow (Intr. by H. Roder), Dept. of Physiology, University of Pennsylvania, Philadelphia, PA 19104.

By 'supercharging', patch clamp time response can be dramatically improved without altering the normal headstage configuration described by Hamill et al. (1981). The method permits resolution of such fast events as calcium and sodium tail currents. Digital computer modelling and analog electronic simulation were used to identify appropriate shapes for the command voltage and the voltage applied to a capacitor tied to the input of the headstage. The voltage command pulse consists of a step with a brief (5-15 us) spike on its leading edge. Spike amplitude is a function of the membrane capacitance and the access resistance. The spike drives current through the access resistance and speeds charging of the membrane capacitance, making it possible to complete a voltage step within 5-15 us. The second function of the patch clamp amplifier is current measurement, and good time resolution requires suppression of the capacity transient. This can be accomplished by applying an appropriately shaped voltage (as will be described) to the small capacitor tied to the input of the headstage. Clamping speed is independent of the electrode and feedback resistance over a wide range. In whole cell recordings of calcium and sodium currents in GH3 cells, the supercharger markedly enhances the time resolution of tail currents. The method should also be useful in single channel and bilayer recording.

W-Pos71 THE SYNTHESIS AND DEVELOPMENT OF FLUORINATED "SPIN-TRAPS" FOR THE IN VIVO DETECTION OF FREE RADICALS USING ^{19}F NMR SPECTROSCOPY. Barry S. Selinsky, Louis A. Levy, and Robert E. London. National Institute of Environmental Health Sciences, Laboratory of Molecular Biophysics, Box 12233, Research Triangle Park, NC 27709.

We have synthesized several fluorinated analogs of the commonly used spin-trap phenyl-tert-butyl nitrone (PBN; see structures below) for use in the detection of free radicals using ^{19}F NMR spectroscopy. The traps synthesized have been characterized with respect to stability to heat and photolysis, and were found to be similar to PBN. Using the thermal decomposition of phenyl-azo-triphenylmethane to generate phenyl and triphenylmethyl radicals at a controlled rate, we have demonstrated that our spin traps do react with radicals in solution to give radical-spin trap adducts distinguishable from the spin trap by ^{19}F NMR. The NMR resonance corresponding to phenyl adduct is shifted 1-3 ppm from the resonance for unreacted spin trap, depending upon the spin trap used. NMR and ESR competition experiments demonstrate that the fluorinated traps have similar trapping efficiencies to PBN. We hope to extend the use of these fluorinated spin traps to in vivo studies, which are difficult to carry out using conventional ESR methods due to in situ reduction of nitroxide and loss of ESR signal.

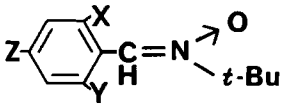

I. X = CF_3; Y = Z = H
II. X = Y = F; Z = H
III. X = Y = H; Z = CF_3
IV. X = Y = H; Z = F

W-Pos72 PHOTOLYSIS MECHANISM OF P^3-1(2-NITRO) PHENYLETHYLADENOSINE 5' -TRIPHOSPHATE, 'CAGED ATP'. J.A. McCray, Dept. of Physics, Drexel Univ., Philadelphia, PA 19104 & D.R. Trentham, Nat. Inst. for Med. Res., Mill Hill, London U.K.

On laser pulse photolysis of caged ATP, I, at 347nm a colored intermediate is formed, presumed to be an aci-nitro compound, II, whose decay can be monitored at 406nm. ATP release is thought to be concomitant with this decay (McCray et al. PNAS 77, 7237-41, 1980). However, 2-nitrosoacetophenone, IV, forms much more slowly at pH 6 than II decays. We have therefore reinvestigated the kinetics of ATP formation on photolysis by following the fluorescence change associated with ATP-induced actosubfragment 1 dissociation; actin being labelled with the fluorescent probe pyrene. ATP formation is as least 10-fold faster than that of IV at pH 6.3. An additional kinetically important intermediate must exist for which III is a possible structure. Rate constants relate to pH 7, 20° C and I (0.05 M). In the Presence of Mg^{2+} and I (0.15 M) ATP forms at $118s^{-1}$.

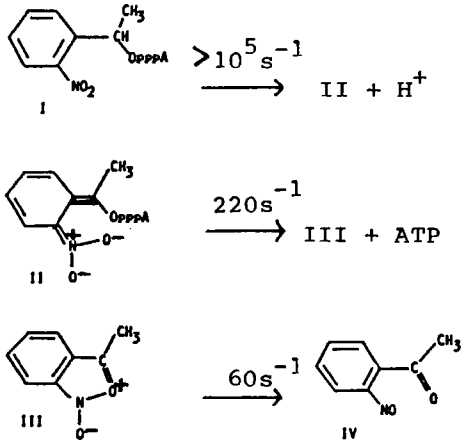

W-Pos73 A TWO-DIMENSIONAL EXTRACELLULAR VIBRATING PROBE FOR THE DETECTION OF TRANSCELLULAR IONIC CURRENTS. R. Nuccitelli, Zoology Department, University of California, Davis, CA. 95616.

The ultrasensitive vibrating probe developed in 1974 by Jaffe and Nuccitelli detects extracellular steady currents in the horizontal plane in one dimension. It has been used most often to detect the normal component of the extracellular current crossing the plasma membrane at various positions around the cell. When the more complete two-dimensional current pattern is desired, a tangential measurement in the same region and time interval is also required, and the vectorial sum of the two provides the net current flow in the horizontal plane. I have developed (with design ideas from the National Vibrating Probe Center at Woods Hole, MA) a circularly oscillating probe and computer analysis system that displays a two-dimensional vector representing the current direction superimposed on the video image of the preparation being studied. A platinum-black electrode is caused to move in a circular path in the horizontal plane using a parallelogram linkage suggested by Gordon Ellis. The signal from this electrode is subtracted from that of a stationary reference electrode by a differential preamp, and connected to a two-phase lock-in amplifier that detects both the normal and tangential components of the signal. These two components are added vectorially by an IBM PCXT computer and the resulting current vector is displayed on the video screen superimposed on the photomicroscope image of the cell under study. The computer displays the vector on the monitor in the position indicated by the operator who uses a light pen to touch the monitor. The magnitude and direction of each vector are also stored on the hard disk for future data analysis and the composite video image is recorded on a time-lapse video recorder.

W-Pos74 EFFECT OF CONTACT LENSES ON OXYGEN TENSION IN THE TEAR FILM OF A RABBIT. B.R. Masters, Dept. of Ophthalmology, Emory University Eye Center, Atlanta, Georgia 30322.

This study is an application of an optical method to measure oxygen concentration in the tear film of a living rabbit and to measure the effect of various contact lens materials on it. The oxygen flux across the contact lens is given by Dk/L times the difference in partial pressures across the contact lens. D is the oxygen diffusion coefficient, K is the oxygen solubitity (both properties of the material) and L is the contact lens thickness. There are also boundry layer resistances on both sides of the contact lens. The method is based on measurements of the NADH fluorescence from the corneal epithelial cells which varies with oxygen concentration. The system was first calibrated in vitro with a perfused cornea yielding a plot of oxygen concentration versus epithelial NADH fluorescence intensity. A contact lens was placed on the rabbit eye and the fluorescence intensity measured, after 30 minutes the steady state value was measured, and compared to the calibration curve to yield the oxygen concentration in the tear film under the contact lens. The PMMA contact lens under open eye conditions had 0.1% oxygen in the tear film, with a Dk/L =0 The Boston II lens (Dk/L=7) had 0.8%, the Boston IV contact lens (Dk/L=12) had 3.0% oxygen in the tear film, and the Equalens (Dk/L= 27.5) had 7% oxygen in the tear film under the contact lens. Since the metabolism of the corneal epithelial cells is dependent on the oxygen concentration in the tear film, we investigated the effect of different contact lens materials and thicknesses using the noninvasive, optical technique. Support from NEI EY06958-01

W-Pos75 ORIENTED SCATTER FROM BIOMOLECULES USING THE NCSASR SHEAR CELL. G.J. Bunick, J.B. Hayter, E.C. Uberbacher, and G.D. Wignall (intro. by J.S. Cook), The National Center for Small-Angle Scattering Research, Oak Ridge National Laboratory, Oak Ridge, TN 37831.

Small-Angle Scattering has been increasingly used to study biological structures. This technique provides information about the overall properties of the macromolecule (i.e., its size, shape, molecular weight, volume, and surface area). When a molecule's detailed structure is known, small-angle scattering is useful to determine changes that occur as the environment of the macromolecule is changed, often providing important information about how the macromolecule functions. With a shear cell, information lost to angular averaging in normal solution scattering can often be recovered when all the particles have the same orientation. Use of the shear cell is appropriate for highly anisotropic macromolecules, long biopolymers, colloidal dispersions, and gels formed from anisotropic supramolecular assemblies. Examples of the application of the NCSASR shear cell system for alignment of biological macromolecules will be presented. Additional potential applications of the cell will be discussed. The National Center for Small-Angle Scattering Research (NCSASR) is sponsored by the National Science Foundation (NSF) through an interagency agreement with the Department of Energy (DOE). It makes state-of-the-art equipment for neutron and X-ray small-angle scattering experiments available to qualified investigators free of charge. NCSASR facilities include use of the 30-m small-angle neutron scattering (SANS) instrument at the High Flux Isotope Reactor (HFIR), the 10-m SANS at the Oak Ridge Research Reactor (ORR), the 10-m X-ray scattering instrument (SAXS), and a high intensity Kratky camera with a linear position-sensitive detector. (Operated by Martin Marietta Energy Systems, Inc. with the U.S. Department of Energy.)

W-Pos76 DETERMINATION OF THE TIME REQUIRED FOR EXONUCLEASE DIGESTION BY AN IN-GEL HYBRIDIZATION TECHNIQUE, John D. Brantley and Michael Beer, Dept. of Biophysics, Johns Hopkins Univ., Baltimore, Maryland 21218.

It is occasionally necessary to produce a specific single strand tail on a DNA fragment large enough to allow annealing of a complementary oligonucleotide. We have developed a method to determine the time required for digestion with an exonuclease to produce such a single stranded tail. The technique involves hybridization directly in agarose gels followed by in-gel detection of non-radioactive probes (Brantley and Beer, 1986). The oligonucleotide is end-labeled by controlled addition of biotinylated nucleotides using terminal deoxynucleotidyl transferase. A time course digestion is performed on the DNA fragment using a non-processive exonuclease such as Exonuclease III or T_7 Gene 6 Exonuclease. The digested fragments are then electrophoresed on a thin vertical agarose gel. After visualization by ethidium bromide staining the gel is allowed to air dry. The probe is hybridized to the DNA fragments in the gel and visualized by streptavidin-coupled alkaline phosphotase (BRL DNA Detection Kit 8239SA). The time at which the probe is first visualized is the minimum digestion time at which a significant number of fragments are sufficiently digested to allow the annealing of the oligomer.

Brantley, J.D. and Beer, M., Proc. 26th Ann. Mtg. ASCB, Washington, D.C. (1986). Also supported by NIH grants RR01214 and RR07041.

W-Pos77 Al-INDUCED CONFORMATIONAL CHANGES OF SPINACH CALMODULIN, LABELLED AT Cys 27. S. Yuan and A. Haug, Department of Microbiology and Pesticide Research Center, Michigan State University, East Lansing, MI 48824. (introduced by D. McConnell)

Al toxicity is a problem of global significance for crop and biomass production. Because Al ions seem to interfere in part with calcium regulation, we investigated the influence of stoichiometrically applied Al ions on calmodulin conformation, a crucial calcium-regulating protein. Since spinach calmodulin harbors a single thiol group at site 27, we labelled this group with a fluorescence probe, mercuric dansyl cysteine. This probe binds to the protein with a molar ratio of unity. Following titration with Al ions, the fluorescence intensity (520 nm) reached a plateau at 3 Al ions per protein. The fluorescence excitation anisotropy spectrum of labelled calmodulin, measured in the presence of Al ions (with Ca present), was different from that in the absence of Al ions. The fluorescence emission of labelled calmodulin can be analyzed in terms of two components. Addition of 2 Al ions per protein increased the apparent lifetime of the long-lived component twofold. It seems that the probe's site interacts more strongly with an adjacent hydrophobic calmodulin domain as a result of Al application.

W-Pos78 SIALIC ACID SUSCEPTIBILITY TO NEURAMINIDASE IN DIFFERENT POPULATIONS OF HUMAN OROSOMUCOID. Ann Villalobos and H. Brian Halsall, Dept. of Chemistry and Biomedical Chemistry Research Center, Univ. of Cincinnati, Cincinnati, OH 45221-0172.

The heavily N-glycosylated glycoprotein orosomucoid (OMD) can be fractionated into two populations containing biantennary and, nominally, tri/tetra-antennary glycan chains terminated in NeuAc. These populations are expressed differentially in the acute phase response. Each OMD molecule contains five primary glycan chains, and therefore, each population has a different NeuAc content. We have previously reported the lack of interaction between the NeuAc termini of these species and the protein core (Biochem. J. 236 (1986) 149), and of the greater access permitted to the core by the biantennary form to monoclonal antibodies (this meeting; Fed. Proc. 45 (1986) 1574). Neuraminidase from Cl.perfringens was used to determine the kinetics of NeuAc cleavage from biantennary and tri/tetraantennary OMD. Production of released NeuAc was followed by a microthiobarbituric acid assay, and the data processed according to Eisenthal/Cornish-Bowden. Using NeuAc content, and not OMD concentration, as indicative of the substrate concentration, Km bi was 82 μM and Km tri/tetra was 235 μM, and V_{max} bi/V_{max} tri/tetra was 1.25. In addition, this neuraminidase was only able to cleave ~ 90% of the tri/tetra NeuAc, but 97% of the bi NeuAc. These results reflect either differences in local conformation for substrate attachment or steric hindrance. This may be of some significance in a host acute phase response to those viral and bacterial incursions containing endogenous neuraminidase, since the proportion of biantennary OMD is significantly elevated in that condition.

W-Pos79 SEPARATION AND CHARACTERIZATION OF THE GENE PRODUCTS OF HUMAN OROSOMUCOID. Brian N. Stretcher, H. Brian Halsall, Dept. of Chemistry, University of Cincinnati, Cincinnati, OH 45221-0172.

Despite extensive characterization, no specific function has yet been assigned to the human serum glycoprotein, orosomucoid. Difficulties in evaluating its observed biological activities in terms of structure in attempts to define function are compounded by the heterogeneous primary structure of the molecule. This has also led to problems in sequencing, fragmentation, and X-ray studies. Recent evidence has shown that there are two different genes that code for orosomucoid, which presumably account for the previously observed heterogeneity. It therefore becomes paramount to develop a technique whereby the two gene products can be separated prior to further structural and functional studies. The technique and results achieved in employing a p-hydroxymercuribenzoate-agarose affinity column to separate the two gene products is reported herein. The organomercurial is specific for sulfhydryls; one of the gene products (hereafter Gene Product II) has a cysteine instead of arginine at position 149, and therefore binds reversibly to the matrix whereas Gene Product I does not. Gene Product II is eluted by adding a low molecular weight thiol, in this case cysteine, to the running buffer, since elution with mercuric chloride appears to be inefficient and inteferes with subsequent analysis of the products. Results from multiple runs show orosomucoid peaks both unbound (peak 1) and bound (peak 2), in contrast to an earlier report in which orosomucoid failed to bind to a thiol specific matrix. Integration of peak areas gives a ratio of peak 1 to peak 2 very close to the predicted theoretical yield of 3:1. The differential chemical, physical, and immunological properties of the separated products will be described.

W-Pos80 ANALYSIS OF THE STRUCTURE-FUNCTION RELATIONSHIP IN PROTEINS USING TWO-DIMENSIONAL ENERGY PROFILES, M.N. Liebman (1) and T.F. Kumosinski (2), Departments of Physiology and Biophysics and of Pharmacology, Mount Sinai School of Medicine of the City University of New York, New York, NY (1) and Eastern Regional Research Center, U.S. Department of Agriculture, Philadelphia, PA (2).

We have recently described an algorithm which computes an energy profile of a protein in terms of dipole-dipole, charge-dipole and charge-charge interactions. This representation can be readily correlated with the three-dimensional structure of a protein when known and permits for examination of the relationship between structure and function at a level not previously accessible.

The present analysis separates the contributions from the polypeptide backbone and the amino acid side-chains. This capability has been explored for use in comparing families of proteins for evaluating characteristics as to their dependence or independence on amino acid substitution i.e. potential for influence by site-directed mutagenesis. In addition we have been using this form of energy profile representation to evaluate the contributions of the various levels of protein organization on the physical properties which can be measured in solution studies (see Liebman and Prendergast). This methodology has also provided insight into the analysis of protein trajectory data as resulting from molecular dynamics studies.

The application of this methodology to several protein systems will be presented representing each of the three areas described above.

This research was funded by a generous grant from ImClone Systems, Inc.

W-Pos81 CONFORMATION OF POLYPEPTIDES: CRYSTAL AND MOLECULAR STRUCTURE OF GLYCYL-L-LEUCYL-L-TYROSINE. E. Subramanian*,**, R. Murali**, V. Lalitha**, S. Fridey*, T. Srikrishnan*, and R. Parthasarathy*. *Roswell Park Memorial Institute, Buffalo, New York 14263, USA and **Dept. of Crystallography and Biophysics, University of Madras, Guindy Campus, Madras, India.

A systematic structural study of sequentially related peptides is of great importance for the elucidation of structure-function relationship of peptides and in deducing possible conformations of polypeptides. In this line of investigation, the crystal structure of glycyl-L-leucyl-L-tyrosine (GLT) was undertaken in our laboratory. Crystals of GLT were grown from a dimethyl sulfoxide/water solution. These crystals are triclinic, space group P1 with the unit cell dimensions a = 9.339(2), b = 10.999(1), c = 12.409(2)Å, α = 84.65(1), β = 83.88(2), γ = 79.99(1)°, V = 1244.5Å^3, Z = 2, D_o = 1.23 g.cm^{-3}, D_x = 1.241 g.cm^{-3}, CAD-4 diffractometer data. The structure was obtained after much difficulty by multisolution techniques using the RANTAN procedure, R = 0.072 for the observed 2620 reflections with $I>3\sigma(I)$. The two independent molecules of GLT are, as expected, transplanar, and zwitterionic with (NH_3) and COO^-. The two molecules differ in an important way in the conformation of the leucyl side chains (χ_1, χ_2, χ_3 angles are, respectively, -58, -70, 170 and -176, -153, -89° for molecules I and II). The ϕ, ψ and (ω) values along the peptide chains are: 170,(178); -129,146,(172); -145,-178 in I and 154,(178); -144,134,(178); -139,-170 in II, respectively. The molecules are linked together to form an infinite sequence of head-to-tail antiparallel β-sheets. There are, in addition, eight molecules of water and two molecules of dimethyl sulfoxide (one of which is disordered), which form a solvent channel in the crystal lattice. Supported in part by NIH GM-24864 and CA-23704.

W-Pos82 COMPUTER SIMULATION OF DIFFUSE X-RAY SCATTERING FROM PROTEIN CRYSTALS. George N. Phillips, Jr., Depts. of Biochemistry and Physiology & Biophysics, University of Illinois, Urbana, IL 61801.

Motions of proteins in crystals give rise to two effects in X-ray diffraction patterns. There is a general fall-off in the intensity of the Bragg diffraction with scattering angle, and 'diffuse' scattering appears in the background. In principle, this X-ray scattering between the strong Bragg peaks contains information about the deviations of the protein structure from its average.

Studies of the diffuse scatter of tropomyosin crystals have yielded information about the direction, extent, and coupling of motions of these molecules in the lattice (Boylan and Phillips, Biophys. J., 49, p. 76-78). It may be possible to examine the dynamic modes of globular proteins, as well. Towards this goal, computer programs have been developed for simulating the diffuse X-ray scattering from myoglobin crystals using various models for the dynamic behavior of the protein. Different models result in different diffuse scattering patterns. If suitable corrections for contributions of incoherent (Compton) scattering and the scattering from the bulk water can be devised, these patterns can be compared with actual diffuse scattering measurements to yield information about the dynamic behavior of the protein in the lattice.

Supported by NIH grant AM32764. GNP is an Established Investigator of the American Heart Association.

W-Pos83 **TITLE: STRUCTURAL MODELS OF TYPE IV COLLAGEN**

AUTHORS: Boryeu Mao, Henry H. Shih, Gabriel Vogeli, and Paul S. Kaytes, The Upjohn Company, Kalamazoo, Michigan 49001.

Type IV collagen molecules are found in the basement membranes, which are extracellular matrices separating cells from connective tissues. Like other types of collagen molecules, they consist of three polypeptide chains, two identical alpha-1 chains and one alpha-2 chain. The amino acid sequence of the mouse alpha-1 and alpha-2 proteins, deduced from cDNA clone, contains segments that deviate from the normal Gly-X-Y triplet pattern found in other types of collagen molecules. In the triple-stranded molecule, several of these segments that interrupt the triplet pattern have been modeled: (a) the substitution of an alpha-2 glycine with a serine residue, (b) the substitution of an alpha-2 glycine with an Asn-Thr dipeptide and (c) the insertion of an extra residue in each of the three polypeptide chains. In the former case, the substitution was computationally accomplished by "mutating" the glycine residue into a serine residue in a stepwise manner. For the dipeptide substitution, the Ser residue was further mutated into either an Asn or a Thr residue, followed by the creation of a break in the alpha-2 chain, and then the insertion of the extra residue into the break. Serine substitutions have minimal effects on the structure of the triple helix while the dipeptide substitution requires a kink of ca. 50 degrees. These results, and the effects of the third type of interruption on the triple helical structure will be presented.

W-Pos84 LINEAR GRAMICIDINS CAN FORM CHANNELS THAT DO NOT HAVE THE $\beta^{6.3}$ STRUCTURE. J.T. Durkin and O.S. Andersen, Cornell Univ. Med. Coll., New York, NY; F. Heitz, CNRS, Montpellier, France; Y. Trudelle, CNRS, Orleans, France; R.E. Koeppe II, Univ. Arkansas, Fayetteville, AR.

The formation and properties of hybrid channels (heterodimers) can test whether the parent peptides form channels that have the same conformation (Durkin et al., 1986, Biophys. J. 49: 118). We have used this approach to show that fourteenmer, fifteenmer, and sixteenmer analogues of gramicidin form channels that are head-to-head dimers of $\beta^{6.3}$ helices of the same handedness. The fourteenmer, formyl-des(formylvalyl) gramicidin C, and the optically-reversed analogue, gramicidin M^- (Heitz et al., 1982, Biophys. J. 39: 87), should therefore not form hybrid channels in planar bilayers. Nevertheless, a new type of hybrid channel forms in this mixture. These channels are distinguished by their extremely long durations: the average lifetimes of the parent channels are 40 and 200 ms (1.0 M CsCl, 200 mV), the average lifetime of the hybrid channels 140,000 ms. The hybrid channels have the same reversal potential as the parent channels, showing that they are equally cation-selective. The sixteenmer formylglycyl-desformyl gramicidin C does not form hybrid channels with gramicidin M^-, but the fourteenmer and the sixteenmer form channels that have the $\beta^{6.3}$ conformation. The new hybrid channels therefore cannot be head-to-head dimers of $\beta^{6.3}$ helices. The long lifetime of these channels suggests an aggregation joined by a large number of hydrogen bonds, such as one of the intertwined double helices shown to be the conformation of gramicidins in organic solvents (Veatch et al., 1974, Biochemistry 13: 5249). These data show that sequence modifications of a peptide can result in a fundamentally different, yet still active, conformation.

Supported by grants from NIH, NSF, and CNRS.

W-Pos85 THE STRUCTURAL BASIS FOR THE CALMODULIN-AMPHIPHILIC PEPTIDE INTERACTION

Karyn T. O'Neil, Susan Erickson-Viitanen, Henry R. Wolfe, Jr., and William F. DeGrado (Intr. by Mark L. Pearson), E. I. du Pont de Nemours & Company, Central Research & Development Department, Wilmington, DE 19898

Calmodulin is a small acidic protein that plays a key role in the activation of several regulatory enzymes including myosin light chain kinase and phosphorylase B kinase. In addition, it has been shown that a number of basic amphiphilic peptides can bind to calmodulin and inhibit the activation of these enzymes. We have designed and synthesized a series of peptides to test the hypothesis that a basic amphiphilic helix is a key recognition feature for binding of these peptides to calmodulin. We have synthesized a seventeen residue peptide (Leu-Lys-Trp-Lys-Lys-Leu-Leu-Lys-Leu-Leu-Lys-Lys-Leu-Leu-Lys-Leu-Gly) that binds to calmodulin in a helical manner with a subnanomolar K_{diss}. In addition, we have generated a series of sixteen peptides that systematically moves the tryptophan through each position in the peptide keeping all other positions invariant. The fluorescent properties (i.e., accessibility to acrylamide, blue shift, and anisotropy) of these peptides have been monitored and found to be modulated in a manner consistent with the peptide being in a helical conformation upon binding to calmodulin.

W-Pos86 MONTE CARLO STUDIES OF EQUILIBRIUM GLOBULAR PROTEIN FOLDING. HOMOPOLYMERIC LATTICE MODELS OF β-BARREL PROTEINS. Andrzej Kolinski, Jeffrey Skolnick and Robert Yaris, Institute of Macromolecular Chemistry, Department of Chemistry, Washington University, St. Louis, MO 63130.

Dynamic Monte Carlo studies have been performed on various diamond lattice models of β-proteins. Unlike previous work, no bias towards the native state is introduced; rather the protein is able to freely hunt through all of phase space. Thus, these systems may aid in the elucidation of the rules governing protein folding. Three models (A-C) were examined. In Model A, in addition to the preference for trans ($\underline{t}$) over gauche states, ($\underline{g}_+$ and $\underline{g}_-$) (thereby perhaps favoring β-sheet formation) attractive interactions are allowed between every non bonded, nearest neighbor pair of segments. If the molecules possess a relatively high fraction of $\underline{t}$ states in the denatured form, spontaneous collapse to a well defined β-barrel is observed. However, the denatured state possesses too much local structure to fully model the globular protein collapse transition. Thus in Models B-C, the local stiffness was reduced. In Model B, $\underline{t}$ and $\underline{g}$ states are equally weighted, and cooperativity is introduced by favoring formation of adjacent nonbonded (but not necessarily parallel) $\underline{t}$ states. In the denatured state, these systems behave like random coils, but their collapse is to a poorly defined, globular structure. Model C retains the cooperativity of Model B but has a slight preference of $\underline{t}$ over $\underline{g}$ states. The denatured state is indistinguishable from a random coil, and the globular state is a well defined β-barrel. The collapse is well represented by an all-or-none model. Thus, these studies are highly suggestive that the uniqueness of the native state requires some residual secondary structure to be present in denatured state.

W-Pos87 COMPARISON OF SCALES OF AMINO ACID SIDE CHAIN PROPERTIES. Leslie A. Holladay and Lenore Kelly, Dept. of Chemistry, Louisiana Tech University, Ruston, LA 71272.

Eighteen published scales for the hydrophobicity, hydrophilicity, and secondary structure of amino acid residues were compared by determining the degree of conservation of each scale in 60 vertebrate myoglobins, 31 vertebrate ribonucleases, 29 vertebrate cytochrome c's, 28 eukaryotic plant cytochrome c's, and 29 insulin A and B chains. The rationale for this study is that relevant side-chain properties must be reasonably conserved during evolution for correct protein folding and biological activity. Sequences were obtained from the Protein Identification Resource, Georgetown University. Each scale was adjusted to a mean of zero and a standard deviation of unity. In all, the data base comprised 20,627 residues.

As might be expected, all scales were most highly conserved in the cytochrome c family. The most conserved scales were the mean area buried scale of Rose et al. (Science 229,834-838(1985)) and the optimized matching hydrophobicity scale of Sweet and Eisenberg (J. Mol. Biol. 171,479-488 (1983)). The Chou-Fasman secondary structure predictors are the least conserved scales. Examination of subsets of the myoglobin sequence database showed that at least fifteen to twenty different sequences are needed before a reliable ranking of scales emerges. The scales which are most conserved over the evolution of these protein families may well be the best predictors of structural homology.

W-Pos88 THE STRUCTURE OF A STABLE MEMBRANE PROTEIN FOLDING INTERMEDIATE. John F. Hunt, Thomas N. Earnest(*), Kenneth J. Rothschild(*), and Donald M. Engelman, Department of Molecular Biophysics and Biochemistry, Yale University, and (*)Department of Physics, Boston Univeristy.

We have used a variety of spectroscopic and biochemical techniques to study the structure of a chymotryptic fragment of the bacteriorhodopsin (BR) molecule reconstituted into unilamellar phospholipid vesicles. This 71 residue amino-terminal fragment, which is called "C-2", probably corresponds to two of the seven putative transmembrane alpha-helices in the electron density map of BR. Previous studies have suggested that the isolated C-2 fragment forms a stable membrane protein folding intermediate when reconstituted into phospholipid vesicles. Solution CD spectroscopy has shown that this intermediate contains approximately 80% alpha-helix. We have produced oriented samples by drying down the C-2 containing vesicles onto suitable transparent substrates for spectroscopic studies. At high relative humidity, the phase preference of the phospholipids leads to the formation of protein/phospholipid multilayers organized largely parallel to the plane of the sample substrate. Ultraviolet CD spectra of such samples deposited on quartz slides suggest that the alpha-helices of C-2 are oriented predominantly perpendicular to the plane of the membrane. Moreover, polarized FT IR linear dichroism studies of multilamellar samples deposited on AgCl disks indicate that the alpha-helices of C-2 are inclined away from the membrane normal at an angle less than 36 degrees. These results suggest that the C-2 fragment forms a hairpin of membrane-spanning alpha-helices and indicate that it adopts the same general conformation when reconstituted into a phospholipid bilayer in the absence of the remainder of the protein molecule as it does when incorporated into the native tertiary structure of BR. Supported by NIH grants GM22778 and AI20466 to DME and NSF grants DMB-8509857 and PCM-8212709 to KJR.

W-Pos89 The periodic association of type VI with type I collagen in bovine corneal stroma as demonstrated by synchrotron X-ray diffraction.

Rita S. Wall, Gerald F. Elliott, Tracy J. Gyi, Keith M. Meek, Christopher J. Branford-White*
Open University, Oxford Research Unit, Boars Hill, Oxford, U.K.
*Bath College of Higher Education, Bath, U.K.

The low-angle meridional X-ray diffraction from collagen in the bovine corneal stroma is unusual because of the absence of the first order reflection, suggesting the presence in the gap zone of some additional electron dense material. Treatment of corneal stroma with SDS prior to X-ray analysis removes at least some of this material with the consequent appearance of the first order reflection. Analysis of the extracted material using SDS-PAGE shows the presence of a prominent 135,000 MW glycoprotein accompanied by small amounts of two higher molecular weight proteins (MW ~ 200,000). Our experimental evidence supports the view that these extracted proteins are subunits of type VI collagen: The 135,000 MW glycoprotein compares well with the 140,000 MW chains of type VI and both are strongly periodic acid/Schiff positive; type VI preparations from other tissues also contain similar higher molecular weight proteins; both our proteins and type VI are extracted under dissociative conditions and both run as a very high molecular weight complex under non-reducing conditions during gel electrophoresis. Type VI collagen is thought to form beaded filaments with a 100nm periodicity. Our results show that these filaments alter the electron density within the gap zone of the type I fibrils (with a 65nm periodicity). For this to be the case the filaments may either run transversely between the gap zones of adjacent fibrils or they may associate helically with the surface of the fibrils. In either case it would appear that they play an important structural role in the tissue.

W-Pos90 EFFECTS OF GLUCOSYLATION AND CALCIUM BINDING ON CALMODULIN STRUCTURE STUDIED BY SMALL ANGLE X-RAY SCATTERING. N.W. Downer, A. Kowluru, R. Kowluru, M.W. Bitensky, D.B. Heidorn and Jill Trewhella, Life Sciences Division and Neutron Scattering Center, Los Alamos National Laboratory, Los Alamos, NM 87545.

Glucosylation of proteins is a possible mechanism underlying some forms of diabetic pathology. We have used solution scattering techniques to study the effect of non-enzymatic glucosylation of lysine residues on the conformation of calmodulin in the presence and absence of calcium. Radii of gyration (Rg) and interatomic distance distribution functions, P(r), were obtained from analysis of scattering data. For the non-glucosylated calcium free control, the Rg measured was 20.8(.4) Å and was not significantly changed by calcium binding. However, the P(r) function indicated a very slight redistribution of electron density accompanying calcium binding. Glucosylation to a level of 3 mol glucose/mol calmodulin in the presence of calcium caused a significant decrease in Rg to 18.7(.2) Å. Removal of calcium from glucosylated calmodulin resulted in a further reduction in Rg to 17.7(.2) Å. Furthermore, the P(r) functions for glucosylated calmodulin were bimodal showing a distinctly different conformation to the non-glucosylated forms whose pair distribution functions showed only a single maximum. Glucosylated calmodulin is known to be functionally impaired (Kowluru, Kowluru and Bitensky, unpublished results). We will interpret the conformational changes in terms of the lysine sites modified and the regions of calmodulin structure important for activation of enzymes.

This work is supported by DOE/OHER. Project #HA-02-02-03/B04664

W-Pos91 MODELLING STUDIES OF X-RAY SOLUTION SCATTERING DATA FOR CALMODULIN: A COMPARISON OF THE X-RAY CRYSTAL AND SOLUTION STRUCTURES. D.B. Heidorn, D. Torney, and Jill Trewhella, Life Sciences and Theoretical Divisions and Neutron Scattering Center, Los Alamos National Laboratory, Los Alamos, NM 87545.

Calmodulin is a biologically important, ubiquitous clacium-binding protein whose crystal structure has been determined (1). X-ray soltuion scattering data have been measured for both the calcium free and calcium bound forms. From this data we have determined the P(r) functions and radii of gyration for the two forms. P(r) is the distance distributiuon function of vectors connecting each scatterer with all other scattering centers in the protein and is derived by an inverse Fourier transform of the scattering intensity. We have calculated P(r) for a simple model constructed of two homogeneous spheres and a connecting rod-shaped ellipsoid based on the crystal structure of calmodulin. The calculated P(r) is significantly different from the experimentally determined P(r) in that it shows a bimodal distribution with distinct maxima at approx. 12 A and 47 A and a maximum vector length of 65 A. The observed P(r) function shows a single maximum at 17 A, with a slight shoulder near 40 A and a maximum length of 60 A. Moreover, the calculated radius of gyration is greater than the observed value from solution scattering. Future modelling calculations will include more structural detail based on the alpha carbon atomic positions and the amino acid sequence, thus accounting for internal density fluctuations.

(1) Babu et al., Nature (1985) 315:37.

This work is supported by DOE/OHER. Project #HA-02-02-03/B04664

W-Pos92 STRUCTURAL STUDY OF A NATURAL INSECTICIDE

MARJORIE E WILKE, ALOK MITRA, TAKASHI YAMAMOTO, ROBERT STROUD

We have made a 22A resolution reconstruction of a natural insecticide from Bacillus thuringiensis (MW 30kd). The missing cone problem has been solved by collecting tilt series from two perpendicularly related planes of thin crystals grown on formvar coated grids. We are using this low resolution map generated by electron microscopy to help in the phase determination of the X-ray data.

The Fourier transform of the hydrophobicity of the sequence shows three strikingly amphipathic stretches of at least 20 amino acids at a frequency of 1/3. This suggests that there are 40A long stretches of amphipathic 3_{10} helix in the protein. To see how amphipathic these sequences are we have modeled them on a PS300 using Proteus. All the helices have a hydrophilic and a hydrophobic side that runs the length of the helix. These are the only amphipathic regions in the protein that are long enough to cross a membrane. At least one of the proposed 3_{10} helices is 100% conserved in another B. thuringiensis with a completely different host range. 3_{10} helices are not common because the hydrogen bonds that brace the structure are bent and therefore weak. In the hydrophobic environment of a membrane there are fewer possibilities for competing hydrogen bonds so the strained bonds of a 3_{10} helix may be relatively favorable. Beta sheet is the secondary structure predicted by the method of Chou and Fasman, however, there is no prediction for 3_{10} helix.

We believe the pore proposed to cause insect death may be formed by the aggregation of a few toxin molecules in the membrane with each molecule providing one to three amphipathic 3_{10} helices because 1) the only amphipatic secondary structures long enough to cross a membrane have a frequency of 1/3. And 2) at least one of the proposed helices is conserved through evolution.

W-Pos93 ANALYSIS OF THE SOLVENT STRUCTURE OF THE PEA LECTIN DIMER AT 2.48 A RESOLUTION.

Susan R. Phillips[a], Elizabeth H. Parks[b], Howard Einspahr[c], and F.L. Suddath[a] a) School of Chemistry, Georgia Institute of Technology, Atlanta, GA 30332, b) Department of Biochemisty, University of Alabama in Birmingham, Birmingham, AL 35294, c) The Upjohn Company, Physical and Analytical Chemistry Research, Kalamazoo, MI 49001

The structure of the pea lectin dimer has been determined to 2.48 A resolution based on MIR phasing to 6.0 A resolution and a combination of SIRAS and density modification to 3.0 A resolution. The pea lectin model is being optimized by restrained least-squares refinement against the data between 7.0 A and 2.48 A resolution. The current model at 2.48 A resolution gives an R factor of 0.24 and an r.m.s. deviation from ideal bond distances of 0.04 A. The two monomers in the asymmetric unit are related by noncrystallographic twofold symmetry to form a dimer. Currently, the solvent structure around the dimer is being studied and water molecules are being added to the refinement model. Details of the metal binding regions, the chain termini, and the area near the cis-peptide bond are also being examined.

1. H. Einspahr, E.H. Parks, K. Sugana, E. Subramanian, and F.L. Suddath, J. Biol. Chem., in press.

W-Pos94 INVESTIGATIONS OF THE ROLE OF CYSTEINE RESIDUES IN THE STRUCTURE AND FUNCTION OF THE PP12 PROTEIN FROM AVIAN MYELOBLASTOSIS VIRUS. Lisa M. Smith and Joyce E. Jentoft. Department of Biochemistry, Case Western Reserve University, Cleveland, OH 44106.

pp12, the nucleic acid binding protein of avian myeloblastosis virus (AMV), contains two homologous regions of polypeptide sequence that are also found in similar retroviral proteins, namely, C X X C X X X G H X X X X C. All of the cysteine residues in pp12 are in these regions. It has been suggested (Berg, J.M. (1986) Science 232, 485-487) that pp12 and other proteins with similar regions of sequence bind zinc through the conserved cysteine and histidine residues. AMV pp12 protein that was isolated without detergent or chelating agents was analyzed for bound metal ions by plasma emission spectroscopy which screened simultaneously for 40 metals. No bound metal ions were detected for pp12. Other structural or functional roles for the cysteine residues were subsequently investigated by chemical modification with 5.5'-dithiobis(2-nitrobenzoic acid) (DTNB). Under nonreducing, nondenaturing conditions, one cysteine reacts rapidly with DTNB, and a second reacts very slowly (overnight incubation). Thus, 4 or 5 of the cysteines appear to be buried in the interior of the protein. Disulfide bond formation and other factors that determine the folding of this small protein (9.5 kd) are currently under investigation. Secondary structure predictions using a variety of algorithms will be combined with chemical modification and circular dichroism data to analyze those aspects of the primary structure of pp12 likely to contribute to tertiary structure.

W-Pos95 ASSIGNMENT OF PROTEIN SECONDARY STRUCTURES TO FOURIER-TRANSFORM INFRARED SPECTRA BY APPLICATION OF LINEAR PLOT ANALYSIS. Steven J. Prestrelski. Department of Physiology and Biophysics, Mount Sinai School of Medicine of the City University of New York. New York, NY.

Recent studies (Biopolymers, 25 , 469 (1986)) using deconvolved Fourier-transform infrared (FTIR) spectra in the Amide I region (1620 to 1690 cm-1) of globular proteins show components at 11 well-defined frequencies. Ideally, each absorption band is associated with specific structures/conformations which exist in proteins in solution. Previous analysis has concentrated on correlation of percent composition with limited structural models. Application of linear distance plot (LDP) analysis allows us to expand the definition of protein secondary structure based on their X-ray crystallographic structures and also to correlate physicochemical and spectral properties with three-dimensional organization and substructures of proteins in solution. These relationships enable analysis of measured spectra in terms of assignments of structural components from a more encompassing set of secondary and tertiary structure descriptors. Molecules used in this analysis include carboxypeptidase, chymotrypsin, chymotrypsinogen, elastase, lysozyme, papain, ribonuclease A, ribonuclease S, trypsin, trypsinogen and pancreatic trypsin inhibitor. Applying the results of LDP analysis to FTIR spectra suggest the suitability of this combined approach for rapid secondary structure determination of proteins in solution.

This research has been funded by a generous grant from ImClone Systems Inc.

W-Pos96 EFFECT OF MUTATIONS ON THE CATALYTIC RATE OF SUBTILISIN : A THEORETICAL APPROACH F. Sussman, A. Warshel. Department of Chemistry, University of Southern California, Los Angeles, CA 90089

Site directed mutagenesis provides a unique opportunity to probe the influence of a given residue on the catalytic rate of an enzyme. Here we apply a very recently developed theoretical methodology (P.N.A.S. 83, 3806 (1986)) to a very basic mutation in subtilisin, that is the replacement of the nucleophilc center serine by the more reactive cysteine. An assessment based on the difference in reactivity would indicate that the mutant thiosubtilisin would be more reactive than the native subtilisin. The experimental outcome is exactly the opposite. With the help of our methodology we have solved this puzzle and have been able to point out the structural underlying causes for the difference in catalytic activity.

W-Pos97 HELICAL FORMATION OF AN ISOLATED FRAGMENT FROM BOVINE GROWTH HORMONE D.N. Brems, S.M. Plaisted, and E.W. Kauffman
Control Division, The Upjohn Company, Kalamazoo, Michigan 49001

Folding studies of bovine growth hormone (bGH) has demonstrated that the secondary structure (helix) is stable in the absence of tertiary structure (Brems et al. 1985, Biochemistry 24, 7662). As a result, we have searched for small peptides derived from bGH that when isolated have measurable helix structure.

One peptide, 109-133, was found to be near 100% helical in aqueous solutions as determined by circular dichroism. The helical content of this fragment is dependent on pH and peptide concentration. This helical structure is most likely amphipathic. We suggest that the unexpected helical stability of this peptide is due to specific electrostatic interactions and intermolecular packing of the hydrophobic surfaces of the amphipathic helix.

W-Pos98 CRYSTALLIZATION OF ACANTHAMOEBA PROFILINS. Karen A. Magnus, Eaton Edward Lattman, Masahiko Sato and Thomas D. Pollard, Department of Biophysics and Department of Cell Biology and Anatomy, The Johns Hopkins University School of Medicine, Baltimore, Maryland 21205 USA

Profilins are actin-binding proteins of low molecular weight that are found in a wide variety of non-muscle cells. They are believed to effect regulation of the extent of actin polymerization by sequestering actin monomers into non-polymerizable complexes. In Acanthamoeba castellanii there are two major forms of profilin, I and II, with distinct primary structures and slightly different actin-binding properties. Both forms have been crystallized from ammonium sulfate. Although grown under the same conditions, the two crystal forms have different morphologies. The profilin II crystals appear rhombic or cubic while the profilin I is monoclinic. The crystals of profilin I have been more completely characterized and are suitable for high resolution x-ray analysis--reflections to Bragg spacings of 1.7A have been observed. They have the symmetry of the space group C2 with a = 110.4A, b = 31.7A, c = 33.5A, beta = 112.4 degrees. There is one profilin monomer, Mr = 12,800, per asymmetric unit. Intensity data to 2.4A were collected from a single native crystal. Two putative heavy atom derivatives, K2PtCl4 and K2HgI4, have been identified and are currently being analyzed at 2.5A and 3.0A respectively.

This work supported by grants GM-26332 and GM-35171 from the National Institutes of Health.

W-Pos99 EPIDERMAL GROWTH FACTOR: ROLE OF CYSTINE DISULFIDE BRIDGES IN STRUCTURE AND DYNAMICS.

R. C. Cavalli, C. Burke and K. H. Mayo from the Department of Chemistry, Temple University, 13th and Norris Streets, Beury Hall, Philadelphia, PA 19122.

The protein hormone, epidermal growth factor (EGF) stimulates the growth and differentiation of various epidermal and epithelial tissues. EGF from the mouse (mEGF) consists of 53 amino acid residues and, like other protein hormones, contains mostly β-structure and a number of cystine disulfide bonds. This present study focuses on the role which the three disulfide bonds play in the structure and dynamics of mEGF. Disulfide bond reduction rates have been followed by high performance liquid chromatography (HPLC) which not only serves to stop the DTT reduction reaction, but also allows resolution and separation of the various reduced species (i.e. one, two or three reduced bonds). Reaction of each reduced species with dithionitrobenzoic acid (DTNB, Ellman's reagent) gave the number of reduced bonds. Study of the reduction kinetics and thermodynamics which vary greatly gives one a relative measure of the cystine environment since structure and dynamics are reflected in these physical parameters. mEGF is known to undergo a pH induced conformational change via breakage of the His-22 inter-residue linkage. Reduction rates reflect this transition and decrease several orders of magnitude from pH 8.5 to 5.5. Proton-NMR spectroscopy has been used to study the overall structural effect of disulfide bond reduction,and amide proton/deuteron exchange rates have been used to probe protein dynamic changes.

This work was supported by a grant from the National Institute of General Medicine (GM-34662).

W-Pos100 UNFOLDING OF IRON AND COPPER COMPLEXES OF HUMAN LACTOFERRIN AND TRANSFERRIN. John P. Harrington, Jan Stuart, and Arlene Jones; Department of Chemistry, University of Alaska, Anchorage, Alaska 99508.

Human lactoferrin and transferrin are capable of binding two iron or copper ions into specific bindings sites in the presence of bicarbonate. The application of visible spectroscopy and circular dichroism has been effective in assessing the modification and extent of secondary and tertiary unfolding of these metal-protein complexes in the presence of urea and several alkyl ureas. Our findings provide additional support for the uniqueness of each of the two specific metal binding sites within lactoferrin as well as within transferrin. This is evident from the biphasic nature of the transitions as determined by direct spectral analysis suggesting the release of iron(III) and copper(II) ions from both of these metal-binding proteins during the unfolding process. Greater stabilization and increased resistance to protein unfolding is observed for all the complexes of iron(III) compared to the copper(II) complexes of lactoferrin and transferrin as determined by isothermal unfolding and thermal denaturation. Relative stabilization of the different metal-protein complexes investigated within this study were determined to be as follows: Lf-Fe(III) > Lf-Cu(II); Tf-Fe(III) > Tf-Cu(II); and Lf-Fe(III)> Tf-Fe(III); Lf-Cu(II)> Tf-Cu(II).

W-Pos101 CALCULATED AMIDE I AND II INFRARED INTENSITIES: VAL-GLY-GLY, A PARALLEL β-SHEET STRUCTURE. J. Bandekar and S. Krimm, Biophysics Research Division, University of Michigan, Ann Arbor, MI 48109.

We have shown (1) that normal mode calculations of peptides and polypeptides permit a detailed analysis of their infrared (IR) and Raman (R) frequencies in terms of three-dimensional structure. Ab initio determination of dipole derivatives of the peptide group (2) now also make it feasible to calculate IR intensities of amide modes, thus enabling further testing of structural proposals. We have analyzed the IR and R spectra of Val-Gly-Gly, a tripeptide known from crystal structure studies to adopt a parallel β-sheet conformation. Amide I frequencies (and intensities) for the two molecules comprising the spectroscopic repeat unit are calculated at 1661 (1.7), 1654 (1.5), 1645 (9.4), and 1643 (5.4) cm^{-1}. Bands are observed at 1663 (IR, weak), 1657 (R, very strong), 1645 (IR, very strong), and 1642 (R, shoulder) cm^{-1}. Amide II mode frequencies (and intensities) are calculated at 1595 (0.7), 1531 (0.1), 1564 (0.5), and 1541 (12.4) cm^{-1}. Subtraction of the IR spectrum of the N-deuterated molecule from that of the protonated molecule, based on the ~1410 cm^{-1} CO_2 band, shows observed amide II bands at 1566 (weak) and 1542 (strong) cm^{-1}. Satisfactory agreement is also obtained between calculated and observed amide III [1264 and 1264 (R, weak); 1228 and 1219 (R, strong) cm^{-1}] and other modes. These results support our analysis of the general β-sheet structure (3). Supported by NSF grants DMB-8517812 and DMR-8303610.

1. S. Krimm and J. Bandekar, Adv. Protein Chem. 38, 181-364 (1986).
2. T.C. Cheam and S. Krimm, J. Chem. Phys. 82, 1631-1641 (1985).
3. J. Bandekar and S. Krimm, Biophys. J. 49, 295a (1986); manuscript in preparation.

W-Pos102 STRUCTURAL STUDIES OF HEXABRACHIONS FROM EMBRYONIC AND ADULT CHICKEN. Hope C. Taylor, Gina Briscoe, Virginia A. Lightner, Harold P. Erickson (Intr. by Jane S. Richardson), Anatomy Dept., Duke Univ. Medical Ctr., Durham, NC 27710

Hexabrachions, a class of extracellular matrix proteins, may be purified readily from conditioned chick embryo fibroblast medium by immuno-affinity adsorption. Gel electrophoresis of reduced hexabrachions shows a prominent band at 220 KDa, with a weaker doublet at 200 and 190 KDa. Rotary shadowed EM specimens of a 13S fraction from a glycerol gradient show mostly hexamers (A), while the 9S fraction consists mainly of trimers (or half hexabrachions), some including the central particle (B). Limited α-chymotrypsin digestion reduces hexabrachions to trimers missing the central knob, as observed by EM. Though the length of the arms remains the same (avg. 67 nm), reduced gels show that chymotrypsin removes about 10 KDa from all three bands of the native protein. Limited trypsin cleavage results in a mixture of double arms (avg. length 128 nm. with a knob at each end (C)) and single arms (avg. length 62 nm, with one knob (D)). On non-reducing gels, this digest shows major bands at 350 and 180 KDa. Hexabrachions purified from embryo and adult brain have slightly shorter arms (avg. 64 nm). Protein from adult gizzard contains a significant fraction of hexamers with one or more much shorter arms (30 to 50 nm); lower molecular weight bands from 115 to 160 KDa were seen on reduced gels. These short arms may be the result of differential expression of the arm proteins.

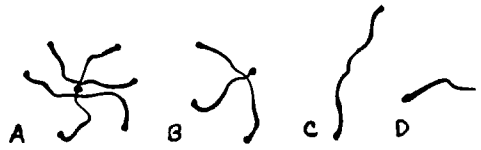

W-Pos103 WATER VAPOR MAY ALTER THE ROTAMER DISTRIBUTION OF A PEPTIDE AROMATIC SIDECHAIN IN NON-POLAR ENVIRONMENT: Wilson Radding, Dep't. Biochem. and Mol. Biophys., Columbia, 630 W. 168th St., NYC. A difference circular dichroism spectrum has been obtained by subtracting the CD spectrum of cyclobis-N-methyl-L-phenylalanine (N-methylphenylalanyl diketopiperazine) in dry iso-octane from that of the same solution exposed to water vapor. The difference spectrum exhibits a roughly Gaussian positive peak at 244nm and a positive shoulder at about 213nm. When alternatives are investigated, one appears almost certain: negative n-π^* CD disappears from the 244nm region and positive n-π^* CD appears in the 213nm region. The probable implications of this shift of wavelength and change of sign are: 1) The sidechain rotamer distribution is altered by coordination of water with non-bonded carbonyl p electrons. 2) The N-methylphenylalanyl diketopiperazine ring is in the pseudoequatorial conformation. This experiment reinforces the possibility that in the hydrophobic core of globular proteins aromatic sidechain dynamics may sometimes be controlled by water molecules hydrogen bonding to the backbone.

W-Pos104 STRUCTURE OF METAL-NUCLEOTIDE COMPLEXES OF PORCINE ADENYLATE KINASE. Bruce D. Ray, and B. D. Nageswara Rao, Physics Department, IUPUI, P.O. Box 647, Indianapolis, IN 46223 and P. Rosch, Max-Planck Institute, D-6900 Heidelberg, W. Germany.

Structures of metal-nucleotide complexes bound to porcine adenylate kinase (E.C. 2.7.4.3) were studied by measuring paramagnetic effects of two dissimilar activating paramagnetic cations, Mn(II) and Co(II), on the spin-relaxation rates of the ^{31}P nuclei of the nucleotides in these complexes. Measurements were made exclusively on enzyme-bound complexes as a function of temperature from 5 to 30°C in order to determine the effect of exchange on observed relaxation rates. The relaxation rates in E•MnATP and E•MnGDP yield activation energies (ΔE) in the range 5-8 kcal/mol. Thus, these rates are exchange limited and are incapable of providing structural data. Relaxation rates in E•CoATP and E•CoGDP exhibit ΔE values in the range 1-2 kcal/mol and yield Co-^{31}P distances. The distances for the β- and γ-P of ATP and for the β-P of GDP denote direct coordination between Co(II) and these phosphate groups. However, in both cases, a significantly greater distance between α-P and Co(II) is indicated. ^{31}P relaxation rates of AMP in the E•MnGDP•AMP and E•CoGDP•AMP complexes exhibited ΔE in the range of 3.5 to 4 kcal/mol. These rates appear to include partial contribution from the lifetimes of the complexes, and therefore, need to be interpreted carefully to determine the cation-^{31}P(AMP) distance.

Work supported by a grant from the NSF (DMB 83 09120). The NT-300 was purchased with support from the NSF (PCM 80 18725).

W-Pos105 STRUCTURAL AND FUNCTIONAL STUDIES WITH SPIN LABELED MELITTIN

Christian Altenbach and Wayne L. Hubbell (Intr. by B. Cohen), Jules Stein Eye Institute and Department of Chemistry & Biochemistry, University of California, Los Angeles, CA 90024

The bee venom protein melittin interacts strongly with phospholipid bilayer membranes and is known to show voltage dependent pore formation. In order to study the molecular mechanism involved we synthesized all 15 possible spin-labeled derivatives which can be obtained by specifically reacting some of the four amino groups of the protein (N-terminal, Lys-7,21,23) with succinimidyl 2,2,5,5-tetramethyl-3-pyrroline-1-oxyl-carboxylate. Labeling an amino group with this label removes a positive charge but it was shown previously by Hanke et al. (Biochim. Biophys. Acta 727 (1983), 108) that even the removal of four out of six positive charges by acylating all amino groups does not significantly change the physical and electrical properties of the melittin. For most studies we used one of the four derivatives with only one spin-label attached to the protein thus minimizing the perturbance introduced by the label. In aqueous solution the EPR spectra of the spin labeled derivatives show dramatic changes during salt induced monomer to tetramer transition. These changes reflect a decrease in rotational correlation time and appearance of spin-spin interaction. The mobility of the N-terminal label is consistent with the correlation time of the tetramer, indicating a rigid attachment. All derivatives bind strongly to neutral or negatively charged phospholipid bilayer membranes. Broadening experiments with chromium oxalate show that in the membrane bound state the spin-label attached to Lys-21 is most shielded from the aqueous environment.

Methods to clamp transmembrane potential in phospholipid vesicles even in the presence of open channels have recently been developed, and together with the spin-labeled melittin derivatives will provide an outstanding opportunity to investigate the molecular details of voltage dependent conformational changes in membrane bound proteins.

W-Pos106 DISCRETE CHANGES IN LATERAL PACKING OF COLLAGEN MOLECULES CAUSED BY GLYCATION. Eric F. Eikenberry, Shizuko Tanaka, Gad Avigad, and Barbara Brodsky, Departments of Pathology and Biochemistry, UMDNJ-Robert Wood Johnson Medical School, Piscataway, NJ 08854.

Incubation of rat tail tendon with reducing sugars results in non-enzymatic glycosylation (glycation) of lysyl and hydroxylysyl residues of collagen and the subsequent formation of sugar derived cross-links. This process results in an increase in the spacings of the near-equatorial x-ray diffraction maxima which indicate an expansion in the cross-section of the unit cell. The expansion is directed along the $1\bar{2}$ planes and appears to be continuous and dependent on the amount of sugar bound. Since the observed direction is confined to one of the three nearest neighbor intermolecular spacings in the quasi-hexagonal unit cell, we modeled the expansion as a one-dimensional process, using an array of identical units representing the collagen molecules. These units were perturbed to represent the effects of glycation. The diffracted x-ray intensity distribution was calculated with the assumptions that: (i) the perturbation was fixed in size; (ii) the crystalline domain size was limited (about 100 nm for rat tail tendon); (iii) the location of the perturbations was stochastic in nature; (iv) a large number of independently diffracting domains contributed to the resulting intensity; and (v) the pattern was slightly blurred by instrumental broadening. When the perturbation is less than 25% of the unit size (about 0.35 nm for collagen), this model predicts the presence of a sharp peak of scattered intensity, indistinguishable from a Bragg reflection, located in reciprocal space at the position of the mean cell size. We conclude that some collagen molecules are pushed apart by sugar derived cross-links and the observed expansion represents the average spacing of normal and cross-linked molecules.

W-Pos107 REOXIDATION OF REDUCED BOVINE GROWTH HORMONE FROM A STABLE SECONDARY STRUCTURE
Thomas F. Holzman, David N. Brems, and John J. Dougherty, Jr., Control Division, The Upjohn Company, Kalamazoo, Michigan 49001

In order to determine solution conditions appropriate for reoxidizing reduced bovine growth hormone (bGH), we have examined the possibility of using a particular denaturant concentration to poise the secondary and tertiary structure of the reduced protein in a stable, nativelike state. Dilution of concentrated samples of reduced and unfolded protein from 6.0 M guanidine into 4.5 M urea followed by air oxidation indicated it was possible to induce refolding and reoxidation to an oxidized monomeric species in high yield (~90%). The choice of solution conditions was based on comparison of urea equilibrium denaturation data. Denaturation supports the existence of equilibrium folding intermediates and demonstrates that chemical modification is capable of inducing differences in the denaturation behavior of these intermediates. The changes in the protein absorption and helix-related CD signals, along with direct titration of protein sulfhydryl groups, indicated that refolding/reoxidation is a multistate process. The ordered nature of the kinetic changes in these probes during reoxidation indicates that disulfide formation is a sequential process, with little mispairing in 4.5 M urea, and that it proceeds through one or more obligatory kinetic folding events. The denaturation behavior, together with the reoxidation data, indicated that the protein maintains a high degree of secondary structure without intrachain disulfide bonds. The formation of these disulfide bonds is a discrete process which occurs after a framework of protein secondary structure is established.

W-Pos108 ENTHALPIES OF INTERACTION OF MELITTIN AND MASTOPARAN X WITH CALMODULIN.
*Jakubowski, H. V., †Brandts, J. F., and *Prendergast, F. G. *Depart. of Biochem. and Mol. Biology, Mayo Fdn., Rochester, MN, †Dept. of Biochemistry, Univ. of Mass., Amherst, MA.

Titration calorimetry was used to determine ΔH of interaction of melittin (MLT) and mastoparan X (MX) with calmodulin (CAM). CAM was purified from chicken gizzards (single band on 15% SDS-polyacrylamide gels). MLT (Sigma Chemicals) was further purified by ultra-filtration (Amicon YM 10 membrane). MX (BaChem) was used without further purification. CAM and the peptides were dissolved in 20 mM HEPES, pH 7.44, +/- 1 mM $CaCl_2$. Trace Ca^{++} was removed from buffers with Chelex-100. Calorimetry was performed using a titration calorimeter kindly supplied by JFB. CAM (1.8 ml, 2.7-3 mg/ml) was added to the sample cell and MLT (1-10 µl, 11 mg/ml) or MX (1-10 µl, 15 mg/ml) was injected with constant stirring. ΔH's, determined at 25, 30 and 35°C, were corrected for ΔH's of dilution of the peptide into buffer. For each peptide, +/- Ca^{++}, ΔH was strongly dependent on temperature, the interaction proceeding with a large negative ΔCp. For each peptide, - Ca^{++}, the absolute value of ΔH and the magnitude of the negative ΔCp were greater than for the peptide + Ca^{++}. ΔH (kcal/mole) varied from +4.4 to -3.4 (MLT - Ca^{++}), +4.6 to +0.16 (MLT + Ca^{++}), -0.95 to -18 (MX - Ca^{++}) and -1.9 to -8.0 (MX + Ca^{++}), as T varied from 25-35°C. The higher ΔH values in the presence of Ca^{++} may reflect an enthalpic-entropic compensation resulting from a decreased electrostatic attraction and increased hydrophobic interaction. Dissociation constants for the peptides with CAM are being determined so that ΔS of interaction can be calculated. Other techniques (fluorescence spectroscopy, sedimentation equilibrium) are being utilized to determine if aggregation and ionization effects contribute to ΔH's. Supported by GM34847.

W-Pos109 THERMOTROPIC TRANSITIONS IN COMPLEMENT PROTEIN C9 AND INTERACTION WITH CALCIUM.
Karl Lohner, Nicole Thielens and Alfred F. Esser, Department of Comparative and Experimental Pathology, University of Florida, Gainesville, FL 32610.

Human complement protein C9 dissolved in buffers of physiological ionic strength undergoes endothermic transitions centered at 42°C and 52°C. The ratio of the calorimetric to the van't Hoff enthalpy change (ΔH) was found to be substantially larger than one indicating that each of the transitions involves unfolding of more than one single domain. Above 52°C C9 aggregates irreversibly. Increasing the salt concentration to 1.0 M removes the lower transition and prevents aggregation. Incubation of C9 at 42°C with ≈10 molar excess EDTA in buffered physiological saline causes loss of hemolytic activity, aggregation and release of calcium ions as measured by spectrophotometric titration with Quin-2 (in the absence of EDTA). High salt concentrations prevent EDTA-induced aggregation and protect hemolytic function. These results indicate that C9 is a multi-domain, Ca-binding protein that is poised to unfold at physiological temperatures. This structural transition may be important for insertion of C9 into target membranes and cytolysis. (Supported by NIH Grant R01 AI-19478)

W-Pos110 SIMULATION OF ELECTROSTATICALLY ENHANCED DIFFUSION OF SUPEROXIDE DIMUTASE.
K. Sharp[1], R. Fine[2], K. Schulten[1] & B. Honig[1]. [1]Dept. of Biochem. & Molecular Biophysics, Columbia Univ., N.Y., N.Y. 10032. [2]Dept. of Biological Sciences, Columbia Univ., N.Y., N.Y. 10027 & Dept. of Structural Biology, Brookhaven National Lab., Upton, N.Y. 11973.

Diffusion of superoxide to the active site of Cu,Zn superoxide dimutase in the presence of the electrostatic field of the protein is simulated by means of Brownian dynamics. The field is calculated from the protein shape and charge distribution, derived from the crystal coordinates, by a finite difference solution to the Poisson-Boltzmann equation (Klapper et al., Proteins 1, 47 (1986). The complex field and protein shape are accurately represented in the simulation by mapping them on a fine grid, and indexing into this grid using the instantaneous position of the superoxide trajectory. With no field, the efficiency (E) of finding the active site copper compared to the whole protein is less than 4%. At an ionic strength (I) of 0, the field increases E by over an order of magnitude. Neutralization of the catalytically important ARG 141 decreases the association rate by 30%. The rate decreases with increasing ionic strength for both the native and modified ARG 141 enzyme. Neutralization of all lysines reduces the rate 100 fold for zero ionic strength, but reverses the dependence on ionic strength. These changes in association rate with ionic strength and amino acid modification parallel the measured changes in enzyme catalytic rate, indicating that the latter depends on the field enhanced diffusion of the substrate to the active site.

W-Pos111 OPTICAL MICROSCOPY OF TROPOMYOSIN CRYSTALS: A BIREFRINGENCE AND MORPHOLOGY STUDY.
T. Ruiz, R. Oldenbourg, Dept. of Physics, Brandeis Univ., G. Phillips, Depts. of Physiology and Biophysics and Biochemistry, Univ. of Illinois, and C. Cohen, Rosenstiel Center, Brandeis Univ.

Tropomyosin crystals have a uniquely high water content (95%), and are made up of an open meshwork of cross-connected filaments. The high solvent content means that there is only limited contact of the filaments in the lattice. Correspondingly, the crystals show some remarkable dynamic features. For our optical studies, capillaries containing single crystals were mounted in a goniometer and immersed in a water bath for temperature control and refractive index matching. When seen through a microscope equipped with crossed polarizers, the clear crystals showed several colors arising from their optical anisotropy. The morphology was used to determine the orientation of the crystal axes. The crystals were observed to be optically biaxial with their principal axes of refraction parallel to the crystallographic axes. The birefringence values for light traveling along each of the three axes were measured to be Δn_a 32.5 10^{-5}, Δn_b 96 10^{-5}, and Δn_c 66 10^{-5}, respectively at 20°C. Model calculations treating the tropomyosin filaments as infinitely long rods with n=1.53, immersed in a medium of n=1.33, reproduced the measured birefringence values within 20%. No intrinsic birefringence was taken into account for these α-helical coiled-coil filaments. As the temperature was lowered, the birefringence Δn_a and Δn_b increased ($\delta(\Delta n)/\delta T$=2.5 10^{-6} 1/°C), but Δn_c did not change with the temperature in the range of -13°C to +30°C. Possible explanations for the temperature dependence of the birefringence are changes in the dimensions of the unit cell or increasing order in the arrangement of the filaments at lower temperatures.

W-Pos112 DOCKING SITES IN PROTEIN AND ENZYME SUBSTRATE REACTIONS.
Chance, B., Chance, M.*, Powers, L.*, Zhou, Y-H. & Reddy, K.S. Dept of Biochem/Biophys, Univ of Penna; and Inst. Struct. & Functional Studies, Univ. City Sci. Ctr., Phila., PA; and *AT&T Bell Labs, Murray Hill, NJ

We have continued our studies on the structural dynamics of myoglobin using optical and X-ray absorption spectroscopy (EXAFS) techniques at low temperatures. Our previous studies by EXAFS on photolyzed MbCO using steady state illumination has indicated that the ligand is trapped very near to the iron at 4°K (1), whilst it is trapped at a larger distance at 40°K. The heme configuration is similar in the photoproduct at 4°K and 40°K. Thus our method is capable of identifying different states in photolyzed myoglobin. We believe that these correspond to different states from those identified by Frauenfelder (2). Recently we have reported (3) that the recombination kinetics of photolyzed myoglobin (Mb*) with CO using steady state illumination is not only dependent on temperature, but also on the time of illumination. This also indirectly indicates that the states populated at low temperature using steady state illumination are different from those identified by Frauenfelder (2) using transient observations such as laser pulse photolysis. In the present study, we report low temperature kinetics of photolyzed Mb-CO recombination reaction using optical spectroscopy at different concentrations, different times of illumination. However our EXAFS and optical spectroscopic studies indicate that 40°K may be the key importance as a docking or alignment site for the ligand entry to its final position and such sites should be sought in other biological reactions, particularly those of enzyme and substrate where orientation of the substrate is important. (1) Chance, B. et al (1983) Biochem. 22:3820; (2) Austin, R.H. et al (1975) Biochem. 14:5355; Chance, B. et al (1986) Fed.Proc. 45:1641. SUPPORT: NIH Grants HL 18708, GM 33165, RR 01633, GM 31992; & SSRL Project 107B.

W-Pos113 THE STRUCTURE AND DYNAMICS OF METHIONINE. E.V. Curto and F.W. Dahlquist, Institute of Molecular Biology, University of Oregon, OR 97403

The side chain motions of a protein can affect what it is and how it works. We are modeling methionine side chain motions in protein based on careful measurements of the structure and dynamics of methionine in crystals of the amino acid using temperature dependent X-ray crystallography and deuterium quadrupole nuclear magnetic resonance (DQNMR). It was shown previously that this crystal undergoes a thermodynamic phase transition at about 32°C (Hutchens et al., J. Biol. Chem. 239, 591 (1964)), which makes it an attractive model for physical study. We have found that the crystal unit cell volume appears to follow this phase transition, changing about 5% from 735 to 780 Å^3 over the temperature range of -20 to 94 °C. The crystal structures of the molecule were solved at -20, 20, 32, and 75 °C to help us understand the nature of this transition. The temperature dependent dynamics of the methionine methyl group were studied in crystal powders using DQNMR. The first moment of the powder pattern also appears to change with temperature much like the enthalpy and volume changes. The motion is highly asymmetric and appears to be undergoing fast exchange between two states. The amplitude of the motion ranges from the rigid limit for methyl rotors to about the square of the methyl rigid limit. The asymmetry parameter of the powder pattern for at least one of the two methionine conformations in the unit cell changes sign at about 45 °C. Models for the symmetry, amplitude and rate of motion of the methionine methyl group are presented and are compared with similar studies in T4 lysozyme.

W-Pos114 SIMULATION OF THE SUPEROXIDE DISMUTASE-SUPEROXIDE REACTION FOR A REALISTIC TOPOGRAPHICAL MODEL. S. Allison, Dept. of Chemistry, Georgia State University, Atlanta, GA 30303; R. Bacquet and J.A. McCammon, Dept. of Chemistry, University of Houston, Houston, TX 77004.

The diffusion controlled reaction between superoxide dismutase (SOD) and superoxide has been studied using a model which accounts for the detailed topography of the enzyme and active site channels. Rate constants under a variety of different conditions will be presented and were derived using a Brownian dynamics trajectory method. At distances greater than 30 angstroms from the center of SOD (outer zone), screened Coulomb potentials derived from Monte Carlo simulations were used to compute the force between enzyme and substrate. At shorter distances (inner zone) pairwise additive forces arising from the charged residues of SOD were used. Counterion effects in the inner zone were either ignored or Debye-Huckel point ion screening was assumed. The latter assumption leads to reaction rates which decrease strongly as the salt concentration increases. The dielectric constant was 78 in the outer zone but was variable in the inner zone. In summary, electrostatic forces greatly enhance the reaction rate over that of a "neutral" enzyme.

W-Pos115 NON-PHOTOCHEMICAL HOLEBURNING IN A PROTEIN MATRIX: CHLOROPHYLLIDE IN APOMYOGLOBIN. Steven G. Boxer, David S. Gottfried, David J. Lockhart and Thomas R. Middendorf, Department of Chemistry, Stanford University, Stanford, California 94305

Non-photochemical holeburning spectroscopy has been used to study a chlorophyllide chromophore substituted for heme in apomyoglobin. The observed holewidths were compared with those found for the same chromophore embedded in the polymeric glass polystyrene. Hole formation occurs with comparable efficiency in the protein and in the polymeric matrix. A temperature exponent of 1.26±0.07 was measured for the pure-dephasing contribution to the homogeneous linewidth (Γ_h) for the chromophore in the protein between 1.35 and 2.5K (see data). This temperature dependence is very similar to that observed for many chromophores in amorphous host matrices. This suggests that the characteristic properties of the matrix responsible for pure dephasing in glasses and in the protein are very similar. Measurements over a wider temperature range and for chromophore aggregates will be discussed, as will possible implications for energy and electron transfer in proteins.

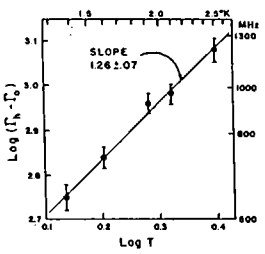

W-Pos116 THERMODYNAMICS OF Zn^{2+}-INDUCED STACKING OF GLUTAMINE SYNTHETASE DODECAMERS.

Ann Ginsburg and Marlana B. Blackburn, NHLBI, NIH, Bethesda, MD 20892

The stacking of glutamine synthetase (GS) dodecamers of M_r 600,000 from E. coli has been studied by calorimetry in order to investigate the forces governing macromolecular self-assembly reactions. The 12 subunits of GS are arranged in 2 superimposed hexagonal rings ~ 140 Å in diameter and Zn^{2+} binds to a site distinct from the active site of each subunit with K_A = 5 X 10^6 M^{-1} at pH 7.0. The binding of Zn^{2+} deforms the enzyme in such a way that when 50 mM $MgCl_2$ also is present, spontaneous face-to-face aggregation of GS dodecamers and later side-to-side interactions between twisted single strands occur. Kinetic studies of Zn^{2+}-induced polymerization of GS along the 6-fold axes of symmetry indicate that the initial process has a second-order rate constant of 5 X 10^4 M^{-1} s^{-1} at 25°C and that the reaction rate increases with increasing temperature with an Arrhenius activation energy of 17.7 kcal/mol. Enthalpy changes (ΔH) for (1) the binding of Zn^{2+} to GS with accompanying proton release (1 eq H^+/Zn^{2+} bound) and protein conformational changes and (2) the Zn^{2+}-induced aggregation of GS dodecamers and, as confirmation, (3) the reversal of reactions in (1) and (2) by addition of the Zn^{2+} chelator pyridine-2,6-dicarboxylate were measured by calorimetry at pH 7.0. A batch calorimeter equipped with a microtitrator was used at 22.5, 30 and 38°C. In the absence of $MgCl_2$, the addition of 0.66 eq of Zn^{2+}/subunit produces no aggregation of GS (as monitored by light scattering) and ΔH = 115 kcal/mol of GS dodecamer for (1) at 38°C with $\delta\Delta H/\delta T \approx$ 1500 cal/K•mol for Zn^{2+} binding. Subtracting the latter value from that obtained for (1) + (2) gave $\Delta Cp \approx$ -850 cal/K•mol for protein-protein interactions in (2). The large ΔCp value for (2) implicates a dominant role of water in the stacking process.

W-Pos117 RAPID LENGTH CHANGES IN MYOCARDIAL SEGMENTS: ASSESSMENT OF STIFFNESS AND FORCE REDEVELOPMENT. D.A. Martyn and L.L. Huntsman. University of Washington, Seattle, WA 98195. Stiffness and force redevelopment were measured in the central segments of isolated ferret papillary muscles. Segment length (SL) was determined using an area sense coil technique. Segment stiffness (K) was calculated by imposing rapid (≤1 msec) changes in muscle length during a twitch and measuring the corresponding changes in force (F) and SL. Isometric force production was altered by changing initial SL and by changing extracellular calcium (Ca_O) levels. When measured at the time of peak force production, K was found to have properties similar to those reported for skeletal muscle. K was proportional to F and the rapid decrease in SL needed to drop F to zero was less than 1%. From 95-85% SL_{max}, F and K have similar SL dependencies. When Ca_O was changed over a range from 4.5 to 1.125 mM, K measured at a given SL changed in proportion to the resulting change in peak force. The SL change needed to obtain zero force (ΔSL_O) did not depend on calcium. At SL ≤85% SL_{max} there was a tendency for K to increase relative to force, and for ΔSL_O to decrease. This tendency was greatest at low Ca_O. These observations indicate that for length at or below 85% SL_{max} (about 1.7-1.8 μm sarcomere length) an internal load may be contributing to the stiffness measurements. The results indicate that over a major part of cardiac F-SL relations changes in force are caused by changes in the numbers of force producing crossbridges. We have also observed that rapid releases of ≤1% SL_{max} imposed during the rising phase of the twitch do not cause a decrease or deactivation of subsequent redeveloped force. However, releases >1% SLmax always cause redeveloped force to fall below what it would have been had the isometric contraction occured at the released length. This result indicates that for mechanical deactivation to occur crossbridges must be detached.

W-Pos118 **BOUND Ca^{2+} AND FORCE DEVELOPMENT IN DETERGENT-EXTRACTED CARDIAC MUSCLE BUNDLES: EFFECT OF SARCOMERE LENGTH.** Polly A. Hofmann and Franklin Fuchs, Department of Physiology, University of Pittsburgh School of Medicine, Pittsburgh, PA 15261

There is evidence that the steep ascending limb of the force-length curve in cardiac muscle (Frank-Starling relationship) is based on a length-dependence of myofilament Ca^{2+} sensitivity (Hibberd and Jewell, 1982; Allen and Kentish, 1985). Previous work from this laboratory has indicated that in the sarcomere length range corresponding to the ascending limb of the force-length curve the Ca-Tn-C affinity may be length-dependent. In this study Ca binding to chemically skinned bovine cardiac muscle bundles was measured during ATP-induced force generation. The muscle chamber was mounted on an inverted microscope so that sarcomere length could be measured and adjusted in each experiment. Sarcomere lengths were maintained at either 2.16-2.37 μm or 1.51-1.84 μm. A double isotope technique was used to make concurrent determinations of the force-pCa and bound Ca^{2+}-pCa relationships at different sarcomere lengths. It was established that at the longer sarcomere lengths the fibers bound an amount of Ca^{2+} equivalent to ~3 moles Ca^{2+}/mole Tn-C and that force development was coupled to titration of the low affinity, Ca^{2+}-specific site. In the pCa range 7.0-6.0 sarcomere length had no effect on Ca^{2+} binding or force generation. In the pCa range 5.7-5.0 the Ca^{2+} bound at sarcomere lengths 1.51-1.84 μm was 20-30% less than that bound at sarcomere lengths 2.16-2.37 μm. Thus sarcomere length appears to determine Ca^{2+}-Tn-C affinity in the pCa range in which the regulatory site is titrated. These data provide direct evidence, obtained under more physiological conditions, that length-dependent modulation of Ca^{2+}-Tn-C affinity may provide a basis for the force-length relationship in cardiac muscle. Supported by grants from the NIH (AM10551) and Western Pennsylvania Heart Association.

W-Pos119 TENSION CONTROL OF FAST-TWITCH FIBERS BY CARDIAC-TnC.

A. Babu, E.H. Sonnenblick, S. Scordilis* and J. Gulati, Albert Einstein College of Medicine, Bronx, NY and *Smith College, Northampton, MA.

Because of the differences in one of the Ca-specific sites of skeletal(S) and cardiac(C) TnC's (site I of CTnC, residues 28-40 from the N-terminus, lacks the Ca-binding function), the fiber studies with native TnC exchanged for CTnC are of interest. Recently, on hamster psoas fibers we found CTnC to be relatively ineffective for tension recovery (Babu: J Mol Cell Cardiol 18, 10a, 1986). Subsequently, Moss (J Biol Chem 261, 1986) indicated near full tension with CTnC in rabbit fibers. But, STnC extraction was more complete in our study, and ionic strength was higher (residual STnC 26% in Babu vs 53% in Moss; ionic strength, physiological 180mM vs 140mM). To study these parameters, systematically, the extraction time was here varied between 1-30 min (Gulati & Babu, this vol). After loading with CTnC, pCa4 activations were made in 180 and 100mM ionic strengths. We found that the tension recovery with CTnC was (i) related to the level of residual force (presumably also residual TnC), being higher with limited extractions, and (ii) greater in 100mM than in 180mM. This confirms our earlier finding that CTnC alone is ineffective in skeletal fibers. The results suggest that the presence of STnC has a cooperative effect on the action of CTnC. The effects with reduced ionic strength (100mM) are explained: (1) By increased cooperativity in the thin filament. (2) By modification of TnC properties by the cross-bridges (Ridgway & Gordon: J Gen Physiol 83, 1984), since the major pathway for the flux of cross-bridges shifts to AM states in low ionic strength (Hibberd & Trentham: Ann Rev BBC 15, 1986). (3) If CTnC were effective in replacing STnC during the force step (weak→strong conformation) but not during weak bridge formation in dual regulation (Gulati & Babu, this vol). (NSF-8303045; NIH-AM 33736 & HL 18824)

W-Pos120 MAXIMAL Ca^{2+}-ACTIVATED FORCE AND MYOFILAMENT Ca^{2+}-SENSITIVITY IN INTACT FERRET HEARTS: DIFFERENTIAL EFFECTS OF PROTONS AND INORGANIC PHOSPHATE

Eduardo Marban and Hideo Kusuoka. Dept. of Med., The Johns Hopkins University, Baltimore, MD 21205

We describe a novel approach to determine maximal Ca^{2+}-activated force and to deduce changes in myofilament Ca^{2+}-sensitivity from isovolumic pressure in intact hearts. This approach is combined with P-NMR to estimate the relative contributions of changes in myofilament sensitivity and maximal force to the negative inotropic effects of acidosis and hypoxia. Ferret hearts were perfused with HEPES-buffered solution (37°C, 2 mM $[Ca]_o$), and P-NMR spectra were obtained every 2-4 min. Acidosis was induced by bubbling with 95%O_2/5%CO_2, and we determined the relation between intracellular $[H^+]$ and simultaneous twitch pressure. After recovery from acidosis, hearts were exposed to ryanodine (3 μM), and maximal Ca^{2+}-activated pressure (MCAP) was determined during tetani induced by 10 Hz pacing at $[Ca]_o \geq 10$ mM. Acidosis was re-induced to determine the relation between $[H^+]$ and MCAP. When normalized, the two relations between $[H^+]$ and pressure (twitch and maximal) would be identical if there were no change in myofilament sensitivity, assuming $[Ca^{2+}]$ transients are unchanged. Instead, the relation for twitches had a significantly steeper slope than that for MCAP (n=5;p<.001 in 4,p<.05 in 1). We used the same approach to investigate hypoxia (which rapidly increases inorganic phosphate, Pi). The relations between [Pi] and normalized pressure were not significantly different for twitches and MCAP (n=6;p>.05). $[Ca^{2+}]$ transients as indicated by aequorin in ferret ventricular muscle are not changed during hypoxia, and increase during acidosis (which would tend to minimize the perceived decrease in myofilament sensitivity). We conclude that Pi accumulation during hypoxia decreases maximal force, but does not shift myofilament sensitivity. In contrast, acidosis induces both a decrease in maximal force and a shift in sensitivity, as expected from skinned muscle.

W-Pos121 EXTRACELLULAR FACTORS SLOW SARCOMERE REEXTENSION IN ISOLATED HEART MUSCLE. John Krueger and Gerard Siciliano. The Albert Einstein College of Medicine. Bronx, N.Y. 10461

A persistent yet untested assumption is that sarcomere shortening distorts extracellular elements elastically in isolated heart muscle. This should a) increase the speed of relengthening (Vl), b) slow the speed of shortening (Vs), and c) increase the ratio Vl/Vs in intact heart muscles as compared to unattached myocytes. RV trabeculae from guinea pigs were bathed in solutions containing 2.0 mM $CaCl_2$ and stimulated to contract at 2 hz (34 °C). Enzymatically isolated cells were bathed in $1.0 \leq CaCl_2 \leq 3.0$ mM to bracket the uncertain $[Ca^{2+}]$ at the cell surface within muscle. The cellular relengthening ratio (Vl/Vs) was 1.04 ± 0.24 in 1 mM $CaCl_2$ (59 cases) and decreased to only 0.74 ± 0.28 in $2 \leq CaCl_2 \leq 3.0$ mM (30 cases). The decrease was due to the constancy of relengthening speed at high contractility, as seen when shortening speed was increased by altering stimulus rate (0.1 to 3 hz). In the intact muscle, the velocity of shortening and relengthening of the sarcomemere approaches 2.4 L/s and 0.4 L/s, respectively, at zero load. Thus, a muscle's relengthening ratio is only about 1/6: i.e., fully 4 to 6 times slower than in the isolated cell. With comparable stimulus rates, shortening speed in the isolated cell, 2.3 ± 1.1 L/s (N= 16), was comparable to muscle. A selective slowing of muscle relengthening refutes the extracellular origin of an elastic restoring force in isolated heart muscle preparations (barring any drastic difference between right and left ventricular muscle mechanics). Conversely, the force which reextends isolated cardiac muscle must originate within the cell (Krueger et al., J. Gen. Physiol. 76: 587, 1980). Interstitial [ion] fluctuations during contraction and/or viscosity might slow reextension in intact muscle.
Supported, in part, by HL 21325 and the Martin Fund.

W-Pos122 MECHANICAL PERFORMANCE OF THE MYOCARDIUM IS MODULATED BY THE ENDOCARDIUM
Dirk L Brutsaert, Ann L Meulemans, Karin R Sipido and Stanislas U Sys
University of Antwerp, Antwerp, Belgium.

The function of the endocardium is as yet unknown. The mechanical properties of mammalian ventricular myocardium were therefore studied in the presence and in the absence of a functional endocardial endothelium.

Isotonic and isometric twitch contractions were obtained from papillary muscles of the right ventricle of cat (n=25) and left ventricle of rat (n=13) at different extracellular calcium concentrations [Ca++]o and at different initial muscle lengths.

Either gentle abrasion of the muscle surface with a plastic blade or immersion of the muscle for 1-2 s with 1% Triton X-100 induced an immediate and irreversible abbreviation of the contractions with a decrease in peak isometric tension, except at the highest [Ca++]o. This abbreviation resulted in an asymmetrical shift of the peak tension-[Ca++]o relationship and in a symmetrical shift of the length-tension relationship, significantly more pronounced (p<0.01) at 37 C than at 29 C.

The asymmetrical shift of the tension-[Ca++]o relationship and the shift of the length-tension relationship at submaximal [Ca++]o, induced by the removal of a functional endocardial endothelium, suggest that the endocardium-mediated chain of events may eventually lead to changes in the sensitivity of the contractile proteins to Ca++.

W-Pos123 ISOPROTERENOL ALTERS MYOCARDIAL MYOSIN-ACTIN KINETICS. Michael R. Berman, Jon N. Peterson, David T. Yue and William C. Hunter. Department of Biomedical Engineering, School of Medicine, Johns Hopkins University, Baltimore, Maryland 21205.

Since catecholamines affect the rates of rise and fall of myocardial force, we investigated whether they might affect the kinetics of the fundamental force generating interaction of myosin with actin. Right ventricular papillary muscles from rabbits were put into barium contracture at Lo. Length was perturbed by both small amplitude (<1% Lo) rapid stretch and sinusoids (0.1-30 Hz, 30 frequencies). Isoproterenol (10 uM) was then added to the bath and the length perturbations were repeated. Force transients in response to stretches had 3 phases: a rise in force coincident with stretch, a rapid fall in force, and a slow rise in force. Isoproterenol had no effect on the time course of the rapid fall in force, but it did reduce the duration of the slow rise of force from 242±29 to 184±23 ms (mean ± SD, n=8). Sinusoidal stiffness (stress/strain) amplitude spectra were "flat" at low frequency, had a minimum near 1-2 Hz, then increased with frequency. Isoproterenol shifted the frequency of the minimum in the stiffness spectra from 1.5±0.13 to 2.1±0.36 Hz, n=5. Since both the time course of force transients and the frequency of the minima in stiffness amplitude spectra are thought to reflect the kinetics of myosin-actin interaction these results demonstrate that isoproterenol, whatever its other mechanisms of action, does alter the kinetics of the fundamental force generating interaction of myosin with actin. Further, these changes in force transients and in stiffness amplitude spectra are similar to changes seen when myocardium shifts its isomyosin pattern from V3 to V1, with an accompanying decrease in thermal economy. It is tempting to speculate that catecholamines might cause a similar decrease in thermal economy.

W-Pos124 RELAXATION IN ISOLATED CARDIAC MYOCYTES IS ENHANCED BY LOW EXTRACELLULAR CALCIUM AND ISOPROTERENOL. Rashid Nassar[+] and Page A. W. Anderson[*]. Departments of Physiology[+*] and Pediatrics[*], Duke University Medical Center, Durham, N.C.

We have previously shown, using changes in the pattern of stimulation as a means to alter cytosolic calcium in externally unloaded cardiac myocytes, that the slope of the relationship between the maximum velocity of sarcomere re-extension ($\dot{r}$) and that of shortening ($\dot{s}$) was constant over a wide range of sarcomere shortening. This suggested that uptake of calcium by the sarcoplasmic reticulum (SR) determines the rate of sarcomere re-extension. In order to test this further, we studied the effect of extracellular calcium concentration ([Ca]o) and isoproterenol on the relationship between $\dot{r}$ and $\dot{s}$. Enzymatically isolated, externally unloaded, calcium tolerant myocytes from the rabbit heart were electrically stimulated at room temperature. [Ca]o was varied from 0.5 to 2.0 mM, and at each concentration the pattern of stimulation was perturbed to obtain a wide range of $\dot{s}$ and $\dot{r}$ in extrasystoles and potentiated post-extrasystoles. Lowering [Ca]o increased the slope of $\dot{r}$ vs. $\dot{s}$. Isoproterenol (3×10^{-7} M) caused an increase in the slope. Thus both a reduction of [Ca]o and isoproterenol produced an enhancement in the re-extension velocity relative to shortening velocity. A common effect of both perturbations is the enhancement of Ca pumping by the SR: low [Ca]o because of lower Ca loading in the SR, and isoproterenol through phosphorylation of the SR.

(Supported by NIH HL20749, HL12486, and HL33680).

W-Pos125 **Halothane Depresses Myocardial Contractility By Reducing Sarcolemmal Ca^{2+} Transport**
P.D. Allen, J.G. Murphy*, D. Kim*, J.D. Marsh*, T.W. Smith, The Departments of Anesthesiology and Medicine (Cardiology), Brigham and Women's Hospital, Boston, MA 02115

The effects of halothane on myocardial contractility and exchangable Ca^{2+} pools were studied in monolayers of spontaneously beating cultured chick embryo ventricular cells. The cells were prepared as described previously[1]. Cells were superfused with HEPES buffered physiological salt solution, pH 7.4, 37°C containing 1% heat inactivated fetal calf serum. Test solutions were equilibrated with gas delivered from a calibrated vaporizer and the halothane conc. confirmed by GLC. Contraction rate as well as amplitude and velocity of contraction were monitored using an optical video system. Five min. $^{45}Ca^{2+}$ exchangeable pool size was determined as described previously[1]. Halothane produces a concentration dependent depression of amplitude and velocity of contraction ($p<0.01$) which is quantitativly and qualitatively similar to its effects on systolic function in papillary muscle and isolated heart preparations. Furthermore, 2% halothane lowered 5 min $^{45}Ca^{2+}$ uptake by 25% from 2.64 ± 0.08 to 2.03 ± 0.06 nmol/mg protien ($p<0.0005$). This rapidly exchangable Ca^{2+} pool has a $t_{1/2}$ of 11 sec and plateaus at 5 min. It is attributed to sarcolemmal flux via the slow Ca^{2+} channel and Na^{+}-Ca^{2+} exchange. These data demonstrate that the depression in contractility induced by halothane is accompanied by a depression in rapid $^{45}Ca^{2+}$ entry, and supports the hypothesis that halothane exerts its negative inotropic effect, primarily, by altering sarcolemmal Ca^{2+} transport. SR Ca^{2+} transport may be secondarily effected as a result of reduced sarcolemmal Ca^{2+} entry. Presumably this decreased Ca^{2+} exchange results in a reduced $[Ca^{2+}]_i$, but this direct observation has yet to be made.

(1.)Barry and Smith, J. Physiol. 325: 243-260,1982 Supported by AHA(Mass Affiliate) PDA and NIH HL35781 JM

W-Pos126 THE EFFECTS OF LOCAL ANESTHETICS ON CULTURED HEART CELL CONTRACTILE PERFORMANCE
S.P. DESAI, J.D. MARSH*, T.W. SMITH, AND P.D. ALLEN, THE DEPARTMENTS OF ANESTHESIOLOGY AND MEDICINE (CARDIOLOGY), BRIGHAM AND WOMEN'S HOSPITAL, BOSTON, MA 02115

The effects of lidocaine (25,50 and 100μg/ml) and bupivacaine (5, 10, and 20μg/ml) on amplitude, velocity and rate of contraction were studied in monolayer cutures of spontaneously beating chick embryo ventricular cells. The cells were prepared and the physiologic parameters of contraction rate, amplitude and velocity of shortening measured with an optical video system as described previously (Barry and Smith, J. Physiol. 325:243-260 1982). All experiments were conducted at 37°C using HEPES buffered physiologic salt solution, pH 7.4 containing 1% heat inactivated fetal calf serum. Parallel studies were carried out in the presence of 1μM TTX to isolate effects caused by TTX sensitive Na^+ channel blockade from other possible mechanisms. Both lidocaine and bupivacaine produced a concentration dependent reversable decrement in all three measured physiologic variables. Bupivacaine demonstrated a 5 fold higher potency than lidocaine but no other differences were noted between the two drugs. TTX (1μM) produced a 38% decrease in rate of contraction and a 23% decrease in amplitude and velocity of shortening. Addition of bupivacaine or lidocaine to TTX resulted in further decreases in amplitude and velocity of shortening but no further decrease in contraction rate. It is well known that local anesthetics block Na^+ channels of excitable membranes. Our observations suggest that both lidocaine and bupivacaine have at least one locus of action at a site other than the TTX blockable site. Previous studies on cultured chick cells have demonstrated that their amplitude and velocity of contraction are highly Ca^{2+} dependent. We propose that both drugs exert some of their effect by altering sarcolemmal Ca^{2+} transport with a subsequent reduction in $[Ca^{2+}]_i$, but these direct observations remain to be made. Supported by AHA(Mass affiliate) PDA and NIH HL 35781 JM

W-Pos127 THE TEMPERATURE-DEPENDENCE OF P-LIGHT CHAIN PHOSPHORYLATION AND TWITCH POTENTIATION IN MOUSE EDL MUSCLE. Moore, R.L.[1], S. Williams[2], H. Tanabe[2], L. Zapp[2] and M.E. Houston[3]
[1]The Division of Cardiology, The Pennsylvania State University, Hershey, PA. 17033, and the Departments of Kinesiology at [2]The University of Colorado, Boulder, CO. 80309, and [3]The University of Waterloo, Waterloo, ONT N2L 3A7.

Isolated mouse EDL muscles were maintained at 25°, 30° and 35°C. and measurements of isometric contractility made prior to, during and following condition stimuli (5 Hz, 20 sec). Before the stimulus train peak twitch forces (mN) were 45.6 ± 2.3, 29.9 ± 1.6 and 20.1 ± 1.4, time-to-peak tensions (msec) were 22.8 ± 0.4, 15.1 ± 0.3 and 10.4 ± 0.3 and half-relaxation times (msec) were 22.2 ± 0.6, 9.2 ± 0.4 and 4.8 ± 0.2 at 25°, 30° and 35°C., respectively. The relative extent of isometric twitch potentiation (ITP) following stimulation was directly proportional to muscle temperature (16 ± 3, 22 ± 3, 33 ± 2%) whereas peak P-light chain (PLC) phosphate content was inversely proportional to temperature (0.71 ± 0.05, 0.43 ± 0.05, and 0.25 ± 0.04 mol P/mol P-light chain) at 25°, 30° and 35°C. The latter observation might be explained by: 1) a smaller fractional activation of myosin light chain kinase (MLCK) due to a reduction in the duration of sarcoplasmic Ca^{2+} transients associated with muscle twitches, 2) an increase in the rate of inactivation of active MLCK, and 3) an increase in the rate of myosin dephosphorylation following stimulation as temperature was increased from 25° to 35°C. Myosin dephosphorylation and ITP decay rates following stimulation were directly related to temperature. A temperature-independent, temporal relationship between ITP and PLC phosphate content existed whereas the quantitative relationship varied as a function of temperature. Whether this relationship is causal or coincidental remains to be determined.

W-Pos128 RESTING TENSION IMPLICATIONS OF STIFFNESS CHANGES AND SHORTENING OF RAT CARDIAC MYOCYTES IN HIGH SALT. A.J. Brady & K.P. Roos, Dept. Physiology, UCLA Med. School, Los Angeles, CA 90024

Stiffness declines in attached detergent skinned cardiac myocytes in elevated salt concentrations(>0.09M KCl). Unattached myocytes shorten in these solutions at a rate that increases with salt concentration. Higuchi & Ishiwata (1985) showed that A-band width declines concomitantly with the stiffness decline and Trinick & Cooper (1980) found that native thick filaments shorten at elevated salt concentrations. The stiffness decline and the shortening might be due to either an extraction of myosin or to a salt induced shift of myosin and actin molecules from an ordered α-helix to a random coil disorder (Mandelkern et al., 1965). In crosslinked glycerinated skeletal muscle fibers the latter study showed that shortening in high LiBr solutions was nearly completely reversible. In our experiments, rigor produced in ATP-free perfusate, was used as a method of temporary contractile filament crosslinking and also as a measure of myosin extraction. Alternate exposure of cardiac myocytes to rigor solution, to 0.47M KCl and then to rigor solution results in a decline in rigor stiffness in both the high salt and at the second exposure to rigor solution. This indicates that 1) some myofilaments have been extracted by the high salt rather than myosin and/or actin filaments having melted, or that 2) myofilaments have melted but the melting effects are small since neither the stiffness decline nor the shortening in high salt is reversible. These results suggest that the cytoskeleton of cardiac myocytes is normally stressed so that disassembly of the thick filaments in high salt results in a relief of that stress with consequent shortening or a fall in cell stiffness. Supported by USPHS HL29671 and HL30828.

W-Pos129 POWER OUTPUTS OF FAST AND SLOW SKELETAL MUSCLES OF THE MOUSE. John A. Faulkner, Susan V. Brooks, and Doris A. McCubbrey. Department of Physiology and Bioengineering Program University of Michigan, Ann Arbor, Michigan, 48109

The hypothesis was tested that fast skeletal muscles develop higher power outputs than slow muscles over any given time period up to 30 min. For fast extensor digitorum longus (EDL) and slow soleus muscles of the mouse, peak instantaneous power outputs were calculated from force-velocity relationships. Measurements were made with a Cambridge 300-H ergometer with the muscle at 35-37°C. The values for peak power were 418±18 w/kg for EDL muscles and 166±8 w/kg for soleus muscles. Maximum power outputs were measured during single contractions. Each contraction was at the optimal velocity for power output and displacement was through 10% of the fiber length (L_f) with L_f optimized for force development. The EDL and soleus muscles were stimulated at a frequency that produced 85% of maximum isometric tension, 150 and 80 Hz for EDL and soleus muscles, respectively. Because of differences in optimal shortening velocity and L_f, the contraction time required for the EDL muscle was 40 ms and for the soleus muscle 180 ms. The maximum power output was 360±27 w/kg for the EDL muscles and 41±6 w/kg for the soleus muscles. The power output that could be sustained for 30 min. was determined systematically by increasing the train rate for each contraction from 0.05 Hz to the train rate that produced the highest sustained power output. The train rates that could be sustained for 30 min were 2 Hz for the EDL muscles and 0.1 Hz for the soleus muscles. The sustained power outputs for EDL and soleus muscles respectively were 12.1±0.8 w/kg and 0.52±0.08 w/kg. These data are in reasonable agreement with peak, maximum, and sustained power outputs of humans. We conclude that fast muscles develop and sustain higher power outputs than slow muscles. Supported by NIH grant AG 06157.

W-Pos130 THE TRANSFER FUNCTION OF HYPOXIC CARDIAC MUSCLE SUGGESTS RIGOR Jeroen J Bucx and Henk EDJ ter Keurs. Departments of Medicine and Medical Physiology, The University of Calgary, Canada

The mechanism that underlies the increase in resting force following hypoxia of myocardium was studied by analysis of the transfer function with sinusoidal length changes. Force was measured with a quartz strain gauge, sarcomere length (SL) with laser diffraction techniques. The muscles (n=8) were superfused with Krebs-Henseleit medium (30 C, pH 7.35, 1 Hz, Ca++ 1.5 mM, pO2 600 mm Hg)(N). Tetani (T) were induce by stimulating at 10 Hz (4 mM Ca++, 10 mM caffein); hypoxia (H) by superfusion with glucose-free medium at pO2 6-9 mm Hg (H). Both during N (at rest and during T) and at maximal hypoxic diastolic tension the modulus (MF) and phase shift (PS in degrees) of the force response to the SL change was measured (0.1 to 400 Hz).

MF (N and H) did not vary with the frequency of the length change; MF during H was 12x MF at N. MF during T was constant up to 0.8 Hz and increased steeply from 3 to 100 Hz. PS during N and H was +10 and independent of frequency. PS, during T, was - 15 (0.1-0.8 Hz) and increased at higher frequencies to + 80.

These observations are consistent with cyclic active force generation during tetani, and completely passive behaviour during normoxia at rest and at hypoxia when maximal diastolic force has developed. The last observation strongly suggests that the increase of the diastolic tension as a result of hypoxia is caused by rapidly developing rigor.

W-Pos131 THE EFFECT OF IONIC STRENGTH ON CROSSBRIDGE KINETICS AS DETECTED BY SINUSOIDAL ANALYSIS, ATP HYDROLYSIS RATE, AND THE LATTICE SPACING MEASUREMENTS IN CHEMICALLY SKINNED RABBIT PSOAS FIBERS. M. Kawai*, K. Güth#, and J. Wray#. *Department of Anatomy and Cell Biology, Columbia University, New York, N.Y. 10032, U.S.A.; #Abteilung Biophysik, Max-Planck Institut Heidelberg, D-6900 Heidelberg, F.R.G.

The ATP hydrolysis rate was measured by the NADH fluorescence method, and the results were correlated with crossbridge kinetics obtained from the tension transients in response to sinusoidal length alterations during maximal Ca activation. When ionic strength (IS) was increased (100-300mM), both isometric tension (60%) and ATPase rate (20%) decreased. Three rate constants of the transients were not altered, but there was a proportionate decrease in the magnitude parameters. The IS effect did not resemble that of MgATP, MgADP, phosphate, or Ca. There was only a slight expansion (6%) in the lattice spacing when IS was increased at 20°C as detected by equitorial X-ray diffraction during relaxation. The result from the ATPase rate imply that IS does not affect a slow step(s) which limits the hydrolysis rate; the results from the sinusoidal analysis imply that IS does not affect steps whose rate constants are in the medium range (1-2000 sec^{-1}). Thus we conclude that IS affects a fast step (>2000 sec^{-1}) such as the rapid equilibrium between the detached state and the pre-tension state (higher IS favors a more detached state), and that IS does not affect the steps influenced by MgATP, MgADP, Pi, and Ca. The results from the X-ray diffraction measurement indicates that the change in the rate constant(s) is based on the genuine effect of IS, and that it is not based on the distance between the filaments.

W-Pos132 THE EFFECTS OF pH, ADP, INORGANIC PHOSPHATE (Pi), AND AFFINITY ON THE MAXIMUM VELOCITY OF SHORTENING AND FORCE PRODUCTION OF SKINNED RABBIT MUSCLE FIBERS. D.J.E. Luney and R.E. Godt; Dept. of Physiology and Endocrinology; Med. College of Ga.; Augusta GA 30912. (Intr. by Keith Green).

Using chemically skinned rabbit psoas fibers, the effects of changes in [ADP], [Pi], pH and the affinity for ATP hydrolysis (A) were studied at maximal activation (pCa 4) and 10°C using the slack test. Increasing Pi to 30mM had no effect on Vmax but reduced maximum force by almost 50%. Adding 1mM ADP (in the presence of a myokinase inhibitor) increased force slightly but decreased Vmax to 87% of control. As compared to pH 7, force and Vmax increased at pH 7.5 and decreased at pH 6.5, with the effect of pH greater on force than on velocity. Reducing A to 42.5 kJ/mol by adding both Pi and ADP had no additional effect on Vmax as compared to ADP alone but the effect on force was a slightly greater reduction than would be expected from the combined effects of ADP and Pi. In intact fibers, Edman and Mattiazzi (J. Muscle Res. Cell Motil. 2:321, 1981) suggested that the decline of force and Vmax with fatigue was due to the decrease of intracellular pH. Our data for pH effects in skinned fibers were quantitatively consistant with their relationship between the reduction of Vmax and force, while our data for ADP, Pi and A changes were not. This supports the conclusion that pH changes play a major role in reducing force and velocity in fatigued muscle fibers. (Support: NIH/AM 31636).

W-Pos133 MECHANICAL OSCILLATIONS RECORDED ACOUSTICALLY FROM FROG MUSCLE, D. T. Barry, University of Michigan, Ann Arbor, MI

Acoustic, force, and compound muscle action potential signals were recorded simultaneously during maximal isometric twitches of frog gastrocnemius muscles. The muscles were mounted between a Konigsberg F-5A force transducer and a fixed post, suspended in a temperature controlled bath of frog Ringers. Stimulation was via the peripheral nerve. Acoustic signals were transduced with Bruel and Kjar 8103 hydrophones (bandwidth 0.1 Hz - 150 KHz ± 3 dB).

The onset of sound production occurred after the onset of muscle depolarization but before the onset of force production. Acoustic waveforms consisted of oscillations that initially increased in amplitude and frequency and then decreased. Hydrophones positioned on opposite sides of the muscle recorded acoustic signals that were 180 degrees out of phase.

These results provide evidence that acoustic signals are produced by lateral oscillations of muscle during contraction. The oscillation frequency is dependent on structural properties of the muscle, the contractile state, and the tension generated. As force increases, the longitudinal stiffness of a muscle increases due to greater numbers of attached cross-bridges. Since muscle is not a homogeneous material, longitudinal and transverse mechanical properties will differ. Nevertheless, transverse oscillations should exhibit a resonant frequency related to longitudinal stiffness, and the acoustic signal may prove useful in monitoring muscle stiffness changes without actually touching or contracting the muscle.

W-Pos134 EFFECTS ON THE FORM OF THE ASCENDING LIMB OF THE SARCOMERE LENGTH-TENSION RELATION IN SKINNED SKELETAL MUSCLE FIBERS DUE TO OSMOTIC COMPRESSION AND VARIATIONS IN THIN FILAMENT ACTIVATION. J.D. Allen and R.L. Moss, Dept of Physiology, Univ of Wisc, Madison 53706.

Factors which influence isometric tension development at lengths below the optimum (i.e., the ascending limb of the L-T relation) were investigated using skinned single fibers from rabbit psoas muscle. During maximal Ca^{2+} activation, the ascending limb (AL) demonstrated first a shallow phase and then a steeper phase as SL was reduced though both phases were shallower than expected. AL obtained in the presence of 5% (w/v) dextran to compress fiber diameter more nearly resembled the AL predicted for mammalian muscle than did AL from untreated fibers. As SL was reduced between 2.46 and 1.54 um, tension-pCa relations from both control and dextran-treated fibers shifted to higher [Ca^{2+}]. These length-dependent changes in Ca^{2+} sensitivity did not appear to be the result of shortening induced dissociation of Ca^{2+} from TnC, since fibers submaximally activated in the absence of Ca^{2+} by the partial removal of whole Tn complexes produced AL similar to those seen in the same fibers activated at low [Ca^{2+}] prior to Tn removal. Stiffness measurements at 3.3 kHz indicated that at low [Ca^{2+}] tension fell more rapidly than stiffness in the shallow part of the AL while at high [Ca^{2+}] tension and stiffness declined in parallel. Thus, the shape of the AL at high [Ca^{2+}] can be explained on the basis of filament overlap, with the possibility that some of the fall off in tension results from an increase in filament lattice spacing. In addition, the depression of the AL observed at low [Ca^{2+}] may involve the presence of an internal load in the form of slowly dissociating cross-bridges which would be expected to progressively reduce total tension as the fiber is shortened. Supported by NIH.

W-Pos135 DO MUSCLE LENGTH TRANSIENTS CORRESPOND TO SARCOMERE PAUSES AND STEPS?
Henk L.M. Granzier, Alicia R. Mattiazzi and Gerald H. Pollack, Center for Bioengineering, University of Washington, Seattle, WA 98195

If the load on a tetanized fiber is quickly changed, the ensuing muscle length signal shows transients. A.F. Huxley (1) suggested that these transients relate to stepwise sarcomere shortening. We tested this by quickly changing the load and measuring the sarcomere length, using two independent methods, employed simultaneously. Single semitendinosus fibers from the frog Rana temporaria were used. Sarcomere length was measured (i) by optical diffraction; and (ii) by measuring the distance between thin cat hair markers attached to the upper fiber surface, 200-500 μm apart.

The muscle length signal typically showed a single transient; the temperature and load dependence was similar to described before (2,3). The low velocity phase of this transient showed up as a pause in sarcomere shortening, with both diffraction and segment length methods. In 9 out of 32 fibers, the first transient was followed by a second one. In each case the low velocity phase occurred simultaneously with a pause in sarcomere shortening. Occasionally, pauses in the laser diffraction signal or segment length signal occurred without corresponding muscle length transient. It is concluded that quickly changing the load synchronizes fiber dynamics; all sarcomeres along the fiber first shorten with high speed and then stop shortening for some time. In some regions of the fiber this synchrony persists, and additional sarcomere length pauses can be detected. If the region over which synchrony is maintained constitutes a large enough fraction of the fiber, more than one transient may show up in muscle length.

(1) Huxley, A.F., 1986. Circ Res., 59, pp. 9-14.
(2) Civan & Podolsky, 1966. J. Physiol., 184, pp. 511-534.
(3) Sugi & Tsuchiya, 1981. J. Physiol., 319, pp. 219-238.

W-Pos136 MECHANICAL MEASUREMENTS ON SKINNED MUSCLE FIBRES FROM BALANUS NUBILUS. Griffiths, P.J., Bedford, L.A. & Ashley, C.C. Univ. Laboratory of Physiology, Parks Road, Oxford, OX1 3PT.

Barnacle muscle fibres have been used for x-ray diffraction measurements and calcium indicator studies, but little is known of their mechanical properties. Step length changes (step time <1 ms) were imposed on myofibrillar bundles from B. nubilus whose sarcomere length was determined as 9 μm by laser diffraction. Force was measured by an AE801 force transducer (sensitivity 122 $mV.mN^{-1}$, resonance frequency 3.8 kHZ) in order to obtain a plot of length step versus tension change (T_1 curve). Extrapolation of the curve for small stretches to zero force gives an intercept (y_o) of 0.4% on the length axis which is less than half that obtained for skinned frog muscle fibres under the same conditions. The half-time of the quick recovery of force after the step was comparable to that of frog muscle, although the actomyosin ATPase activity of barnacle muscle is 5 fold lower than that of vertebrate muscle (Hasselbach, W. 1966, Ann. N.,Y. Acad. Sci. 137, 1041-1048). This has also been reported for Limulus muscle (Kuhn, H.J., Kulik, R., Winker, H. & Pferrer, S. 2985, J. Muscle Res. & Cell Motl., 6, 106). The maximum shortening velocity in barnacle is 0.24 muscle lengths/sec. compared to 2 muscle lengths/sec for frog. These findings are consistent with the view that the cross-bridges are the main source of compliance in a contracting muscle fibre. Barnacle muscle, having long myofilaments, should therefore have proportionally smaller values for y_o. Furthermore, the rapid recovery of tension observed in barnacle fibres following a length step suggests that their low actomyosin ATPase activity may not due to a slow 'power stroke', but to some other step in the cross-bridge cycle. Supported by the MRC & NIH.

W-Pos137 IONIC STRENGTH DEPENDENCE OF RIGOR TENSION IN MECHANICALLY SKINNED MUSCLE FIBRES OF BALANUS NUBILUS. P.J. Griffiths, N. Stoneham and C.C. Ashley. University Laboratory of Physiology, Parks Rd, Oxford OX1 3PT, UK.

At physiological ionic strength in the absence of Ca^{2+} and ATP, skinned barnacle muscle (100-200μm diam) fibres do not develop rigor tension. When the ionic strength of the rigor solution is reduced to 5mM (1mM EGTA, 6mM TES, 3.7mM K+), tension development occurs. We have investigated the dependence of rigor tension and fibre stiffness on ionic strength. Stiffness was determined from force responses to length steps (step time 700μs). Glucose (1mM and hexokinase (30 $units.ml^{-1}$) were included in rigor solutions to ensure removal of residual ATP. On elevation of the ionic strength by addition of either KCl, bis (2-hydroxyethyl) dimethyl ammonium chloride or TES/EGTA solution resulted in a rapid and reversible loss of tension which was 90% complete at an ionic strength of 40mM. Fibre stiffness and diameter remained unchanged over this range of ionic strength variation. The quick recovery of tension (T_2) following a length step was almost absent in rigor solutions, and the stiffness to tension ratio was 2.5x bigger than that obtained in Ca^{2+} activation. Addition of Ca^{2+} to rigor solutions of physiological ionic strength did not induce rigor tension. On restoration of ATP at physiological ionic strength, preparations showed normal Ca^{2+} sensitivity. This suggests that rigor tension at low ionic strengths is not due to the loss of some Ca^{2+}-dependent regulatory component. The results are consistent with two reversible states of rigor crossbridge attachment, one associated with force, the other not, and where force generation occurs as a result of a reduction of electrostatic screening between charged sites. (Supported by the NIH, MDA & MRC Support).

W-Pos138 TIME RESOLVED MEASUREMENTS OF FREE Ca^{2+}, X-BRIDGE MOVEMENT & FORCE IN INTACT, ISOLATED B. NUBILUS MUSCLE FIBRES. C.C. Ashley, P.J. Griffiths, Y. Maeda* and J.D. Potter+. University Laboratory of Physiology, Parks Road, Oxford. OX1 3PT, EMBL (DESY) Hamburg* and Dept. Pharmacology, University of Miami, FL 33156.+

Isolated, intact arthropod muscle fibres provide a valuable preparation for time resolved Xray diffraction studies (Ashley et. al. 1986). However, in these experiments it is important to know the relation between sarcomere length and isometric force. Intact single muscle fibres from B. nubilus were pressure injected with the calcium sensitive photoprotein aequorin. The relation between mean sarcomere length determined by laser diffraction, aequorin light emission (free Ca^{2+}) and force development was studied. Despite myofilament length variability in this preparation (Hoyle et al., 1973), there is nevertheless a distinct maximum force development between 8 to 10μm. The aequorin light emission on the other hand is much less dependent on sarcomere length. At 8 to 10μm, isometric tensions of up to 600kN.m^{-2} can be developed and a marked change in intensity, recorded with a 1D detector, of the first actin layer line (axial spacing 38nm and laterally at 12.5nm) can be interpreted in terms of cross-bridge movement. The half-time of this intensity change precedes that of force development by 80 ms while that of the deconvoluted aequorin response leads force by 174ms at 11-13°C. Supported by M.R.C., M.D.A. and N.I.H. grants.

References.

Ashley, C.C., Griffiths, P.J., Maeda, Y, and Potter, J.D. (1986) J. Physiol Abstract, Oxford.
Hoyle, G., McNeill, P.A. & Selverston, A.I. (1973). J. Cell Biol. 56, 74-91.

W-Pos139 LASER FLASH PHOTOLYSIS OF CAGED-ATP IN SKINNED MUSCLE FIBRES FROM BALANUS NUBILUS. I.P. Mulligan, P.J. Griffiths, C.C. Ashley. University Laboratory of Physiology, Oxford OX1 3PT. U. K. and NIMR, Mill Hill, London, U.K.

The development of an inert photolabile precursor of ATP, P^3-1 (2-nitro) phenyl ethyl adenosine 5'-triphosphate (caged -ATP), has enabled the study of the reaction kinetics of the force generating system in skinned muscle fibres (Goldman, Hibberd, McCray and Trentham (1982), Nature 300 701). These observations have been extended to crustacean muscle and the preliminary results of experiments using this compound in mechanically skinned fibres from Balanus nubilus are reported. Rigor tension was not altered by the addition of 4mM caged -ATP. The muscle was illuminated by a pulse of laser light (100 mJ in 200 msec at 347nm). In the presence of calcium, tension increased to at least 90% of the level resulting from activation in a solution containing calcium (pCa 3.8) and Mg-ATP (2mM). The rise of tension was exponential with a rate constant of ca. 5 sec^{-1}. In the absence of calcium tension decreased biphasically suggesting protein cooperativity. Thus the response of barnacle muscle is qualitatively similar to that of rabbit skeletal muscle. The rate of tension rise is slower (rate constant 5 sec^{-1} cf. 28 sec^{-1} in rabbit (Firenczi, Homsher and Trentham, 1984) consistent with the slower steady state ATPase rate and the results of experiments with imposed mechanical transients where the rate of tension recovery from a 2% release; sufficient to discharge isometric tension, had a $T1/2$ 335 msec at +7°C. (rate constant 2 sec^{-1}) in barnacle. (MRC & NIH Support).

W-Pos140 TIME-RESOLVED MEASUREMENTS OF FILAMENT LATTICE SPACING IN RABBIT PSOAS MUSCLE FIBRES FOLLOWING RAPID PHOTOGENERATION OF ATP FROM CAGED-ATP. Ferenczi, M.A.*, Goody, R.S.@, Irving, M.,+ Maeda, Y.,$ Peckham, M.,+ Poole, K.J.V.@ & Rapp, G.@ * National Institute for Medical Research, Mill Hill, London. @Department of Biophysics, Max Planck Institut fur Medizinische, Heidelberg. +Department of Biophysics, King's College London. $European Molecular Biology Laboratory, Deutsches Electronen Synchrotron, Hamburg.

Rapid release of ATP in rigor fibres by flash photolysis of caged-ATP produces synchronised transitions within the crossbridge cycle. The structural basis of these transitions has been studied by X-ray diffraction (Goody et al. (1985) J.Physiol. 364, 75P) and birefringence measurements (Irving et al, this meeting). Birefringence is sensitive to crossbridge orientation but also depends on the fractional volume occupied by contractile filaments and thus on their transverse spacing. We have used time-resolved X-ray diffraction to monitor the spacing following ATP release under the conditions used for the birefringence measurements. Bundles of about 50 demembranated fibres were initially in rigor in a solution containing 5mM caged-ATP, 5mM EGTA, 10mM imidazole, 3.3mM $MgCl_2$, 30mM reduced glutathione, ionic strength adjusted to 0.1M with potassium propionate, pH7.0; temperature 25°C, sarcomere length 2.6μm. A pulse of UV light produced photolysis of caged-ATP followed by rapid mechanical relaxation with no detectable change in d_{10}, although a change of about ½% would have been resolved. Similarly, no change in d_{10} was detected when isometric contraction was initiated by photolysis of caged-ATP in the presence of calcium (pCa 4.5). Thus the birefringence changes recorded under these conditions are likely to be produced by changes in crossbridge orientation rather than in lattice spacing.

W-Pos141 A MODEL OF THE FORM BIREFRINGENCE PROPERTIES OF MUSCLE. F. D. Carlson, R. C. Haskell* and P. S. Blank. Depts. of Biophysics, Johns Hopkins Univ., and Physics, Harvey Mudd College.

The theory of form birefringence for a multi-component system is used to model the birefringence of muscle. Mylofilament structures are approximated by a suspension of dielectric ellipsoids in a dielectric solvent. The ith species of ellipsoid is assigned a set of dimensions, a refractive index and an orientation distribution function. The birefringence of the system, B, is developed from its bulk refractive index, n, given by: $(n^2 - 1) = \Sigma f_i(n_i^2 - 1)(E_i/E_o)/\Sigma f_i (E_i/E_o)$; f_i and n_i are respectively the volume fraction and refractive index of the ith ellipsoid, E_i/E_o is the ratio of the field inside the ith ellipsoid, E_i, to the applied field, E_o. For E_o parallel or perpendicular to the fiber axis, the corresponding values of n are $n_{\parallel}$ and $n_{\perp}$ respectively and $B = (n_{\parallel} - n_{\perp})$. The modeled mylofilament structures were developed from published data to obtain approximate values for f_i, n_i, and the dimensions of the thick and thin filaments and the S1 and S2 subfragments of myosin. Using Osborne's tables (Phys. Rev. **67**:351-257) values of (E_i/E_o) were determined for each component of the model on the assumption that S1 and S2 are rigid ellipsoids. These values of (E_i/E_o) were used in the above equation to evaluate $n_{\parallel}$, $n_{\perp}$ and B for selected orientation distributions of S1 and S2. Rotation of S2 away from the fiber axis by 15° diminished B by 2%. Rotations of S1 from its long axis parallel to its long axis perpendicular to the fiber axis systematically reduced B from 2.00×10^{-3} to 1.00×10^{-3}. If, however, S1 and S2 only change their shape, i.e., from a prolate ellipsoid to a sphere or oblate ellipsoid at constant volume, B also changes its value. Supported by USPHS AM12803 to F.D.C.

W-Pos142 THE FILAMENT LATTICE OF VERTEBRATE STRIATED MUSCLE. MODELLING FILAMENT POSITION AND CROSS-BRIDGE MOVEMENT. Thomas C. Irving and Barry M. Millman, Biophysics Interdepartmental Group, Physics Department, University of Guelph, Guelph, Ontario, N1G 2W1, Canada.

We have used improved procedures to refine Fourier reconstructions of the equatorial X-ray diffraction patterns from vertebrate striated muscle in the relaxed, rigor and contracting states. In particular, we have studied the effects of lattice disorder: both overall disorder and disorder in the thin filaments only, and the effects of a limited lattice. This has resulted in an improved fit to experimental data. Our modelling consistently supports the phasing choice of + + - - + for the first five observable orders from relaxed muscle; the choice used by Haselgrove et al. (Nature 1976, 261:606), in contrast to that used by Yu et al. (Biophys. J., 1985, 47:311). New X-ray diffraction patterns have been obtained using a new two-dimensional, TV-based X-ray detector which was designed and built for us by K. Kalata of Brandeis University (Nucl. Instr. Methods, 1982, 201:35). Using the new modelling calculations, we have compared filament sizes and crossbridge positions to changes in the position of the charge on the thick filaments inferred previously from studies on the swelling and shrinking of the filament lattice in osmotic stress experiments.

W-Pos143 DOES THE HUXLEY-SIMMONS THEORY ALLOW THE CROSSBRIDGE TURNOVER IN ISOMETRIC CONTRACTION ? Tsukasa Tameyasu, Department of Physiology, St.Marianna University, Japan (Present address: Center for Bioengineering, WD-12, University of Washington, Seattle, WA 98105.)

Suppose that there is a steady turnover of the crossbridges (XBs) at the plateau of isometric contraction, it is deduced from the equilibrium condition that the rate constant K_i for the reaction from i-th position to the next in a series of the tilting steps of the XBs is inversely proportional to N_i, the number of the XBs at the i-th position (no backward reaction is considered): $K_i \propto 1/N_i$. Since the Huxley-Simmons theory assumes the increase in the activation energy barrier as the increase of x, the extension of the elastic element in the XB, the rate from one position to the next in a series of the tilting steps decreases as the progress of the tilting steps, giving a monotonically increasing function for N(x), which represents the number of the XBs with x. However, such a monotonically increasing N(x) cannot explain the recent results of the quick length change experiments by Huxley group. They suggest that the length reduction of ~4 nm/half sarcomere is enough to reduce the tension in the XBs to zero while the complete tilting of the XB head stretches the elastic element by more than 12 nm. To explain their results, it is necessary to assume either a monotonically decreasing N(x) or N(x) with a complex form. To overcome this dilemma, the Huxley-Simmons theory requires either the detachment of the XBs on the way in a series of the tilting steps or no detachment of the XBs in isometric contraction. It will be considered which one of the above two cases satisfies the bulk of the present knowledge.

W-Pos144 OPTICAL STUDIES OF VARIATION IN A- AND I-BAND WIDTH

David H. Burns, Ammasi Periasamy, Dale N. Holdren, and Gerald H. Pollack
Center for Bioengineering, WD-12, University of Washington, Seattle, WA 98195

We describe optical microscopic studies, using advanced digital image processing techniques, of A- and I-band widths. Data were obtained from single intact frog skeletal muscle fibers using polarization microscopy. Images were collected with a vidicon camera, stored on an LSI-11/23 computer and subsequently processed and analyzed. To minimize aberrations caused by imperfections in the optical illumination and collection systems, a background subtraction method was employed. Likewise, to allow estimates of A- and I-band widths with resolution near the optical diffraction limit, digital deconvolution was used. The transfer function of the optical system was determined by imaging a step object and modeling the image with a combination of a Bessel and Gaussian function. This transfer function was used for image restoration. Deconvoluted images demonstrated better distinction of fine structure than unenhanced images. Noise was reduced by summing the striations perpendicular to the fiber axis. To ensure band skewing did not broaden the summed striation pattern, images were straightened with a cross correlation algorithm. Finally, characteristic band widths were determined as distance between midpoints of adjacent A- and I-band maxima and minima. Images were obtained from fibers initially stretched and allowed to shorten at approximately 0.1 sarcomere lengths per second. Measurements from unstimulated fibers confirm expected dimensional changes in both A- and I-band widths. However, measurements of actively contracting fibers seem to indicate dimensional changes in both A- and I-bands with changes in sarcomere length. We are currently investigating whether these changes are influenced by shortening velocity and microscopic methodology, or reflect genuine variations in thick filament length.

W-Pos145 CHANGES OF THIN FILAMENT BASED X-RAY DIFFRACTION PATTERNS DURING CONTRACTION OF LOBSTER MUSCLE

D.POPP, Max Planck Institute for med. Research, Heidelberg
and Y.Maeda, EMBL Outstation at DESY Hamburg, Fed.Rep.Germany.

The lobster muscle gives rise to X-ray diffraction patterns on which the thin filament associated layer-lines are well seperated from the myosin layer-lines (J.Wray et al.,1978). Moreover, since fibres are parallel within a flat thin muscle, artefacts of movement can be minimized.

Medial superficial abdominal extensor muscles of lobster were stimulated with a sinusoidal bipolar external electric field, producing a tension of up to 3 kg/cm^2. The synchrotron radiation from DORIS incidents the X-ray optics X-33. X-ray diffraction patterns were either recorded with a fast linear detector (J.Hendrix et al.,1982) or on "Imaging Plate" (K.Miyahara et al.,1986).

By measuring the axial width of the 59 A layer-line recorded on Imaging Plate, the extent of disordering of thin filaments were estimated, and the layer-line intensities were corrected for the sharpening effect which is associated with activation. On activation at a sarcomere length of 10μm and at a temperature of 12°C, the intensity of the first layer-line (at 380 Å axially and 0.007 - 0.008 Å^{-1} laterally) increased by about 50%, whereas the 59 a layer-line increases by about 5%, compared to the resting level. Although the big increase of the first layer-line has been observed in other arthropod muscles (Y.Maeda et al.,1986 , C.Ashley et al.,1986) the seperation of the layer line from the equator is significantly better in this muscle. The 51 Å layer-line was also intensified on activation. The meridional actin reflextion at 27.3 Å increases substantially both in intensity and in lateral width, which is likely due to conformational change of actin subunits.Among reflexions assignable to troponin repeat at least the 380Å meridional reflexion increases by a factor of two. Supported party by MDA.

W-Pos146 X-RAY DIFFRACTION STUDY OF THE STRUCTURAL CHANGES ASSOCIATED WITH PHOSPHORYLATION OF TARANTULA MUSCLE THICK FILAMENTS.

Sosa, H.; Pantē, N. & Padrón, R. Laboratorio de Biofísica del Músculo, IVIC-BIOFISICA, Apdo. 21827, Caracas 1020-A, Venezuela.

Electron microscopy of negatively stained thick filaments of tarantula muscle reveals that regulatory light chain (LC) phosphorilation is accompanied by loss of the helical ordering of the myosin heads and that the heads sometimes proyect away from the filament backbone (Craig, Padrón & Kendrick-Jones, Biophys. J. 47:469a). This disordering implies a mass movement in the transverse section of the filaments, which we have detected through the equatorial section of the X-ray pattern. We have obtained equatorial X-ray patterns of Avicularia sp. muscles in the relaxed state (LCs non phosphorylated) and in the phosphorylated state (in the absence of calcium) by using a calcium-insensitive myosin light chain kinase (MLCK). The phosphorylation was achieved in the presence of 1 mM ATP-γ-S to produce an irreversible thiophosphorylation of the LCs. The phosphorylation of the LCs was determined by urea/glycerol gel electrophoresis. Equatorial patterns showed a decrease in the intensity of the (10) reflection and an increase in (11) and (20) after phosphorylation. In the bidimensional electron density maps obtained from the Fourier synthesis using these three reflections it was possible to obtain the mass distribution in the hexagonal lattice and the change that occurs after phosphorylation. The electron density maps show that there is an decrease in mass distribution in the surface of the thick filaments. Supported by the Muscular Dystrophy Association MDA (to R.P.) and CONICIT (to R.P. Proyect S1-1460 and fellowship to N.P.)

W-Pos147 EQUATORIAL X-RAY DIFFRACTION FROM FULLY Ca^{++} ACTIVATED SINGLE MUSCLE FIBERS AT LOW IONIC STRENGTHS I.C. Yu† and R. Brenner*. †NIAMS, NIH; and *University of Tubingen, FRG.

It was shown that in rabbit psoas muscle, crossbridges are attached in the relaxed state at low ionic strength (μ) and low temperature (Brenner, et al., 1982; Brenner, et al., 1984). The crossbridges attached in the relaxed state correspond to the weak binding states of the actomyosin ATPase in solution. It has been suggested that force is generated by a transition from the weak to the strong strong binding states. The present study investigated what structural changes, if any, are associated with this transition in Ca^{++} activated fibers. Equatorial X-ray diffraction patterns were obtained from relaxed, rigor and fully Ca^{++} activated single skinned rabbit psoas fibers. To compare structures of the crossbridges attached in weak and strong binding states, relaxed and active patterns were recorded between μ =50-120mM, where a significant fraction of crossbridges are attached in both states. Upon activation, the order of the myofilament lattice was maintained sufficiently such that 5 reflections were discernible. Preliminary data showed that as μ decreased from 120 to 50 mM, force level increased by ~50%, and the intensity ratio I_{11}/I_{10} increased from 2.2 to 2.8. In general, there was a proportionately greater change in I_{10} than in I_{11} upon activation. At μ=50mM, I_{11} was within 10% of the relaxed value, while I_{10} decreased 35%. Previously we showed that increasing the number of crossbridges attached in the relaxed state due to lowering the ionic strength caused a greater change in I_{11} than in I_{10}. Therefore, the significantly greater decrease in I_{10} upon activation cannot be attributed to an increased number of crossbridges in the relaxed attachment configuration. More likely, there is a change in the attachment configuration accompanying generation of active force. Comparing the active with the rigor patterns suggests that there might be further structural changes in the ATPase cycle. Work is partially supported by NATO grant 769/85.

W-Pos148 EFFECTS OF LIMITED RESOLUTION ON DENSITY MAPS RECONSTRUCTED FROM EQUATORIAL X-RAY DIFFRACTION INTENSITIES OF SKELETAL MUSCLE Leepo C. Yu. NIAMS, NIH.

X-ray diffraction from skeletal muscle has been instrumental in providing information on mass distributions within the myofilament lattice. Recently five equatorial reflections have been used to reconstruct 2-dimensional maps of densities projected along the fiber axis (Yu, et al., Biophys.J.1985). With various phase combinations, some of the density maps showed prominent six-fold symmetry of the thick filament. However, the spatial resolution of these maps is limited at ~ 130 Å. Objects with sizes less than 130 Å will be smeared to appear larger than their actual sizes, with their peak densities lowered. Furthermore, artifacts might be introduced in the density maps due to effects introduced by terminating Fourier series in the inverse transform at five reflections. To guard against such factors in interpretation of experimental data, model calculations were carried out which included effects of series termination. In the models, mass distributions were assumed to be centrosymmetric. The unit cell contained a cylindrical thick filament backbone, an annulus of mass surrounding the backbone, and two thin filaments. Series termination was introduced by setting reflections beyond the first five reflections to zero by a smooth function in the reciprocal space. Inverse Fourier transforms were then calculated based on the five remaining reflections. The density maps thus obtained showed that series termination could introduce spurious structural details not included in the original distributions. Apparent six-fold symmetry for the mass surrounding the backbone appears even though the original distribution is uniform. Conversely, an original distribution with six-fold symmetry resulted in a relatively uniform distribution. Modelling also showed that phases associated with each reflection are affected by the radial position of the annular mass surrounding the backbone. The results are not significantly affected by the specifics of the models.

W-Pos149 BACKBONE ORGANIZATION OF SKELETAL MUSCLE MYOSIN FILAMENTS. F. Ashton, J. Weisel, C. Street and F. Pepe. Dept. of Anatomy, Univ. of Penn. Phila. PA 19104.

The backbone structure of the myosin filaments of chicken pectoralis muscle was studied under different conditions. Images of transverse sections of the filaments were analysed by Fourier based rotational filtering as described previously (Pepe et al. Tissue and Cell 18, 499-508, 1986). In all cases the myosin filaments were completely overlapped by actin filaments. Skinned fibers were fixed in the presence of either a) 1 mM AMPPNP, 1 mM EGTA, 3 mM $MgCl_2$, 1 mM DTT, 10 mM imidazole, pH 7.0, b) 5.44 mM ATP, 25 mM EGTA, 7.7 mM $MgCl_2$, 10 mM glutathione, 100 mM TES, pH 7.1., or c) 25 mM EGTA, 7.7 mM $MgCl_2$, 10 mM glutathione, 100 mM TES, pH 7.1. Three different portions along the length of the filament were studied, i.e. the bare zone to C-protein bearing region (C-region), the C-region and beyond the C-region. Two major categories were identified for the arrangement of the 9 subfilaments observed in transverse sections. Category 1 consisted of three central subfilaments and three pairs of subfilaments on the surface with a pair at each apex of the triangle formed by the central subfilaments. In category 2 the three pairs were located at each side of the triangle formed by the three central subfilaments. In the presence of solutions (b) and (c) above, a modification of the category 1 arrangement, with the pairs of subfilaments shifted slightly out of alignment with the three central subfilaments, was also observed. A third category in which all nine subfilaments were on the surface of the filaments probably represents a partially disrupted or altered subfilament arrangement. These different arrangements were observed in all three portions of the filament but the relative representation was different in different portions of the filament as well as under the different conditions studied.

W-Pos150 RIGOR CROSS BRIDGES ARE DOUBLE HEADED Frederique Bard, Clara Franzini-Armstrong and Wallace Ip. Depts. of Biology and Anatomy, University of Pennsylvania; Dept. of Anatomy, University of Cincinnati.

Negative staining of partially decorated actin filaments in vitro shows that the two heads of a myosin molecule can either interact with adjacent monomers of an actin filament (double headed X-bridge, Craig, et al., J. Mol. Biol., 140, 35, 1980), or cross link two actin filaments (single headed X-bridge, Trinick and Offer, J. Mol. Biol., 133, 549, 1979). Rigor X-bridges formed in intact myofibrils are large enough to be double headed (Varriano-Marston, et al., J. Muscle Res., 5, 363, 1984; Taylor, et al., Nature 310, 285, 1984), but the two heads have not been resolved. We compared rigor X-bridges in glycerol extracted crayfish fast adductor muscle (using deep etching rotary shadowing) with those in "natively decorated" thin filaments from the same muscle fibers (using either negative staining, or freeze-drying on mica and rotary shadowing). "Natively decorated" thin filaments were obtained by dissociating the backbone of the myosin filaments of rigor myofibrils in 0.6 M KCl. The X-bridges on the natively decorated actin maintain the original spacing and the disposition in chevrons and double chevrons for several hours, indicating that no rearrangement of the acto-myosin interactions occurs. Thus the natively decorated filament's X-bridges were formed within the geometrical constraints of the intact myofibril. The majority of X-bridges in the intact muscle have the triangular shape indicative of a double headed X-bridge. Negative staining of the natively decorated actin filament resolves the individual heads and shows that "native" rigor X-bridges are double headed. The X-bridges are attached at a uniform acute angle. Unlike those in insect flight muscle (Taylor, et al., 1984), lead and rear elements of the double chevron may both be double headed. Deep etched images also reveal a long pitch helical arrangement of subfilaments in the thick filament backbone.
Supported by NIH HL-15835 to PMI.

W-Pos151 STRUCTURAL STUDIES OF RIGOR CROSS-BRIDGE ORIENTATION Károly Trombitás, Peter H.W.W. Baatsen, and Gerald H. Pollack. Center for Bioengineering, University of Washington, Seattle, WA 98195

It is generally thought that the rigor state represents the final phase of the cross-bridge cycle. Thus, the rigor cross-bridge angle can provide clues about the contractile mechanism. Rigor bridge orientation of insect flight muscle (Honeybee, *Apis mellifera*) was investigated under three different conditions: (a) muscles were stretched in life by various degrees, then transferred to rigor solution; (b) relaxed muscles were slightly stretched, transferred to rigor solution, then stretched again until broken, whereupon they shortened and became slack; (c) stretched in rigor until the thin filaments broke in some sarcomeres. In the presence of resting tension (a) bridges were either perpendicular to the filament axis, or tilted towards the M-line (rigor position). In broken muscle (b) which was slack, rigor bridges remained perpendicular, or tilted oppositely, toward the Z-line (anti-rigor position). Thus, rigor bridge angle appears to depend on the "state" of the thick filament. With the thick filament under stress, the angle may be quite different than at slack length. Whether this effect is "physiological" or artifactual remains to be determined. On the other hand, external force applied directly to the rigor bridges (c) did not change their configuration. The rigor bridge angle remained unchanged, irrespective of the amount of tension applied to the bridges. This implies that a very tight bond exists between the rigor bridge and thin filament, allowing essentially no rotation--even with large applied force. Thus, tension applied directly to rigor bridges does not influence the bridge angle, whereas tension applied to the thick filament shaft may have an important influence.

W-Pos152 THE ULTRASTRUCTURE OF CONTRACTING SINGLE FIBERS Peter H.W.W. Baatsen, Károly Trombitás, and Gerald H. Pollack. Center for Bioengineering, University of Washington, Seattle, WA 98195

Single fibers of Rana temporaria (frog) tibialis anterior muscle were stimulated electrically and allowed to shorten by different amounts. Tension was measured using a strain gauge. Specimens were prepared for electron microscope in several different ways: fibers were fixed chemically by bringing either glutaraldehyde, mercuric chloride, or osmium tetroxide onto the fiber, after which the fibers were embedded in araldite and ultrathin-sectioned; or fibers were mounted in a dual propane jet freezing device and subsequently deep-etched, fractured and replicated, or freeze-substituted. Sarcomeres of fibers allowed to shorten to ca. 2 μm are hard to recognize in freeze-fracture replicas. However, if shortening was terminated at 2.5 μm, well established features such as Z-lines, M-regions, H-zones and overlap zones of thick and thin filaments were easily discerned. In the H-zone, lateral structures (myosin heads), protruding from adjacent thick filaments, sometimes appeared to touch each other and form lateral interconnections. Lateral projections were also observed in filaments of the I-band. Experiments using the above-mentioned methods are in progress.

W-Pos153 **RELAXATION AND ACTIVATION OF SKELETAL MUSCLE FIBERS BY ATPγS AND BY PHOTOLYSIS OF CAGED ATPγS.** J.A. Dantzig+, J.W. Walker*, Y.E. Goldman+ & D.R. Trentham*. Dept. of Physiol+. School of Med., Univ. of Penna., Phila., PA 19104 and Nat. Inst. Med. Res., Mill Hill*, London NW7 1AA, U.K.

ATPγS (Adenosine-5′-O-(3-thiotriphosphate)) interacts with myosin and actomyosin in a manner similar to that of ATP but ATPγS-induced detachment of actomyosin is 10-fold slower (Goody & Hofmann, J. Musc. Res. Cell Motil. 1:101, 1980) and hydrolysis of ATPγS by myosin is 500-fold slower (Bagshaw et al. Cold Spr. Harb. Symp. Quant. Biol. 37:127, 1972). In the absence of Ca^{2+}, tension and stiffness (500 Hz) of glycerol-extracted fibers from rabbit psoas muscle were fully relaxed by 1 mM ATPγS. The transient tension rise observed on photolysis of caged ATP_3 was suppressed in relaxation from rigor following photolysis of caged ATPγS (P^3-O-1-(2-nitrophenyl)ethyladenosine-5′-O-(3-thiotriphosphate)). In the presence of Ca^{2+}, photolysis of caged ATPγS caused tension to decrease fully to the relaxed level while stiffness was maintained at ~30% of the rigor value. Increasing the Ca^{2+} concentration to ~30μM in fibers relaxed in ATPγS also resulted in development of stiffness without tension (Fig. 1). When Ca^{2+}-activated fibers in ATPγS were quick-stretched by 0.2-0.6%, tension declined with $t_{1/2}$=70-170 ms. These results show that attachment of cross-bridges into the low tension state, presumed to be AM.ATPγS, is sensitive to Ca^{2+}. Supported by NIH grant HL15835 to PMI and the MRC U.K.

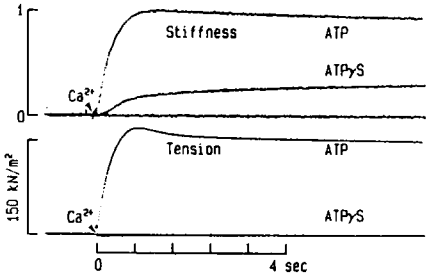

W-Pos154 THE FORCE RESPONSE TO PHOTOGENERATED ADP IN ISOMETRICALLY CONTRACTING GLYCERINATED RABBIT PSOAS MUSCLE FIBERS. J. W. Lacktis and E. Homsher, Dept. Physiology, School of Medicine, UCLA, Los Angeles, Ca, 90024.

Addition of ADP to maximally activated glycerinated skeletal muscle fibers increases the isometric force. To elucidate the mechanism of this effect, the time course of the rise of force following laser flash photolysis of caged ADP (P^2-1-(2-nitrophenylethyl adenosine-5′-diphosphate, c-ADP) to ADP in maximally activated isometrically contracting glycerinated muscle fibers was measured. The inset shows the results of photogenration of 1.0 mM (A) and 1.7 mM (B) ADP in a muscle fiber contracting at 10°C. After the laser flash, force rises exponentially at 12 s^{-1}. In the temperature range 4-20°C, the Q_{10} for this rate constant is ca. 3. Because the photolysis of caged AMP to AMP does not affect the isometric force, the photolysis by-products do not cause the force rise. The rate constant of the force rise is independent of the sarcomere length (at lengths >2.5 um) while the amplitude scales to the pre-flash isometric force. Although the extent of force rise is dependent on the concentration of photogenerated ADP, the rate constant of the tension rise is independent of [ADP]. This result suggests that ADP rapidly binds to rigor (AM) crossbridges (AM+ADP⇌AM•ADP) which does not cause a rise in force. The force rise may stem from an accumulation of an AM•ADP isomer, AM^+•ADP, exerting a force greater than AM•ADP. Since ADP addition to fibers in rigor does not increase the force, the AM^+•ADP crossbridge must be generated from ATP hydrolysis. Supported by USPHS grant AM 30988.

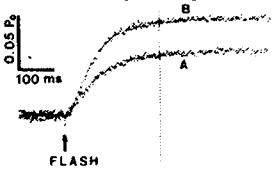

W-Pos155 RATE OF RELAXATION IN SINGLE SKELETAL MUSCLE FIBERS OF THE FROG AS A FUNCTION OF TETANUS DURATION AND TEMPERATURE. Tien-tzu Hou and Jack A. Rall. Department of Physiology, Ohio State University Columbus, OH 43210.

The Ca^{2+}-binding protein parvalbumin (PV) may function to promote muscle relaxation. Effects of PV would diminish progressively with increasing tetanus duration since PV fills with Ca^{2+}. The importance of PV might increase at low temperatures if the Q10 for the sarcoplasmic reticulum (SR) pump rate is greater than the Q10 for Ca^{2+} binding to PV. Rate of relaxation (y), determined as the reciprocal of time for force to fall from 95 to 80% of the value at the last stimulus, was determined as a function of tetanus duration at 0, 10 and 20°C in fibers from tibialis anterior muscles (n=11). y falls exponentially to a steady value, yf, with increasing tetanus duration. Data was fit to the equation: $y=yoe^{-bt} + yf$ where yo is the "extra" rate of relaxation at time t=0 and b is the rate constant for the effect. The following results were found: A) Relaxation rate slows to a steady value with increasing tetanus duration at each temperature. B) The relative magnitude of slowing of relaxation is largest at 0°C, i.e., yo/yo+yf x 100 is 63±3% at 0° (n=8), 33±5% at 10° (n=8) and 37±7% (n=4) at 20°C. C) The Q10 for relaxation in the 0 to 10°C range depends on tetanus duration, ranging from 2.2±0.2 (yo+yf) to 4.0±0.3 (yf). In the 10 to 20°C range the Q10 is independent of tetanus duration, 2.6±0.3 (yo+yf) and 2.4±0.2 (yf). One

W-Pos156 EFFECT OF ACTIVATION ON THE RELATION BETWEEN STIFFNESS AND TENSION IN SINGLE FROG MUSCLE FIBRES. M.A. Bagni, G. Cecchi and F. Colomo. Dipartimento di Scienze Fisiologiche. Università degli Studi di Firenze. Viale G.B. Morgagni 63. I-50134 Firenze. ITALY.

Stiffness was measured in single muscle fibres isolated from the lumbricalis muscle of the frog either during the tetanus rise or during the redevelopment of tension that occurs when shortening at zero load is suddenly stopped. The fibres were mounted between tension and length transducers and were stimulated tetanically for 0.8 s at regular four minute intervals at 4° C and at 2.2 um sarcomere length. Stiffness was measured by applying sinusoidal (5-6 kHz frequency) or step length changes to one fibre end and by measuring the resulting force at the other end. The measurements during the redevelopment of force were performed after 20 ms of shortening at Vmax. In some experiments the effects of the tendon compliance were eliminated by clamping a short fibre segment by means of a laser diffraction servo-system. Development of stiffness preceeded that of tension during the tetanus rise as well as during tension redevelopment, however the delay between stiffness and tension during the redevelopment of tension was about one half that found during the tetanus rise. The relation between relative stiffness and relative tension was the same either during the tetanus rise or during the tension redevelopment. Since the redevelopment of tension occurs presumably in conditions of full activation of the fibre these results suggest that activation may be only partially responsible for the delay between cross-bridges attachment and force generation.

W-Pos157 KINETICS OF HEAT PRODUCTION DURING SHORTENING AT SEVERAL VELOCITIES IN FROG MUSCLE AT 0 AND 10°C. Susan H. Gilbert, Dept. of Anatomical Sciences, SUNY at Stony Brook, Stony Brook, NY

At 0°C, frog muscles shortening at most velocities do not liberate energy at a constant rate, although power becomes stable after shortening less than 4% muscle length (Ford & Gilbert, J. Physiol., in press), which suggests a delay between the mechanical steady state and that of the cross-bridge cycle. To examine the phenomenon in more detail, tension and heat production were measured in frog (R. temporaria) sartorius muscles at 0 and 10°C. The muscles were stimulated for 3.5 s every 5 min. They began shortening (5% ML) after 2 s of isometric contraction at velocities from 0.2 to 2 ML/s. The following ratios of parameters were observed [(x at 10C)/(x at 0C)]: P_o, 1.2-1.3; a/P_o, 1.1; b, 2.2; V_{max}, 2.1; isometric heat rate, 3.5. Although the force maintained during shortening was higher at 10C than at 0C, the drop in force at the beginning of shortening was about the same (maximum of 15% less at 0.3 ML/s), which made the thermoelastic effects about the same at the two temperatures. At both temperatures thermoelastic heat was produced by the drop in tension at the beginning of shortening. Its attenuation by an early heat-absorbing process was more prominent at 10 than at 0C. At 0C most of the heat produced as a consequence of shortening appeared after shortening ended, especially at high velocities, while at 0C most of it evolved during shortening. At 0C heat rate became constant during shortening only at the lowest velocity (P/P_o 0.6), while at 10C it became constant during shortening at 1.0 ML/s (P/P_o 0.3). The results suggest that the delay between the mechanical steady state and the steady state of the cycle is shorter at 10°C than at 0°C and that it does not bear a simple relation to force or velocity.

W-Pos158 pH EFFECTS ON CONTRACTION OF FAST AND SLOW MUSCLE FIBERS. P.B. Chase and M.J. Kushmerick, Department of Radiology, Brigham & Women's Hospital, Boston, Massachusetts 02115

As a product of the myosin ATPase reaction, H^+ may significantly affect the cross-bridge cycle. Muscle intracellular pH can vary *in vivo* by more than one pH unit during activity; pH changes may be biphasic and depend on the relative contributions of the Lohmann reaction and anaerobic glycolysis. During prolonged activation, isometric force (F_{iso}) and unloaded shortening velocity (V_{us}) decline in fast vertebrate skeletal muscle, but do not change in slow muscle. Since other changes parallel altered pH *in vivo*, we used single glycerinated fiber segments from rabbit psoas (fast) and soleus (slow) muscle to study pH effects in an otherwise constant medium. pH was varied from 6.0 to 8.0 at constant ionic strength (200 mM) at 12°C.

At most pH levels, qualitatively similar results were observed in fully activated fibers of both fast and slow types: (1) F_{iso} increased with pH (but in slow fibers it decreased at pH 8.0). The total force change was ~50% of maximal force; (2) V_{us} was maximal at approximately neutral pH. The total change in velocity was ~50% of maximal velocity; and (3) Bode analysis of stiffness, using small (<0.05% L_o) sinusoidal length changes, showed that high frequency stiffness decreased relative to force with increasing pH, and high pH shifted oscillatory work to lower frequencies.

pH decrease is a factor in decreasing F_{iso}, as was the P_i increase reported last year. In contrast to the P_i effects, pH change from neutrality decreased V_{us}. Thus product inhibition by H^+ and P_i can be interpreted by a shift towards a greater fraction of attached low-force states of the cross-bridge cycle; however, pH affects more steps than does P_i.

Supported by NIH grants AM36813 and AM07783.

W-Pos159 MEASUREMENT OF CONSTANT CK FLUX IN GRADED STEADY-STATE STIMULATION IN SLOW-TWITCH SKELETAL MUSCLE. E.W. McFarland, J.M. Krisanda, T.S. Moerland and M.J. Kushmerick, Department of Radiology, Brigham & Women's Hospital, Boston, Massachusetts 02115

The metabolically active ADP concentration in striated muscle (11.5 μM, soleus, 30°C) is far below the K_m for creatine kinase (CK) measured *in vitro*. It is thus possible that the unidirectional reaction velocity will have a nearly linear relationship to small increments in [ADP]. The ^{31}P flux through CK between phosphocreatine (PCr) and γATP is a measure of this velocity, and can be determined by NMR spin transfer techniques. We studied blood-perfused cat soleus muscles (>92% slow fibers), which can be stimulated for long periods of time at levels of ATPase activity more than 10-fold higher than resting (as measured by O_2 consumption). The following results were obtained: (1) In stimulated muscle, [ATP] remained constant throughout the range of stimulations, PCr declined, and Pi increased stoichiometrically; (2) with increasing stimulation rate, the NMR-measured magnetization transfer rate constant (K_a) for PCr to γATP exchange was found to increase, tracking the increased ATPase activity and the NMR-measured [PCr] reduction; and (3) the net PCr to ATP exchange flux remained constant over the 10-fold increase in ATPase activity (flux = $(K_a \cdot PCr)/ATP$ = constant). This result is contrary to reports where the CK flux was found to vary significantly with changes in ATPase activity and PCr/ATP ratio in perfused heart. Our findings are thus inconsistent with the kind of requisite functional coupling between the mitochondria and myofibrils implied by the "PCr shuttle", but are completely consistent with the properties of CK in a homogeneous solution.

Supported by NIH grant AM36281.

W-Pos160 VELOCITY OF SHORTENING (V_{max}) AND MYOSIN HEAVY CHAINS (MHC) OF SINGLE FIBERS FROM EMBRYONIC, NEONATAL AND ADULT CHICKEN SKELETAL MUSCLE. Peter J. Reiser and Richard L. Moss, Dept. of Physiology, University of Wisconsin, Madison, WI 53706.

Previously, we reported that the mean V_{max} of skinned single fibers from the chicken red sartorius (RS) muscle is greater at neonatal compared to adult ages (Reiser, et al., Fed. Proc. 45 (3):453, 1986). This change in V_{max} correlates with a change in the MHC content of samples from the RS at the two ages as determined by SDS-PAGE. Specifically, the adult RS contains two MHC's that co-migrate on SDS gels with the two MHC's, SM1 and SM2, from the slow anterior latissimus dorsi muscle and a trace amount of a third MHC that migrates between the two major MHC's. The neonatal RS contains the same MHC's with the MHC migrating between SM1 and SM2 predominating in amount over the other two. Examination of the MHC content and measurement of V_{max} have now been extended to embryonic RS. The mean V_{max} of embryonic day 18 RS fibers is approx. 2.6 muscle lengths/sec (ML/s) compared to 1.9 ML/s and 0.9 ML/s for neonatal and adult fibers, respectively. The predominant MHC of the embryonic RS co-migrates with the major MHC of neonatal RS with only trace amounts of the SM1 and SM2 MHC's also being present. At each age examined, the fibers with the highest V_{max} also had the greatest amount of the MHC that migrates between SM1 and SM2. Thus, the mean V_{max} of the chicken RS undergoes a progressive slowing during development which is correlated with changes in the MHC content of the RS suggesting that the MHC is, at least in part, a determinant of V_{max}. Supported by NIH.

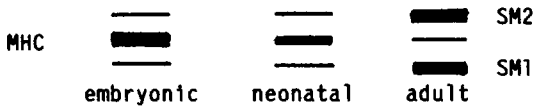

W-Pos161 ANOMALOUS EFFECT OF LOW pH AND HIGH IONIC STRENGTH ON RESTING TENSION OF SKELETAL MUSCLE. R. McCarter, J. Beverly & K. Wang†. Dept. of Physiology, Univ. of Texas Health Science Ctr., San Antonio & †Clayton Fndn. Biochem. Inst. & Dept. of Chemistry, Univ. of Texas at Austin

The functional roles of cytoskeletal matrix and contractile filaments in the generation of resting tension are the subjects of much current interest. It has been shown by several laboratories that either an increased hydrogen ion concentration or an increased ionic strength lead to decreased resting tension. We have observed that a combination of low pH and high ionic strength produced a marked increase in resting tension of mechanically skinned single fibers of rabbit psoas muscles. Under conditions of low pH (4.0 to 5.0) and high ionic strength (500 mM KCl), a highly reproducible generation of extra resting tension was observed. There were two components of the extra resting tension. Component 1 was generated by small degrees of stretch (<50% L_o) and was labile; i.e., it disappeared following an initial stretch-release cycle. Component 2 was present at large degrees of stretch (>70% L_o) and was stable; i.e., it was present in subsequent stretch-release cycles. The structures responsible for the extra resting tension are at present unknown.

W-Pos162 KINETIC ANALYSIS OF OSCILLATORY ACTIVATION OF INSECT FLIGHT MUSCLE FROM LETHOCERUS USING PHOSPHATE-WATER OXYGEN-EXCHANGE. J.Lund*, M.R.Webb+ & D.C.S.White*. *Department of Biology, University of York, York YO1 5DD, UK & +NIMR, Mill Hill, London, NW7 1AA, UK.
Sinusoidal length oscillations were applied to insect flight muscle fibers in the presence of Ca^{2+} over a range of frequencies at zero mean strain. Over the range of frequencies at which the fibers produced positive oscillatory work (2-9Hz, 21°C), the ATPase activity shows a single pathway of ATP hydrolysis as shown by the oxygen exchange in product Pi during ATP hydrolysis in an [^{18}O]water medium. At low (<1Hz) or high (>10Hz) frequencies, the fiber ATPase shows multiple pathways. In other experiments, step stretches and releases of a few percent strain were applied repeatedly to fibers. The cycles were repeated at a constant frequency, but the duration of the stretched phase was varied from 0 to 500ms. With low durations of the stretch phase (5-50ms), multiple pathways were seen, although the oxygen exchange was dominated (>90%) by a single high-exchange pathway. When the stretched phase was longer the fibers hydrolysed ATP by a single pathway (as seen in sinusoidally oscillated muscles). The overall ATPase activity, and the rate constant for Pi release measured by oxygen-exchange, increased with the duration of the stretch. The single pathway of exchange seen may be due to the uniform distortion of cross-bridges, reflecting the common periodicity of the thick and thin filaments in insect fibrillar muscle (Wray, Nature, 280, 325 1979). The single pathway of Pi release caused by even a relatively short stretch phase indicates a slow relaxation of the ATPase mechanism after a change of length. There is also a time-dependent effect on Pi release which may be due to a delay between applied stretch and a change in a strain-dependent rate constant, such as cross-bridge attachment affecting Pi release.
[Supported by the Medical Research Council of Great Britain, Grant G8326496CB.]

W-Pos163 METABOLIC ADAPTATION IN THE SKELETAL MUSCLE OF MICE INTOXICATED WITH A POORLY-METABOLIZED ANALOGUE OF CREATINE. T.S. Moerland and M.J. Kushmerick, Department of Radiology, Brigham and Women's Hospital, Boston, Massachusetts 02115.

Analogues of creatine are commonly used as *in vivo* probes of creatine kinase (CK) function. An implicit assumption is that treatment effects can be attributed primarily to kinetic manipulation of the CK reaction; however, the time necessary for incorporation of the analogue is sufficient for adaptive changes of several types to occur. One such analogue, β-guanidinopropionic acid (β-GPA), was administered via food and water to male CD-1 mice. ^{31}P-NMR spectroscopy of the hindlimb musculature showed that the concentration of phosphocreatine (PCr) at rest was reduced to < 5% of control values after 6 weeks. Pyrophosphate gel analysis showed a 50% decrease in the LC-3f homodimer of myosin in the predominantly fast-twitch EDL muscle of treated animals, and a 70% loss of fast-type myosin from the predominantly slow soleus. Activities of citrate synthase and cytochrome oxidase were 55% and 25% greater, respectively, in EDL of β-GPA mice, but were not significantly different in soleus. CK activity was unchanged in EDL, but decreased 50% in soleus of β-GPA mice. O_2 consumption of isolated muscles following a fused tetanus indicates that the metabolic cost of maintaining tension is approximately 50% lower in both soleus and EDL of analogue-treated animals. The monoexponential time constant of recovery O_2 consumption was not different for soleus muscles of β-GPA mice or controls (1.1 s), but decreased significantly (from 2.3 s to 1.2 s) in EDL. Administration of this analogue has effects similar to endurance training and chronic stimulation in inducing alterations in both contractile proteins and metabolic pathways of energy supply.

Supported by NIH grants AM36281 and AM07763, and by a grant from the Muscular Dystrophy Association.

W-Pos164 HIGH ENERGY PHOSPHATE UTILIZATION AND COMPARTMENTATION IN SKELETAL MUSCLE DETERMINED BY PHOSPHORYL LABELING WITH ^{18}O. R.J. Zeleznikar, R.M. Graeff, S.M. Dawis, T.F. Walseth, E.A. Butz & N.D. Goldberg (Intr. by D. Levitt) Dept. of Pharmacology, University of Minnesota, Minneapolis, MN 55455

The kinetics of ^{18}O labeling of phosphoryls of high energy phosphate-related intermediates were used to study the dynamics and compartmentation of energy metabolism in intact skeletal muscle. This was accomplished with resting or contracting rat diaphragms incubated in medium enriched with ^{18}O-water and subsequent measurement of rates of ^{18}O labeling of the phosphoryls of cellular 5'-nucleotides, creatine phosphate and orthophosphate (Pi). Incorporation of ^{18}O into the phosphoryls of interest results from enzyme-catalyzed hydrolytic cleavages and transfers of ^{18}O-labeled Pi and/or the ^{18}O-labeled γ-phosphoryl of ATP. In the intact cell metabolic recycling of these intermediates yields phosphoryls labeled with multiple atoms of ^{18}O and this time-dependent equilibrium labeling provides information on metabolic rates and size of the cellular compartment in which the metabolic process occurs. The labeling of the γ-phosphoryl of ATP and GTP and the phosphoryl of creatine phosphate proceeds at similar rates with sequential addition of ^{18}O rather than by multiple reversal reactions resulting in saturation with ^{18}O. These rates increase when the muscle is electrically stimulated to contract. Adenine nucleotide β-phosphoryl labeling identified by ^{18}O content to derive from the transfer of the γ-phosphoryl of ATP proceeds at a rate equivalent to less than 2% per min of total cellular ADP and ATP in non-contracting muscle. However in muscle stimulated to contract at a frequency of 2 per sec this β-labeling rate increases to 11% per min. In non-contracting diaphragm a discrete pool comprising less than 50% of the total cellular Pi is metabolically active but during contraction 100% of the cellular Pi becomes recruited to sustain the energy demands. Similarly, equilibrium labeling of the γ-phosphoryl of ATP indicates that a compartment(s) representing only 80% of the total ATP is utilized metabolically in non-contracting muscle compared to over 95% during contraction. Kinetic analysis of ^{18}O incorporation rates into the phosphoryls of these cellular components can be used to provide a direct estimate of high energy phosphate utilization rates in intact muscle with respect to a specific function such as contraction. GM28818.

W-Pos165 A NEW METHOD TO ATTACH SINGLE CARDIAC MYOCYTE TO TRANSDUCERS. Tatsuo Iwazumi, Dept. of Medical Physiology, University of Calgary, Calgary, Alberta, Canada T2N 4N1

Comprehensive investigations into the mechanics of cardiac myocytes have been hampered by the lack of a secure way for attaching the cell to the force and length transducers. A new method has been developed using silicone adhesive and a metal flake to form a sandwitch structure. Wetting force of the monomeric adhesive over the metal surface clamps the cell firmly then the adhesive hardens upon polymerization. It is now possible to utilize the full capability of the force and length transducers originally developed for single myofibril mechanics from nanograms to milligrams weight forces and from picometers to micrometers length changes over 50 KHz bandwidth. The minimum length between the two transducers is about 20 μm allowing a cell segment of only 10 sarcomere long to be tested.

Because of the extremely short segment length, it is possible to perform sarcomere compression as well as stretch. Preliminary tests on passive compression on single myocytes showed a sharp increase of stiffness below 1.6 μm sarcomere length causing the segment to buckle. The stiffness of the myocytes at longer sarcomere lengths was about an order of magnitude smaller than that of trabeculae of comparable size indicating that the characteristic stiffness of cardiac muscles resides in extracellular structures. Supported by Muscular Dystrophy Association.

W-Pos166 **EPR STUDIES OF MUSCLE CROSSBRIDGE ROTATIONAL MOTION USING CAGED ATP.** David D. Thomas, Eric C. Svensson, Todd L. Mitchell, Ben L. Etzkorn, and Piotr G. Fajer, Department of Biochemistry, University of Minnesota Medical School, Minneapolis, MN 55455.

We have used photolysis of caged ATP to obtain transient EPR signals from spin-labeled myosin heads in solution and in glycerinated muscle fibers. As in previous EPR studies, myosin heads were labeled with a maleimide spin probe, and saturation-transfer EPR was used to detect microsecond rotational motions. We have previously reported that ATP induces microsecond rotational motions of spin-labeled myosin heads in myofibrils and muscle fibers, but in these complex cycling systems, it is difficult to determine whether the motion is occurring when heads are attached to actin. To remedy this, we performed experiments on myosin heads covalently cross-linked to actin, and confirmed that ATP induces motions of these "attached" heads. In order to obtain analogous data on heads that are uncross-linked but still attached to actin in the presence of saturating ATP, we have performed STEPR on acto-S1 at very low ionic strength, at 200 micromolar actin. Sedimentation experiments showed that over half of the labeled S1 is bound to actin under these conditions. However, the ATPase activity is so high that only a few seconds are available for EPR data acquisition, not enough time to mix ATP with the viscous acto S1 solution and inject it into the spectrometer. Therefore, caged ATP was mixed with the sample in the dark, and approximately 1 mM ATP was produced by shining an intense pulse of UV light into the EPR cavity. This induced enough motion to indicate that active heads undergo submillisecond motions while bound to actin. These studies are being extended to muscle fibers.

W-Pos167 NEW METHODS FOR MEASURING THE MECHANICS OF FIBER CONTRACTION. E. Pate and R. Cooke, Math Dep, WSU, Pullman, WA 99163, and Dep. of Biochem/Biophys. and CVRI, UCSF, S.F. CA 94143

Estimates of the maximum velocity of contraction (Vmax) of active muscle fibers are commonly obtained by two methods. In one isotonic releases at nonzero loads generate a series of data points which are extrapolated to zero force (Vext) using the Hill equation to obtain Vext. In the other, Vmax is measured at zero load by applying a series of step decreases in length with the time taken to reach the new lengths used to calculate the slack velocity (Vs). A number of investigators have noted that Vs is greater than Vext. We have developed methods that allow easier and more accurate determination of these two parameters. Isotonic releases to very low loads are often not accurate due to drifts in the base line of tension transducers. This problem has been eliminated by applying a load clamp to a low load for 40 msec followed by a step decrease in length to slacken the fiber and determine the actual baseline. This technique allows reproducible load clamps to 1-5% of isometric tension (Po) eliminating much of the variability in Vext. Measuring Vs by standard methods resulted in variable values which exceeded Vext. The variability was due to a nonlinear, time-dependent fiber elasticity . The problem was circumvented by obtaining Vs in a single, continuous series of step changes in length in which a small rise in fiber tension initiated the next release (effective tension less than 1% Po). Finally, both the load clamps and the series of step changes in length must be obtained over the same time period following initial release because of nonconstant contraction velocity noted by Brenner (Basic Res Card 81:54, 1986). Following these protocols, Vs and Vext agree within 5%. Supported by the USPHS, AM30868 and HL32145 and NSF, DCB8641373.

W-Pos168 A NEW SPIN-LABEL ANALOG OF ATP AND ITS INTERACTION WITH MUSCLE FIBERS N. Naber and R. Cooke, Dept. of Biochem/Biophys and the CVRI, Univ. of California, San Francisco, CA. 94143
Paramagnetic probes have proved useful for measuring the orientation and motion of muscle cross-bridges. A major task associated with this technique is that of finding sites where spin probes can be specifically placed . Previous work has found that spin probes can be attached to either the 3' or the 2' position of ATP via an ester bond and that these analogs can then bind to myosin and support contraction. Two problems arise with these analogs: the ester bond isomerizes rapidly between the 2' and 3' positions and it does not support a hydrogen bond with hydrogen bond acceptors on the protein. These problems have been solved by changing the ester bond to an amide bond. The compound 3'(2,2,5,5 tetramethyl-3-pyrroline-1-oxyl-3-carboxyamido)-3' -deoxy ATP was synthesized by reacting succinimidyl-spin-label with 3'-amino-3'-deoxy ATP We have found that the diphosphate form of this analog binds to the myosin site of muscle fibers in a highly ordered array, showing that the ATPase site is well oriented in agreement with other nucleotide analogs. Competition with ADP shows that the analog binds with an affinity that is equal to that of ADP within experimental accuracy. The analog supports the contraction of soleus muscle fibers with tensions and contraction velocities that are similar to those for ATP. However, the analog is only a moderately good substrate for creatine kinase and is a poor substrate for myokinase and pyruvate kinase. Despite the fact that the analog is a poor substrate for some enzymes it will be an excellent tool for investigating muscle cross-bridges.
Supported by a grant from the USPHS: AM30868.

W-Pos169 THE ROTATIONAL DYNAMICS OF MYOSIN HEADS IN MYOFIBRILS AND FIBERS MEASURED BY TRANSIENT PHOSPHORESCENCE ANISOTROPY
R. D. Ludescher, P. G. Fajer, and D. D. Thomas. Department of Biochemistry, University of Minnesota Medical School, Minneapolis, 55455.

We have labeled myosin in glycerinated muscle fibers with the phosphorescent probe eosin-5-iodoacetamide. ATPase activities, dye/protein ratios, and PAGE gels of the labeled fibers indicate that the probe is predominantly located on a specific sulhydryl (SH1) on myosin S1. The transient phosphorescence anisotropy, measured using both analog and digital signal detection, has time resolution ranging from 50 ns to hundreds of milliseconds with a dead time due to transient PMT gating of 200 ns.

The anisotropy decay of eosin-labeled myosin heads in myofibrils in rigor is characterized by a high limiting anisotropy at 1ms; in rigor fibers this value is slightly higher. The difference may be due to orientation effects or to depolarization due to light scattering in the optically dense myofibril solution. Upon addition of ATP the limiting anisotropy decreases, indicating that the myosin heads undergo a greater amplitude of motion in the microsecond time range. The anisotropy in both myofibrils and fibers undergoing contraction is intermediate between rigor and relaxation, indicating either that heads have intermediate mobility or that only some are mobile. We also see intermediate limiting anisotropy values in the presence of AMPPNP and PPi.

W-Pos170 ORIENTATIONAL AND CONFORMATIONAL DYNAMICS OF SPIN-LABELED MYOSIN HEADS IN CONTRACTING MUSCLE FIBERS. **Vincent A. Barnett, Kiandoht Beyzavi, & David D. Thomas, Univiversity of Minnesota Medical School, Minneapolis, MN 55455.**

The conformational dynamics of myosin in contracting muscle fibers are a key point in the determination of the molecular mechanism of muscle contraction. Previously, we have used conventional and saturation-transfer EPR to examine the orientational distribution and rotational dynamics of spin-labeled myosin crossbridges in glycerinated psoas fibers during isometric contraction. We have shown that on average during an isometric contraction only about 20 % of the myosin heads have a well-defined orientation, and that this orientation is identical to that observed for a rigor muscle fiber. We have further shown, using conventional EPR and a spin probe sensitive to local conformational changes induced by nucleotide binding to the active site of myosin, that in relaxed fibers the myosin heads participate in a conformational equilibrium between states that can be correlated with the M*ATP and M**ADP.P_i conformations of myosin. The distribution between these two conformations is perturbed by the interaction of myosin with actin even in relaxation. In the present study we have used conventional EPR to examine the conformational changes of spin-labeled myosin in glycerinated rabbit psoas fibers during isometric contraction. We have analyzed the spectra during contraction in terms of three components, corresponding to two detached states (most likely M*ATP, M**ADP.P_i), and one attached state (indistinguishable from AM*ADP). Just as in relaxed muscle fibers, the conformational equilibrium is perturbed by the transient interactions of the myosin heads with actin in the thin filaments.

W-Pos171

ABSTRACT MOVED TO W-AM-G11

W-Pos172 THE EFFECT OF C-PROTEIN ON ACTOMYOSIN ATPase IN THE PRESENCE OF TROPOMYOSIN AND TROPONIN. D. Stępkowski & C. Moos, Biochem. Dept., SUNY, Stony Brook, NY 11794.

C-protein, a component of the thick filaments of vertebrate striated muscle, is known to influence the ATPase activity of actomyosin (AM) and to bind to both myosin and actin. We have studied the effect of C-protein on AM ATPase activity in the presence of tropomyosin (TM) or TM plus troponin (TT). Proteins from rabbit white skeletal muscle were used, and experiments were done under three conditions: 100 mM KCl at pH 7.0 and 7.5, and 50 mM KCl at pH 7.0. Other conditions were: 1 mM $MgCl_2$, 1 mM MgATP, 0.1 mM $CaCl_2$ or 1 mM EGTA, 20 mM buffer (MOPS at pH 7.0, Tris at pH 7.5), 3.8 mol actin per mol myosin, 1 mol C-protein per mol myosin, and 2 mol TM or TT per 7 mol actin. At 100 mM KCl, pH 7.0 or 7.5, TM alone had little or no effect on AM ATPase but TT + Ca caused 50-100% activation. Under these conditions, C-protein had no effect on the ATPases in the presence of TM or TT, with or without Ca. The pCa-dependence of TT-regulated AM ATPase has been studied only at 100 mM KCl, pH 7.0 (using 2 mM EGTA-Ca buffers), and C-protein had little or no effect on it. However, C-protein caused ca. 50% activation in the absence of TM or TT at pH 7.5, so that addition of TM in the presence of C-protein gives a relative inhibition. At 50 mM KCl, TM activates AM ATPase ca. 30% and TT + Ca activates about 50%, and addition of C-protein abolished the activating effects of both TM and TT. In conclusion, the presence of C-protein in myosin preparations could influence studies of AM ATPase regulation in vitro under certain conditions. Furthermore, it remains possible that C-protein might influence the thin-filament regulatory system in vivo. Similar studies using cardiac C-protein, TT and myosin are currently under way. (Supported by NSF Grant DCB 8317038 and Amer. Heart Assoc. Grant 83-1137.)

W-Pos173 EFFECT OF VANADATE (V_i) ON THE BINDING OF S-1·ADP TO ACTIN AND ON THE ACTO·S-1 ATPase ACTIVITY. Susan Smith and Evan Eisenberg, Lab. of Cell Biol., NHLBI, NIH, Bethesda, MD.

We have studied the effect of V_i on the binding of S-1·ADP to actin and on the acto·S-1 ATPase activity. The dissociation of actin from S-1·ADP was determined at varied $[V_i]$ in direct binding studies using ^{14}C-iodoacetamide labelled S-1. These experiments were carried out at low salt, pH 7, 15°C with < 1 mM V_i, because polymeric V_i species form above this concentration. Using this limited range of $[V_i]$ necessitated considerable extrapolation in determining binding constants. Nevertheless, we could estimate that the binding constant of V_i to the acto·S-1·ADP complex is between $5x10^2$ and $5x10^3$ M^{-1}, while that of actin to the S-1·ADP·V_i complex is between $2x10^4$ and $1x10^5$ M^{-1}. These values are consistent with the data of Goodno and Taylor (PNAS 79, 21, 1982). The maximum rates of dissociation of actin from S-1·ADP·V_i and of V_i from acto·S-1·ADP obtained by light scattering measurements are both > 0.05 s^{-1}. Modelling of these data, assuming that V_i binds in a two-step process to the acto·S-1·ADP complex, predicts that V_i should have very little effect on the acto·S-1 ATPase activity. In agreement with this prediction, we find that, at $[V_i]$ below 0.5 mM, there is very little inhibition of the acto·S-1 ATPase activity. At $[V_i]$ between 0.5 and 1 mM, some inhibition does occur, possibly due to a small amount of polymeric V_i. However, there is no inhibition of the ATPase activity of cross-linked actin·S-1 at these $[V_i]$. Hence, the effects of V_i that we observe are consistent with V_i simply binding to the normal S-1·ADP complex, although we cannot rule out that the ATPase inhibition is due to V_i binding to an S-1·ADP intermediate which occurs only during the steady-state ATPase cycle.

W-Pos174 THE EFFECTS OF PYROPHOSPHATE ON ACTIVE CROSS-BRIDGE CYCLING IN ISOLATED THICK FILAMENTS FROM LIMULUS STRIATED MUSCLE. S.F. Fan, M.M. Dewey and B. Chu. Department of Anatomical Sciences and Department of Chemistry, SUNY at Stony Brook, Stony Brook, NY 11794

Pyrophosphate (PP_i) is regarded as a non-hydrolyzable ATP analogue which affects the kinetics of attachment and detachment of myosin-heads from actin. Makinose and Nagi reported that PP_i enhanced muscle contraction elicited by electrical stimulation (Jap. J. Physiol., 5:49'55). Subsequently evidence was presented which suggested that this effect was due to repetitive firing of muscle fibers following single direct stimulus in the presence of PP_i (Fan and Li, Acta Physiol. Sinica, 26:28'63). Kameyawa et al. (J. Biochem., (Tokyo) 97:635'85) reported that in the presence of PP_i, the decrease of the Ca^{2+} -ATPase which normally occurs upon treatment with 2,4,6-trinitrophenyl groups is reduced. They held that the site of trinitrophenylation is different in the presence of PP_i than in its absence. Limulus striated has been shown to possess both a direct myosin regulatory system as well as the troponin-tropomyosin and calmodulin-myosin light chain phosphorylation systems (Gaylinn et al., Biophys. J., 47:469a'85). If PP_i has an effect on the myosin heads, as suggested by the above data it may act near or at the direct myosin-regulatory system and/or the cross-bridge cycling process. With a quasi-elastic light scattering method (cf. Fan et al., Biophys. J., 47:809'85), we have shown that the increase of the average linewidth of the photocount correlation function at high scattering angles (e.g. 120°) from isolated thick filaments of this muscle by calcium is increased by the presence of 2mM PP_i. The average linewidth of the photocount correlation function of filaments suspended in relaxing and in ATP-free solutions are not affected. This suggests that PP_i may affect the cross-bridge cycling motion in the absence of actin.

W-Pos175 SELECTIVE EFFECTS OF ATP ON EDC-CROSSLINKED PRODUCTS OF ACTO-S1. Rajen Oza and Paul Dreizen. Graduate Program in Biophysics & Department of Medicine. SUNY Health Science Center at Brooklyn, New York.

EDC cross-linking of actin and rabbit fast muscle myosin S1 in 100mM KCl generates a doublet band for acto-HC (170 and 180K). When cross-linking is done in the presence of Mg-ATP, there is diminished complex formation with selective loss of the 180K component at 3mM ATP. It is unclear whether the ATP effect represents selection of sequential conformational states in the ATPase cycle, or non-specific ionic strength effects on the actin-myosin interaction. We have further investigated this question in several ways. First, the ATP effect is highly sensitive to ionic strength. Increase of KCl from 0 to 200mM in the presence of 1mM ATP during cross-linking is accompanied by a marked decrease in the amount of acto-HC, with selective loss of 180K. In the absence of ATP, the extent and distribution of actin-HC doublet is unchanged at KCl concentrations from 0 to 200mM. These findings are consistent with weak and strong-bound states for acto-S1, and also show that 170/180K selectivity is coupled with the presence of ATP and is not a non-specific ionic effect. Also, the ATP effect is highly sensitive to the duration of incubation with acto-S1 prior to EDC cross-linking. For example, in 1mM ATP, 100mM KCl, as incubation time is varied from 30min to 5h, there is progressive decrease of 170/180K doublet with selective loss of 180K. In the presence of 3mM ATP, the same changes occur during less incubation time, with total loss of 170/180K doublet after only 2 hrs incubation. This time-dependent phenomenon may be related to enhanced ligand-induced dissociation of actin-S1, due to progressive conversion of ATP to ADP and Pi during prolonged ATP hydrolysis. The overall results suggest a specific ATP effect consistent with a sequential interpretation for the acto-HC doublet.

W-Pos176 EFFECT OF ETHYLENE GLYCOL ON THE INTERACTION OF S-1 WITH REGULATED ACTIN. Lois E. Greene and Ednan Mushtaq, LCB, NHLBI, National Institutes of Health, Bethesda, MD 20892

To elucidate the structure of the cross-bridge intermediates in the actomyosin ATPase cycle, several laboratories have added both ethylene glycol and AMP-PNP to muscle fibers. These studies suggested that ethylene glycol may shift the structure of S-1 toward the weak-binding conformation, i.e. toward the structure of M·ATP. However, the effect of ethylene glycol on the interaction of S-1 with regulated actin has yet to be determined. We, therefore examined the effect of ethylene glycol on the regulation of the acto·S-1 ATPase activity by troponin-tropomyosin. Although we found that increasing the percentage of ethylene glycol causes a decrease in the extent to which actin activates the S-1 ATPase activity, this decrease was much greater in the presence of troponin-tropomyosin with Ca^{2+}. In fact, at 40% or greater ethylene glycol, there is essentially no activation of the regulated acto·S-1 ATPase activity in the presence of Ca^{2+}. This lack of activation is not due to denaturation of the troponin-tropomyosin since upon reducing the ethylene glycol, we obtained full recovery of activity. One possible explanation for this behavior is that ethylene glycol shifts the regulated actin filament toward the turned-off form even in the presence of Ca^{2+}. If this were the case, the binding of S-1 to regulated actin in Ca^{2+} might be more cooperative in the presence of ethylene glycol than in its absence. We tested this in 40% ethylene glycol and found that there is indeed more pronounced cooperativity in the binding of S-1·ADP to regulated actin both with and without Ca^{2+} than in aqueous solution. Therefore, our data suggest that, in addition to affecting the conformation of S-1, ethylene glycol may shift the tropomyosin-actin units to the turned-off form.

W-Pos177 **THE MgADP INHIBITION KINETICS OF STEADY-STATE CARDIAC MYOFIBRILLAR ATPase.** Stephen M. Krause and William E. Jacobus. Jefferson Medical College, Philadelphia, PA and The Johns Hopkins School of Medicine, Baltimore, MD.

The maintenance of the MgATP pool at the contractile proteins requires the effective regeneration of MgATP by the rapid rephosphorylation of MgADP, since the increased [MgADP] could potentially inhibit the myofibrillar ATPase. We previously demonstrated with cardiac myofibrils that MgATP, provided by rephosphorylation of MgADP via the endogenous creatine kinase, enhanced the kinetics of the steady-state myofibrillar ATPase. It was the purpose of this study to determine if the kinetic enhancement was the specific action of the endogenous M-line creatine kinase or the result of a rapid removal of an inhibitory effect of MgADP. To accomplish this, we studied MgADP inhibition of the myofibrillar ATPase in cardiac myofibrils isolated in the presence of Triton X-100. MgADP inhibition of the ATPase was determined at [MgADP] ranging from 158 μM to 4 mM while [MgATP] was varied from 0.16 to 0.8 mM. Other conditions included a free $[Mg^{2+}]$ of 3.2 mM, pH 7.1, 37°C and an ionic strength of 0.16 M. Maximal Ca^{2+}-ATPase activity was maintained at a free $[Ca^{2+}]$ of 31 μM, resulting in a specific activity of 0.12 ± 0.01 μmols Pi/mg protein-min. Kinetic analysis of substrate-velocity curves indicated that MgADP acts as a non-competitive inhibitor of the steady-state ATPase, (K_i = 5.0 ± 0.1 mM). Therefore, the kinetic enhancement previously observed with the endogenous creatine kinase appears to be the result of the close proximity of the two enzymes and not the rapid removal of an inhibitory effect of MgADP on the ATPase. Overall, these results suggest that because the physiologic free [MgADP] is approximately 40 μM in the heart, MgADP inhibition of myofibrillar ATPase plays little role in the control of normal myocardial contractility.

W-Pos178 BINDING OF MYOSIN HEADS TO ACTIN DURING ATP HYDROLYSIS IN MYOFIBRILS FROM RABBIT SKELETAL MUSCLE. Anh Duong and Emil Reisler, Department of Biochemistry and Chemistry and the Molecular Biology Institute, University of California, Los Angeles, CA 90024.

Measurements of cross-bridge attachment to actin in myofibrils during ATP hydrolysis require prior fixation of myofibrils to prevent their rapid contraction. The optimal cross-linking of myofibrils was acheived by using 10 mM carbodiimide (EDC) under rigor condition, at 4^0C. The fixed myofibrils had elevated MgATPase activity (150%), could not contract, and as judged by chymotryptic digestion and subsequent SDS gel electrophoresis analysis showed the cross-linking of about 25% of the myosin heads. Such myofibrils were employed in the proteolytic rates measurements (Duong & Reisler, Biophys. J.,49, 444a (1986)) of myosin binding to actin. The modified myofibrils were digested with trypsin at a weight ratio of 1:50 under rigor and relaxed conditions, and in the presence of 5 mM MgATP. The relaxed state was obtained by incubating modified myofibrils with 3 mM MgADPVi, 0.1 mM MgATP, in the presence of 0.2 M NaCl. Under rigor condition and in the presence of MgATP, the concentration of NaCl was 0.1 M. Aliquots of tryptic digestion reactions were cleaved with chymotrysin to yield isolated myosin heads and their fragments. Analysis of the decay of myosin heavy chain bands on SDS gels yielded the rates of myosin cleavage under all experimental conditions. The binding information was then obtained by comparing the rates of tryptic cleavage of myosin heavy chain in myofibrils in the presence of MgATP with the rates of their cleavage under relaxed and rigor conditions. Using this approach, we detected the binding of between 20 to 30% of myosin heads to actin in myofibrils during ATP hydrolysis.

W-Pos179 FURTHER STUDIES ON THE TWO PATHWAYS FOR OXYGEN EXCHANGE BY HEAVY MEROMYOSIN WITH ACTIN. Kamal K. Shukla, Harvey M. Levy, Fausto Ramirez and James F. Marecek, Department of Physiology and Biophysics, School of Medicine, SUNY at Stony Brook, Stony Brook, NY 11794.

Studies on the intermediate oxygen exchange catalyzed by myosin in the presence of actin have revealed two pathways for the hydrolysis of MgATP. The oxygen exchange, between water and the γ-P group of ATP, results from the reversible hydrolysis of MgATP while it is tightly bound to the myosin active site; it appears in the product P_i that is ultimately released to the medium. Starting with [γ-^{18}O]MgATP as substrate, the exchange is determined by analyzing the distribution of product P_i species with 3,2,1 or zero ^{18}O atoms, using mass spectrometry. Comparing the measured distributions to theoretical ones reveals two pathways of comparable flux that differ greatly in the extent of exchange they support. For each pathway the extent of exchange is given by R, the rate of the exchange cycle (hydrolysis and its reverse), k_{ex}, divided by the rate of the post-exchange reaction, k, which immediately follows the cycle. With HMM, the low exchange pathway (P1) had a low value for exchange (R=0,4) independent of the actin concentration. In contrast, R2 for the high exchange pathway (P2) decreased with the actin concentration (from 20 at low actin to 2 at high actin). Apparently, actin reduces R2 by activating k_{P2} which is a rate-limiting step along this route. Thus for the HMM, a plot of R2 vs 1/(Actin) gave a straight line. The intercept of this line at infinite actin (1/(Actin)=0) gives a minimal value for R2, designated $R2_{min}$, where k_{P2} is assumed to be maximally activated by actin, leaving minimal time for exchange. Using this graphical method, $R2_{min}$ for HMM had a value between 1 and 2, significantly higher than R1. This difference between $R2_{min}$ and R1 indicates that the low exchange pathway is not equivalent to the high exchange pathway saturated with actin. (Supported by NIH Grant AM 36701)

W-Pos180 BINDING AND ORIENTATION OF THE MYOSIN-ACTIN—NUCLEOTIDE TERNARY COMPLEX IN MUSCLE FIBERS. Fajer, E.A., Fajer, P., Brunsvold, N. and Thomas, D.D., Biochemistry Dept., University of Minnesota, Minneapolis, Minnesota 55455.

We have previously shown [1] that in the presence of 4 mM AMP.PNP, disorientation of spin-labeled myosin heads in muscle fibers is accompanied by increased mobility. We have further confirmed this result under saturating conditions of 16 mM AMP.PNP at 4°C, when 50% of the myosin heads are disoriented and mobile. K_d for AMP.PNP in fibers has been independently obtained by titration of the dissociation effect and by ADP.SL displacement [2]. It was found to be about 3 mM. In order to determine the orientation of the ternary complex, MSL-labeled S1 was infused into an unlabeled fiber. The orientational resolution of EPR spectra allows the simultaneous measurement of actin-binding and orientation of S1. At 4°C in 16 mM AMP.PNP, there was no evidence for a disoriented ternary complex, but the binding of S1 was substantially weaker (10%) than that of intrinsic heads (50%). Increasing the temperature to 13°C resulted in the binding of 50% of S1 to actin. Under these conditions there is still no evidence for any bound but disoriented species, and all of the ternary complexes are oriented as in rigor. We therefore conclude that AMP.PNP causes partial dissociation of crossbridges without a change of conformation in the ternary complex as detected by EPR.

[1] Brunsvold, N., Fajer, E., Fajer, P. and Thomas, D., Biophys. J., 49, 265a (1986).
[2] Pate, E. and Cooke, R.C., Biophys. J., 49, 265a (1986).

W-Pos181 THE APPARENT TWO-STATE TRANSITION IN MYOSIN S-1 IS LINKED TO THE ACTIN BINDING REGION. Utpala Kamath and John W. Shriver. Department of Medical Biochemistry, School of Medicine; and Department of Chemistry and Biochemistry, College of Science; Southern Illinois University, Carbondale, IL 62901
Myosin S-1 exists in at least two structural states as indicated by ^{19}F NMR spectra of a probe attached at SH_1 and also by tryptophan UV difference spectra induced by nucleotides, especially AMPPNP. The energetics of the states may be investigated by the temperature dependence of the equilibria between them. We are using the demonstrated ability of trypsin to nick the myosin heavy chain at two specific sites to probe the topology and function of the structural transition in the myosin head. DSC studies of the denaturation of S-1 show that the protein stability is not affected by nicking. The Mg^{++} ATPase is also essentially unaffected by nicking. The structural transition is significantly perturbed by the nicking of S-1 at both sites, indicating that nicking occurs in the regions participating in the structural transition. Both ^{19}F NMR and UV studies of the 27K-50K-20K species show little evidence of a thermotropic transition over the temperature range of 0 to 25°C. However, the 27K-70K species behaves identically to the uncleaved S-1 at the one or more tryptophans responsible for the UV difference spectra. The 27K-70K species is prepared by digesting S-1 in the presence of actin. This data would imply that the transition observed at these tryptophans is sensitive to the integrity of the actin binding site region or cooperative domain. ^{19}F NMR studies of the 27K-70K species are in progress.
(Supported by a Basic Research Grant from the Muscular Dystrophy Association).

W-Pos182 EFFECTS OF IONIC LIGANDS ON ACTO-S1 ATPASE AND ACTO-S1 BINDING OF CARDIAC VENTRICULAR MYOSIN. Joseph Rivera and Paul Dreizen, Graduate Program in Biophysics, SUNY Health Science Center at Brooklyn, New York.

Cardiac atrial and ventricular S1 have different Vmax and Km values for actin activation, and both isoforms exhibit multisite, competitive inhibition by monovalent anions and ATP, with Ki values stronger for ventricular than atrial S1. The kinetic data have been interpreted in terms of ligand regulation at allosteric sites on acto-S1. We have further explored this hypothesis by equilibrium binding studies of acto-S1 from canine ventricular myosin, as measured by the NH_4^+/EDTA ATPase of free S1 following acto-S1 sedimentation in an Airfuge. In preliminary studies, Kd is approximately 10 μM, as compared with apparent Km of 5 μM under the same (low ionic strength) conditions. This difference is consistent with previous studies of Km and Kd for skeletal and smooth muscle myosin S1 (Stein et.al., 1982; Rosenfeld and Taylor, 1984). Studies of salt effects on acto-S1 binding show that monovalent anions (Cl^-, CH_3COO^- and SCN^-) inhibit the interaction between actin and S1 according to a multisite model (n=3), as in the case of kinetic studies on fast skeletal and cardiac myosin S1 isoforms. Ki values are approximately the same for binding and ATPase for SCN^- (13 mM), Cl^- (20 mM) and CH_3COO^- (30mM). The overall results provide direct evidence that anions regulate the acto-S1 interaction in a highly specific way, and confirm that the predominant kinetic effects of anions on acto-S1 ATPase can be explained in terms of several anion-specific sites on the acto-S1 complex.

W-Pos183 INTERACTION OF ACTIN WITH MYOSIN SUBFRAGMENT 1 (SF-1) PHOTOLABELED WITH 3'(2')-O-(4-BENZOYL)BENZOYL,1,N^6-ETHENOADENOSINE DIPHOSPHATE ($Bz_2\varepsilon ADP$). Christine Cremo and Ralph G. Yount, Biochemistry/Biophysics Program and Dept. of Chemistry, Washington State University, Pullman WA, 99164 (Intr. by Michael J. Smerdon)

The stable trapping of $Bz_2\varepsilon ADP$ on SF-1 by p-phenylene dimaleimide (pPDM) and subsequent specific photolabeling with the fluorescent photoaffinity label has been previously reported (Cremo and Yount, 1985, Biophys. J., 49, 46a). The fluorescence properties (lifetimes, quantum yields and polarization) of the reversibly bound and covalently bound probe at the active site have been characterized in detail. The fluorophore has a high quantum yield only after photoincorporation, a feature that makes it particularily useful for distance measurements using lifetimes to measure energy transfer efficiencies. The covalently modified SF-1 binds to actin in a specific manner with a K_d of 30μM, not significantly different from the binding constant for ADP trapped on SF-1 by pPDM (Greene et al, 1986, Biochemistry 25, 704-709). Polarization studies confirmed the results of Greene et al, indicating that actin binding accelerates the exchange of nucleotide at the active site of pPDM·SF-1. The lifetime of the covalent fluorophore did not change upon addition of actin. $Bz_2\varepsilon ADP$ has been used as a donor in fluorescence energy transfer experiments using DDPM as the chromophoric acceptor on Cys-374 of actin. Preliminary results indicate that the distance between the active site on SF-1 and Cys-374 on actin is greater than 40 Å. Experiments with other acceptors on actin are in progress.

Supported by MDA and AHA of Washington postdoctoral fellowship (C.C) and an MDA grant (R.G.Y.)

W-Pos184 ACTIVATION OF CILIARY BEAT FREQUENCY BY CALCIUM, CALMODULIN, AND cAMP IN RESPIRATORY CILIA. R. Hard and L. Scarcello, Dept. of Anatomical Sciences, SUNY at Buffalo, Buffalo, NY.

Ciliary beat frequency is known to depend on MgATP and temperature. Previously we showed that the beat frequency of demembranated newt lung cilia responds biphasically to varying [MgATP]. This occurs when cilia are isolated at 20°C with a KPIPES-based buffer containing Triton X-100 (1-2%, W/V). Double reciprocal plots (1/F vs 1/MgATP) of cilia reactivated at 20°C show downward curvature with two effective Fmax values: 18-20 Hz over the substrate range, 50 uM-0.5 mM; 45-50 Hz over the substrate range, 0.5 mM-5 mM. We also have shown that cilia, whose outer dynein arms have been removed by high salt extraction, show linear kinetics with an Fmax of 11-12 Hz, suggesting functional differences between inner and outer arms. In the present study, we show that reactivated beat frequencies above 20 Hz are not obtained when cilia are demembranated at 4°C with a KCl-imidazole-based buffer of comparable ionic strength and when the TX-100 concentration is lowered to 0.08%. This is true, regardless of the [MgATP] used in reactivation. Beat frequencies above 20 Hz can be restored by including Ca^{2+}, calmodulin (CAM) and cAMP in KCl-imidazole based reactivation mixtures. The optimal free Ca^{2+}, CAM and cAMP concentrations are in the order of 1 uM, 3 u/ml and 10 uM, respectively. In contrast, high-salt extracted cilia, first isolated with KCl-imidazole, behave the same as those isolated with the KPIPES-based buffer. Ca^{2+}, CAM and cAMP have no effect on the reactivated beat frequencies of these outer-arm-depleted cilia. These data suggest 1) further functional differences between inner and outer dynein arms in newt lung cilia and 2) that the biphasic response of reactivated axonemes is centered around a Ca^{2+}-CAM-cAMP based activation of outer dynein arms. (Med. Res. Fndn. Oregon)

W-Pos185 LASER DOPPLER VELOCIMETRY USING A QUASI-ELASTIC LIGHT SCATTERING (QELS) MICROSCOPE SPECTROMETER. Paul S. Blank, Dept. of Biophysics, Johns Hopkins Univ., Baltimore, MD 21218.

The quasi-elastic light scattering (QELS) microscope spectrometer has been used to examine transport in a model system and isolated cells. Biologically relevant velocities (.1 um/sec and greater) were modeled using a gel filled capillary tube moving with uniform velocity. Velocities could be determined rapidly from analysis of the Doppler shifted power spectrum and were in agreement with direct observation. The dependence between the Doppler shifted frequency and the scattering geometry was linear over scattering angles from 35 to 50 degrees. As predicted by theory, for fixed scattering angles, the dependence between the Doppler shifted frequency and the projection of the velocity vector on the scattering plane was linear over rotation angles from 0 to 90 degrees out of the scattering plane. Cytoplasmic streaming in Nitella was examined over scattering angles from 30 to 50 degrees using a scattering volume 12.5 um in diameter. An average velocity of streaming, ~58 um/sec, was determined from the linear dependence between the Doppler shifted frequency and the scattering geometry. The results are in agreement with earlier light scattering studies. An attempt was made to correlate light scattering results with the fast component of axonal transport. No evidence for a well defined Doppler shifted peak in the averaged spectral data was found. Differences in averaged data following orientational changes and gluteraldehyde fixation implicate motion within the axon as the origin of the light scattering signal. Structure in single spectra indicate that many velocities may contribute to the spectral average. This work was supported by USPH/NIH grant 5R01AM12803-27 to F.D. Carlson, Dept. of Biophysics, JHU.

W-Pos186 ON THE BIOPHYSICAL TRAIL OF THE PHYSIOLOGIC SIGNIFICANCE OF GROWTH FACTORS. Beverly Packard, Alan W. Partin, Donald S. Coffey, and Michael Edidin. Departments of Biology and Urology, The Johns Hopkins University, Baltimore, MD.

In the past 35 years more than 20 polypeptides with growth promoting activity have been isolated, purified, and cloned. Although many growth factors and their respective plasma membrane receptors are now structurally and chemically well characterized in addition to having molecules and ions implicated as second and third messengers in their signal transductory pathways, the physiologic roles of these factors remains largely elusive. In order to gain insight into the potential physiologic roles these factors may play, at least at a single cellular level, we have been studying the effects of three growth factors on the molecular architecture and dynamics of cellular motility. Cells of neural crest origin which have been treated with transforming growth factor, type beta show an increase in their fibrillar actin content. Nerve growth factor and a synthetic fourteen amino acid sequence from thrombin induce a reorganization of the actin network. The effects of these actin changes upon cellular spreading and motility are being studied by time-lapse photography; their role in cellular growth, differentiation, and metastasis are being assessed.

W-Pos187 SOLUBLE MICROTUBULE-BASED TRANSLOCATOR PROTEIN IN ACANTHAMOEBA CASTELLANII EXTRACTS. Bechara Kachar*, Hisao Fujisaki, Joseph P. Albanesi and Edward D. Korn, *Laboratory of Neuro-Otolaryngology, NINCDS, and Laboratory of Cell Biology, NHLBI, NIH, Bethesda, MD 20892.

Bidirectional movement of organelles along microtubules is observed when cytoplasm of Acanthamoeba is extruded into buffer containing ATP and taxol. These cytoplasmic extracts are being used as the initial material for the purification of microtubule-based translocator proteins. Soluble fractions are assayed for translocator activity by adsorbing protein to the surface of latex beads, incubating with purified bovine brain microtubules, and directly observing motility by video microscopy. Latex beads coated with the crude supernatant moved bidirectionaly along microtubules. Within a few hours of extraction the bead movement became unidirectional with a rate of 2-3 μm/s. Movement always occurred from the minus to the plus end of the microtubules as determined with microtubles nuclated from the distal end of sea urchin axonemes. The Acanthamoeba translocator was not inhibited by the myosin innibitor NEM (2 mM), or by the dynein innibitor vanadate (20 μM). Specific activity for movement was enhanced 250x after five sequential chromatography columns. Motility persisted after 200x dilution of fractions containing 0.5 mg protein/ml. After the last purification step, a Coomassie blue-stained SDS gel showed three main bands and several minor bands. Although we do not yet know which band(s) correspond to the translocator protein, a 110-120-kDa band characteristic of kinesin (Vale et al. Cell 42, 39, 1985) was not prominent. Preliminary results with SDS-polyacrylamide gels subjected to immunoblotting with polyclonal antibodies raised against squid kinesin (gift of T.S. Reese) showed cross reactivity with a 175-kDa Acanthamoeba polypeptide.

W-Pos188 ARE LARGER SPERM MORE FRAGILE?

Jay Baltz*, Oneeka Williams and Richard Cone
Jenkins Dept. of Biophysics, The Johns Hopkins University, Balto., MD 21218 and *LHRRB, Harvard Medical School, Boston, MA 02115

Mammalian sperm are subjected to mechanical shear as they are transported through the tubules of the epididymis and vas deferens. Rat sperm in a sheared fluid can easily be lethally damaged (Cardullo and Cone, BOR. 34, 820 1986). We calculated that the sheared fluid exerts tension on the sperm (modelled as rigid rods) proportional to shear, viscosity, and their length squared. We used a "cone and plate" to impose a constant shear on sperm in a test fluid (2% methylcellulose). The viscosity was measured as a function of shear using a capillary viscometer. 50-micron-long human sperm were able to withstand slightly more than twice the shear stress that killed 180-micron-long rat sperm (4500 vs. 2100 Poise/sec). However, the difference in their lengths implies that rat sperm should be 13-fold more susceptible to shear damage than human sperm. Therefore, rat sperm are relatively sturdier for their size. This suggests, perhaps, that the role of the very large dense fibers surrounding the axoneme of rat sperm may be to strengthen them. Fragility may still be a problem, though, since rat sperm are not only large, but they may also experience higher shears *in vivo* due to the smaller tubules through which they are transported. We are currently investigating whether the mucus in which epididymal rat sperm are stored protects them against mechanical damage during transit. (Supported by NIH HD 16800)

W-Pos189 TRACER DIFFUSION OF MACROMOLECULES IN CONCENTRATED SOLUTIONS OF PROTEINS AND IN GEL NETWORKS. Li Hou, Katherine Luby-Phelps, and Frederick Lanni. Center for Fluorescence Research in Biomedical Sciences, and Department of Biological Sciences, Carnegie-Mellon University, Pittsburgh, PA 15213.

The technique of fluorescence recovery after photobleaching (FRAP) has been used in recent studies to measure the rate of motion of fluorescent tracer proteins and fluorescent analogs of native cytoplasmic proteins in live cells (Wojciescyn *et al.* (1981) PNAS **78**: 4407, Wang *et al.* (1982) PNAS **79**: 4660, Kreis *et al.* (1982) Cell **29**: 835, Luby-Phelps *et al.* (1985) J. Cell Biol. **101**: 1245). In order to fully understand the results of the above experiments, in which the tracer may interact with cytoplasmic elements in many ways, it has been necessary to study the transport of size-characterized inert tracer macromolecules, in live cells (Luby-Phelps *et al.* (1986) J. Cell Biol. **102**: 2015) and in model systems. We have used FRAP in a study of size-fractionated tracer polymer (dextran and Ficoll) diffusion in concentrated solutions of globular proteins. Our data show that the normalized tracer diffusion coefficient D(test solution)/D(water) varies inversely with tracer radius and is asymptotic at the inverse relative bulk viscosity of the test solution, as predicted by theories of the obstruction effect and a simple scaling argument. We are extending our experiments to cases in which a gel network of known density is formed in the specimens, to determine whether the steeply-decreasing curve D(cytoplasm)/D(water) versus tracer radius can be modeled simply, *in vitro*. Supported by NIH grant GM34639.

W-Pos190 L-CARNITINE MAY PROLONG SPERM VIABILITY IN THE RAT EPIDIDYMIS. Richard A. Cardullo, Samuel W. Kennedy and Richard A. Cone*, LHRRB, Harvard Medical School, Boston, MA 02115 and *Dept. of Biophysics, The Johns Hopkins University, Baltimore, MD 21218.

As rat sperm progress through the epididymis there is a marked change in their extracellular environment. From caput to cauda epididymis there is approximately a 60-fold increase in the L-carnitine concentration, a 7°C drop in temperature, and an increase in the viscoelasticity that mechanically immobilizes sperm. Here we report that, in the absence of added metabolites, cauda epididymal fluid (CEF) markedly reduces the oxygen consumption rate of rat sperm. It has been previously reported that mechanical immobilization of rat sperm diluted in a variety of test solutions does not detectably decrease their oxygen consumption rate (Cardullo and Cone, BOR, 34, 1986). When 10 mM L-lactate was added to the suspension there was a marked increase in the oxygen consumption rate of these sperm but not in the epididymal tissue that surrounds them. Additionally, the 7°C decrease in temperature leads to a two-fold decrease in the oxygen consumption rate of these sperm (Q_{10}=3.1). Of all CEF components examined, only L-carnitine decreased the the oxygen consumption rate of washed rat sperm to the same low levels as CEF in the absence of added metabolites. These results, taken together, suggest that in the absence of exogenous metabolites, oxygen metabolism of rat sperm may be markedly reduced by L-carnitine. This inhibition of oxygen metabolism may increase the oxygen supply to the epididymis and also reduce the aerobic consumption of the metabolites stored in sperm. Both of these may prolong sperm viability during storage in vivo. (Supported by NIH HD 16800).

W-Pos191 AN APPROACH FOR STUDIES ON THE COUPLING BETWEEN CELLULAR ENLARGEMENT AND INITIATION OF DNA SYNTHESIS. Mary N. Stamatiadou, Department of Biology, Nuclear Research Center "Demokritos", Aghia Paraskevi, Athens, Greece.

Reentry of quiescent Balb/c-3T3 cells into the cell cycle following stimulation by serum is characterized by a 14 h prereplicative (G_0-G_1) phase, during which protein accumulation in the cytoplasm is somehow involved in the control of the ensuing initiation of DNA synthesis. The two parallel processes, i.e., cellular enlargement and progression to DNA synthesis and mitosis may not exhibit the same requirements for a given proliferative stimulant. Whereas quiescent Balb/c-3T3 cells become committed to initiation of DNA synthesis after a relatively short exposure to serum, protein accumulation depends on the continuous presence of serum in the cellular environment. Treatment of these cells with urea during the prereplicative and S phases results in an uncoupling of DNA synthesis from protein accumulation (1). Urea-treated cells are dependent on serum concentration to the same extent as urea-untreated cells for initiation of DNA synthesis, which indicates that the dependency on serum factors as a general characteristic of Balb/c-3T3 cells is not altered by urea treatment. Devoid of an apparent inhibitory action on general protein synthesis, urea appears to act antagonistically to the activity of serum that is required for cell protein accumulation while at the same time it does not affect the entry of the cells into S phase. An approach is thereby provided which permits quantitative studies on the coupling between the two parallel pathways, i.e., between cellular enlargement and progression to DNA synthesis and mitosis.

(1) Stamatiadou, M.N. (1986) IRCS Med. Sci. 14, 171-172.

W-Pos192 DYNAMIC PROTEIN AGGREGATES IN THE MITOCHONDRIAL INNER MEMBRANE PROBED BY TIME-RESOLVED ANISOTROPY MEASUREMENTS OF ERYTHROSIN-LABELED F_1. T.P. Silverstein* and H. Rottenberg, Pathology Dept., Hahnemann Medical Univ., Philadelphia, PA 19102.

Erythrosin isothiocynate (erNCS) attached to purified F_1 from rat liver SMP's shows no anisotropy on a msec time scale, suggesting F_1 in solution rotates fast enough to wipe out the fluorescence anisotropy of erythrosin covalently bound to the protein. As dextran is added to the buffer anisotropy becomes evident, increasing with increasing concentrations (from 5-20% dextran by weight). Anisotropy decayed to zero with a correlation time of .19 ms. When erNCS-F_1 is reconstituted with urea-treated SMP's (F_1-depleted urea particles, UP) anisotropy decayed more slowly (=1.86 ms) to a time-independent residual level of .030, which is indicative of a population (63% in this case) of labels which are rotationally frozen on the msec time scale, presumably by dynamic aggregation of the protein into a large, slowly rotating oligomeric unit. The anisotropy of erNCS-labeled SMP's decayed more quickly (=.54 ms) to a residual level of .020, suggesting about 67% dynamic aggregates.

A cooperative temperature-dependent transition was detected in both reconstituted erNCS-F_1-UP and erNCS-SMP's, with T_{tr} around 20-25°C. In addition, various membrane-perturbing agents were shown to significantly alter the level of residual anisotropy, which was increased by chloroform and palmitic acid but decreased by Triton X-100. These effects were all saturable within the concentration ranges in which the reagents serve as uncouplers of mitochondrial oxidative phosphorylation, suggesting that large, dynamic protein aggregates may play a role in energy transfer in bioenergetic systems.

W-Pos193 REVERSE UNIPORT DEPENDENT Ca^{2+}- RELEASE FROM MITOCHONDRIA: INHIBITION BY EGTA PLUS Mg^{2+}. Urule Igbavboa and Douglas R. Pfeiffer. The Hormel Institute, University of Minnesota, Austin, MN 55912.

When energized, Ca^{2+} loaded rat liver mitochondria are uncoupled, they undergo the nonspecific permeability transformation which results in swelling and the release of normally impermeant matrix solutes. The transformation induced by uncoupler is largely prevented by 400 μM ATP plus oligomycin. Under these conditions, reverse uniport dependent Ca^{2+} release can be investigated without interference from Ca^{2+} release by the nonspecific pathway. At Ca^{2+} loads of 50-60 nmol/mg protein, ClCCP stimulates Ca^{2+} release in a concentration dependent manner with the rate of release being an inverse function of $\Delta\psi$ and approaching the rate of forward uniport at optimal levels of uncoupler. Ruthenium red re-establishes the permeability transformation in Ca^{2+} loaded, uncoupled mitochondria, even in the presence of ATP and oligomycin. The maintenance of mitochondrial integrity following uncoupling thus requires a pathway for rapid Ca^{2+} release (reverse uniport). 0.5 mM EGTA plus 1.0 mM $MgCl_2$ have the same effect as ruthenium red in that they re-establish the permeability transformation in mitochondria which would otherwise remain intact and release Ca^{2+} by reverse uniport. EGTA alone is partially effective in this regard. Based on these findings, we propose that the Ca^{2+} uniporter is regulated by a Ca^{2+} binding site which is located on the cytoplasmic side of the inner membrane. When this site is not occupied by Ca^{2+}, the uniporter is inactive. The binding of Mg^{2+} to this site, or possibly to a distinct but interacting site, apparently further modulates uniporter activity. (Supported by NIH grant HL08214 and by the Hormel Foundation).

W-Pos194 CHANGES IN MITOCHONDRIAL PH AND THE PH GRADIENT DURING METABOLIC AND RESPIRATORY ACIDOSIS IN THE INTACT HEART. Steven D. Buchthal and Truman R. Brown. Fox Chase Cancer Center, Phila., PA 19111. In order to understand the different physiological responses to metabolic and respiratory acidosis in the intact heart, ^{31}P-NMR was employed on the isolated Langendorff perfused rat heart. With the perfusate at 7.40(control), the intracellular pH(pH_I) as determined from the chemical shift of the Pi resonance is 7.05. The mitochondrial phosphate pool is visible as a shoulder on the Pi resonance and corresponds to a pH(pH_M) of 7.38. During metabolic acidosis to pH 7.0(decreased bicarbonate), the pH_I dropped to 6.92 while the pH_M remained at 7.38, increasing the pH gradient(ΔpH=0.46). The pressure rate product(PRP) dropped to 71% of the control value. In contrast, during respiratory acidosis to pH 7.0(increased CO_2), both pH_I and pH_M shifted(6.92 and 7.24, respectively), maintaining ΔpH. The PRP dropped to 49% of control levels. The oxygen consumption during respiratory acidosis was lower than during metabolic acidosis. Upon further acidosis to pH 6.6, pH_I dropped to 6.79 while pH_M remained at 7.38 (ΔpH=0.59) during metabolic but fell to 7.13 during respiratory acidosis(ΔpH=0.34). Since the pH is a component of the proton motive force which is necessary for oxidative phosphorylation, these different responses of mitochondrial pH to different forms of acidosis may explain the physiologically different responses seen in the intact heart.

W-Pos195 CATION/H^+ EXCHANGE REACTIONS IN HEART MITOCHONDRIA. D.W.Jung, M.H.Davis and G.P. Brierley. Dept. of Physiological Chemistry, The Ohio State University, Columbus, Ohio.

K^+/H^+ antiporter activity in isolated heart mitochondria requires major membrane alterations such as swelling or Mg-depletion for activation. We have further charcterized K/H activity in intact mitochondria and submitochondrial particles (SMP) to clarify its physiological role. Mitochondria swell passively in K or Na nitrate (0.1M) at alkaline pH (8.4) and elevated temperature (37C) due to increased cation influx via a pH-sensitive uniport pathway. Initiation of respiration by succinate addition to swollen mitochondria activates cation/H exchange activity resulting in contraction. DCCD treatment of swollen mitochondria inhibits contraction in K but not Na nitrate indicating separate pathways for Na and K. Matrix Mg is also lost during swelling decreasing from 30 nmol/mg to approx 15 after 0.25 Abs unit swelling. This is in line with the activation of a K/H exchanger by declining Mg as proposed by Garlid (JBC 255:11273,1980). However, during contraction a rapid efflux of the remaining matrix Mg takes place along with K efflux. Mg efflux parallels K efflux. Both are faster when the influx path is closed by lowering the pH to 7.2 before contraction. This indicates that either Mg/H and K/H exchangers operate in parallel or there is a nonspecific cation/H exchange reaction. K/H exchange activity was also studied in SMP containing fluorescein isothiocyanate dextran, a fluorescent pH probe. These SMP support an internal pH gradient of 0.6 units with succinate and show K/H exchange activity which is inhibited by DCCD but is insensitive to 10mM Mg. These observations agree with the concept of controlled unspecific sites responsible for electroneutral exchange reactions as suggested by Bernardi et al. (J.Bioenerg.Biomemb.14:387,1982), but oppose the idea of a Mg-regulated K/H antiporter. Supported in part by USPHS Grant HL09364.

W-Pos196 DO MITOCHONDRIA PROVIDE A "MEMORY" OF PAST CYTOSOLIC CALCIUM PULSES? T.E. Gunter, D.E. Wingrove, S. Banerjee, and K.K. Gunter: Dept. of Biophysics, U. of Rochester, Roch. NY 14642.

At least three mechanisms of Ca^{2+} transport function in mitochondria. These are a very rapid uptake mechanism or uniport (V_{max} well over 500 nmol/mg·min, in liver), a Na^+-dependent efflux mechanism ($V_{max} \approx 2.6$ nmol/mg·min) showing simultaneous kinetics, and a Na^+-independent efflux mechanism ($V_{max} \approx 1.2$ nmol/mg·min) showing second order kinetics. While mitochondria regulate Ca^{2+} in vitro, they are badly designed to do so in vivo. The K_m of the uniport is higher than would be expected for a regulator and the uptake rate becomes unmeasurably slow below 100-200 μM ("resting Ca^{2+} level"). Mitochondria are well designed to shape Ca^{2+} pulses, released into the cytosol by hormone action, by blunting the sharp rises of cytosolic Ca^{2+} through rapid uptake by the uniport and by greatly extending the pulse duration at levels only a little higher than the "resting level" through slow release by the efflux mechanisms. Because (in liver) cytosolic Na^+ is well below the saturating Na^+ concentration of the Na^+-dependent mechanism, and because this mechanism is very sensitive to inhibition by Mg^{2+} and spermine, the Na^+-independent mechanism dominates efflux. The flat saturation dependence of the Na^+-independent mechanism should set up circumstances in which efflux is independent of mitochondrial Ca^{2+} load. This would lead to a "quasi steady-state" during the extension of the pulse. Because of the great difference between possible rates of influx and efflux, intramitochondrial Ca^{2+} could remain elevated for periods much longer than the pulse itself, leading to a "calcium memory" of the pulse and perhaps to an extended period of activation of electron transport and phosphorylation rate as proposed by Denton and coworkers. Supported by GM35550.

W-Pos197 *PARTIAL AMINO ACID SEQUENCE OF COUPLING FACTOR B.* *Lakshmi Kantham, Raktima Raychowdhury and D. Rao Sanadi. Boston Biomedical Research Institute, 20 Staniford Street, Boston, MA 02114*

Bovine heart mitochondrial coupling factor B (F_B) was isolated by the procedure of Joshi et al. (JBC 254, 10145, 1979) and alkylated with 4-vinylpyridine. On dialysis vs. distilled water, F_B was precipitated. The alkylated F_B appeared as a single band on silver-stained SDS-PAGE. The partial N-terminal amino acid sequence determined in the Applied Bioscience Microsequencer was as follows:

Phe	*Try*	*Gly*	*Try*	*Leu*	*Asn*	*Ala*	*Val*	*Phe*	*Asn*	*Lys*	*Val*	*Asp*	*His*	*Asp*
Arg	*Iso*	*Arg*	*Asp*	*Val*	*Gly*	*Pro*	*Asp*	*Arg*	*Ala*	*Ala*	*Ser*	*Glu*	*Try*	*Leu*
Leu	*Arg*	*Gly*	*Gly*	*Ala*	*Met*	*Val*	*Arg*	*Tyr*	*His*	*Gly*	*Gln*	*Gln*	*Arg*	*Try*
Gln	*Lys*	*Asp*	*Tyr*	*Asn*	*His*	*Leu*	*Pro*	*Thr*	*Gly*					

Two chains were evident, the second chain starting with Try, the second amino acid. The first 10 amino acids of this 55 amino acid sequence are hydrophobic and the rest strongly hydrophyllic with several charged groups. Further sequencing of the peptides determined by cyanogen bromide cleavage is underway. This sequence shows no homology with the E. coli unc operon, F_6 or OSCP.

W-Pos198 RESPIRATORY CHARACTERISTICS OF PLEIOTROPIC DRUG RESISTANT HUMAN MAMMARY ADENOCARCINOMA CELLS. A. Kong, G. Fiskum, K.A. Kennedy and A.N. Murphy. Departments of Biochemistry and Pharmacology, The George Washington University Medical Center, Washington, D.C. 20037.

The basis for the pleiotropic drug resistance exhibited by various tumor cell sublines has not been established, however NMR studies suggest that alterations of energy metabolism may be involved. In this study, O_2 electrode experiments were performed with adriamycin resistant (Adr^R) and sensitive (MCF-7) cells to determine whether any major differences in mitochondrial respiratory characteristics may exist. In the presence of 5 mM glucose, the consumption of O_2 by intact Adr^R cells was 30% of that of the MCF-7 cells. In the presence of 15 mM 2-deoxyglucose, the rate of O_2 consumption by Adr^R cells was 50% of the rate obtained with the MCF-7 cells, suggesting that an elevated rate of glycolysis in Adr^R cells only partially explains their lower rates of respiration. This was confirmed by direct measurements of phosphorylating (State 3) and resting (State 4) mitochondrial respiration using digitonin permeabilized cells. State 3 respiration by permeabilized Adr^R cells was less than 50% of that expressed by MCF-7 cells in the presence of malate plus glutamate. Due to similar rates of State 4 respiration, the acceptor contol ratio (State 3/State 4) of the drug resistant cells was 50% of the value obtained for the sensitive cell line. These results indicate that both the rate and control of oxidative phosphorylation are reduced in Adr^R cells when compared to the wild type MCF-7 cells. The combination of decreased mitochondrial respiration and increased glycolysis may represent an adaptation which increases the resistance of some tumor cells to a variety of chemotherapeutic drugs. (Supported by NIH grant CA32946 to G.F. and ACS grant CH274A to K.A.K.)

W-Pos199 CONTRACTILE FUNCTION OF NORMOXIC HEART AT LOW LEVELS OF BOTH ATP AND PHOSPHOCREATINE. A ^{31}P NMR STUDY. Hoerter, J.A., Lauer, C. & *Gueron, M. (introduced by Vassort, G.) U241 INSERM, Orsay, France & * Groupe Biophysique, Ecole Polytechnique, Palaiseau, France

It is presently unknown if the impairment of force during hypoxia or ischemia should be ascribed to intracellular acidosis, a reduced ATP and phosphocreatine (PCr) or to a rise in inorganic phosphate (Pi). We have explored this problem in perfused isovolumic rat hearts. A perfusion containing 2DeoxyDGlucose (2DG) together with an oxydative substrate abstracts phosphorus from its normal metabolic pathways. The phosphorylation of 2DG reduces the amount of available phosphorus metabolites. At 20 minutes, minor changes in Pi and pH_i have occurred, PCr has decreased by 50%, but systolic pressure is still unchanged. After one hour both ATP and PCr have decreased to less than 20% of control, but systolic pressure is still quite large (65% of control) and the diastolic pressure is unchanged. The oxygen consumption per unit work is constant suggesting that energetic processes operate normally. Thus low levels of both ATP and PCr are compatible with heart function in normoxia. This is not the case when oxydative phosphorylations are inhibited by amytal a situation where impaired function is related to both a rise in Pi and a decrease in PCr. We shall consider two interpretations of these results: either heart function is directly affected by the Pi level or it does not directly depends on the metabolic pools but rather on the turnover of metabolites.

W-Pos200 EFFECT OF IONOPHORIC PEPTIDES ON ELECTRON TRANSPORT AT COMPLEX III AND IV IN INTACT RAT LIVER MITOCHONDRIA

Amitabha Basu , Sophisticated Instruments Facility,
Indian Institute of Science, Bangalore 560 012, India.

Electron transport is inhibited by Alamethicin and related ionophores at high concentration of phosphate (100 nM). The extent of inhibition follows the order; Alamethicin > Acetylated melittin > FCCP + Melittin > FCCP + Valinomycin > FCCP + gramicidin >> Melittin, at Complex IV, in the presence and absence of the phosphate translocator inhibitor, N-ethylmalimide (NEM). Difference spectroscopic studies established that cytochrome-c is reduced at high phosphate, without reduction of cyt a and a_3 which were slowly reduced with increase in cyt-c red. concentration; with simultaneous increase in oxygen consumption. These uncouplers with the exception of melittin and its derivative inhibit complex III in absence of phosphate, with the pH optimum around 8:0. Difference spectra established that in aerobic state cytochrome b is reduced with little reduction of cytochromes-c, a and a_3. Under anarobic conditions identical difference spectra were obtained with normal mitochondria and mitochandria treated with ionophores. ADP (200 n mole) addition to the ionophore treated mitochondira increases the rate of cyt-c and ferricyanide reduction and oxygen consumption, while phosphate (300 n mole) has little effect. No inhibition was found with prior additon of ATP, ADP or Phosphate. The respiratory activity can be inhibited by oligomycin and NEM. The complex II was unaffected throughout.

W-Pos201 REDOX PROPERTIES OF METHYLAMINE DEHYDROGENASE, AMICYANIN, AND *C*-TYPE CYTOCHROMES FROM *PARACCOCUS DENITRIFICANS*. *K.A. Gray, +V.L. Davidson, +M. Husain, & *D.B. Knaff, *Dept. of Chemistry & Biochemistry, Texas Tech. University, Lubbock, TX; +Dept. of Biochemistry & Biophysics, UCSF; +Molecular Biology Division, VAMC, San Francisco, CA 94121.

During growth on methylamine, *P. denitrificans* synthesizes a periplasmic pyrroloquinoline quinone containing methylamine dehydrogenase [MADH] which donates electrons to a Type I blue copper protein, amicyanin. Also present in the periplasm of these cells are 3 *c*-type cytochromes, *c*-550, *c*-551i, and *c*-553i. The E_m values of the copper protein and cytochromes are: amicyanin, 294±6 mV; cyt. *c*-550, 253±5 mV, cyt. *c*-551i, 190±4 mV; and cyt. *c*-553i, 148±5 mV. Although rapid amicyanin-mediated transfer of electrons from MADH to cyt. *c*-551i occurs, reduced amicyanin did not reduce oxidized cyt. *c*-551i in the absence of MADH, suggesting that the E_m value of amicyanin is shifted when the protein forms a complex with MADH. Reductive titration of MADH indicated the formation of a stable radical intermediate. The absorption spectra of the 3 redox states of MADH are quite distinct and should allow for the potentiometric titration of the two one-electron couples of MADH. Based on this data and induction patterns of these proteins, a scheme for the transport of electrons from MADH to the membrane-bound respiratory chain is presented. [Supported by grants from the NIH (HL-16251), NSF (PCM-8408564), & Robert Welch Foundation (D-710).]

W-Pos202 REDOX COOPERATIVITY IN CYTOCHROME c OXIDASE. Richard. W. Hendler and Hans V. Westerhoff, Laboratory of Cell Biology, NHLBI, and Section on Theoretical Biology, NIDDK, National Institutes of Health, Bethesda, MD 20892.

Mammalian cytochrome c oxidase has 4 known (and possibly additional) redox centers (viz. free radical, Fe^{IV}, Zn). In addition, the molecule appears to be active in both monomer and dimer states. The possibilities for cooperativity between and among various centers as well as a modification of redox properties because of a change in conformation or state are many. Nonetheless, only the simplest of all cooperative models has been explored so far. In this ("neoclassical") model, the interaction of only two, one-electron centers has been considered. However, recent observations (Hendler et al., Biophys. J. (1986) 49: 717-729), in which a continued lowering of the E of the solution first caused an oxidation of heme a_3 followed by a turnaround towards reduction, cannot be explained by this model. This behavior indicates that heme a_3 has at least two different Em values which depend on the redox state of another center (or centers) in the molecule. Models which consider interactions of more centers and allow for changes in redox properties as a result of a change in state of the enzyme can account for these observations, as well as the observed presence of three apparently Nernstian transitions with n values of 2, 2, and 1. In these models, in addition to the 4 electrons needed for O_2 reduction, other electrons which play a regulatory role are considered. Several of these models will be presented.

W-Pos203 EXAFS STUDIES ON CARDIAC CYTOCHROME $\underline{c}_1$

C. H. Kim, G. Bunker*, A. Yencha, B. Chance*, and T. E. King, Laboratory of Bioenergetics and Dept. of Chemistry, State University of New York at Albany, Albany, NY 12222 and *Institute for Structure and Function Studies, University City Science Center, Philadelphia, PA 19104

EXAFS studies on cytochrome $\underline{c}_1$ from beef heart mitochondria were conducted in oxidized and reduced forms at CHESS, SSRL, and NSLS. EXAFS data of highly purified cytochrome $\underline{c}_1$ at 1 - 2 mM in 50 mM phosphate buffer, pH 7.4 and model compounds were collected at ca. -140°C and ca. 23°C. Model compound for Fe-N distance was bis(imidazol)iron tetraphenylphorphin and HiPIP(high potential iron protein), which was kindly supplied by Dr. Cusanovich, was used for Fe-S distance. Obtained data are compared with those of tuna heart and horse heart cytochrome $\underline{c}$. In addition, the effect of the hinge protein(a mitochondrial protein which is essential for the formation of the cytochrome $\underline{c}_1$-$\underline{c}$ complex) to the heme environment of the cytochrome $\underline{c}_1$ was also investigated by comparison of corresponding data. The results show difference between cytochrome $\underline{c}_1$ and $\underline{c}$. The hinge protein exerted rather distinguished effect on the EXAFS behavior of cytochrome $\underline{c}_1$. Detailed analysis and interpretation will be presented.(supported by grant from American Heart Association and NIH grant GM 16167)

W-Pos204 AN ANTIMYCIN A-INSENSITIVE SUCCINATE-CYTOCHROME C REDUCTASE IN PURE SUCCINATE DEHYDROGENASE. Yu, L. and Yu, C. A. Department of Biochemistry, Oklahoma State University, Stillwater, OK 74078

Pure succinate dehydrogenase (SDH) is fully active in reconstitution with Q-binding protein (QPs) to form succinate-Q reductase. In the absence of QPs, SDH is capable of transferring electrons from succinate to an artificial electron acceptor such as phenazine methosulfate or ferricyanide. Recently, we have found that reconstitutively active SDH possesses an antimycin A (AA) insensitive succinate-cytochrome *c* reductase (SCR) activity, and such activity is correlated to its reconstitutive activity. This activity disappears when the enzyme is reconstituted with QPs. The activity is cytochrome *c* concentration dependent. At 100 μM cytochrome *c*, the activity is about 2% of the succinate-PMS reductase activity. Such activity is not stable under aerobic conditions. The half life is about 20 min at a protein concentration of 23 mg/ml. Succinylated cytochrome *c* can also be used as an electron acceptor for this AA insensitive activity but with much lower activity. It is suggested that a free radical, presumably O_2^-, may be generated by active SDH. Free radical formation is confirmed by spin trapping technique, using PBN. Free radical formation and cytochrome *c* reduction are inhibited by oxalacetate. The AA insensitive cytochrome *c* reductase activity of SDH is different from that of the AA insensitive SCR activity detected in isolated SCR because they differ significantly in K_m for cytochrome *c*. The AA insensitive SCR activity of succinate cytochrome *c* reductase preparation has a K_m for cytochrome *c* and for succinate similar to that of AA sensitive activity in reductase, indicating that this insensitive activity results from incomplete AA inhibition. When SDH is reconstituted with the soluble cytochrome *b*-c_1 complex (a QPs containing cytochrome *b*-c_1 complex), the AA insensitive activity of SDH is converted to AA sensitive cytochrome *c* reductase activity. (Supported in part by grants from NIH and OKAES.)

W-Pos205 **PREPARATIVE SCALE PURIFICATION AND CHARACTERIZATION OF THE UBIQUINOL: CYTOCHROME C_2 OXIDOREDUCTASE COMPLEX FROM *RHODOBACTER SPHAEROIDES***

Katherine M. Andrews, Antony R. Crofts, and Robert B. Gennis*
Department of Biochemistry and Department of Physiology and Biophysics*, University of Illinois, 1209 W. California, Urbana, Illinois, 61801

A highly active large-scale preparation of ubiquinol:cytochrome c_2 oxidoreductase (bc_1 complex) has been obtained. The complex was extracted from chromatophores with dodecyl maltoside, in the presence of glycerol, and was purified by ion-exchange chromatography and gel filtration on Sepharose CL-4B. Full spectrum redox titrations, in the presence and absence of antimycin, show two thermodynamically distinct *b* cytochromes and cytochrome c_1, with spectra and midpoint potentials similar to those in chromatophores. Redox titrations monitoring low-temperature EPR spectra at $g=1.90$ and $g=2.00$ show the presence of the Rieske iron-sulfur center and the antimycin-sensitive semiquinone, respectively. Ubiquinol, phospholipid, and iron content have been determined, and the activity of the complex has been shown to be enhanced in the presence of phospholipid. The procedure yields at least 35 mg of purified bc_1 complex from 4 g of membrane protein, at a specific heme content of 10 nmol c_1 per mg protein, and consistently gives a preparation which catalyzes the reduction of horse heart cytochrome *c* with a turnover in excess of 300 mol s^{-1} (mol c_1)$^{-1}$, in the presence of phospholipid. We propose to study the semiquinone binding sites using ENDOR spectroscopy.

This work was supported by NIH grants PHS 5 RO1 GM 26305 and GM 35438. We gratefully acknowledge support by the University of Illinois ESR Research Center (NIH RR 01811).

W-Pos206 A MUTANT OF RHODOBACTER CAPSULATUS UBIQUINOL CYTOCHROME C_2 OXIDOREDUCTASE IMPAIRED IN UBIQUINOL OXIDATION. D.E. Robertson, F. Daldal, C.C. Moser, P.L. Dutton. Intr. by R. Lobrutto. Department of Biochemistry and Biophysics, Univ. of Pennsylvania, Phila. Pa. and Cold Spring Harbor Laboratories, CSH NY.

Mutants of the cyclic electron transfer system impaired in quinone function in the cyt bc_1 complex were isolated. Mutants of R. capsulatus were selected for photosynthetic growth (Ps+) in the presence of the potent ubiquinol oxidation inhibitor myxothiazol. Ps+ mutant MXT102 was able to grow at $5x10^{-6}$M myxothiazol, a concentration which kills its parent strain, MT1131. MXT102 was also resistant to both stigmatellin and 5-n-undecyl-6-hydroxy-4,7-dioxobenzothiazol (UHDBT). Functions linked to ubiquinol oxidation (Qz) were significantly imparied in MXT102: 1) The half-time for the reduction of cyt c_1+c_2 oxidized after a flash varied from about 50 ms at Eh=55 mV to >100 ms at Eh=200 mV. Wild-type mutant (MT1131) values vary from 2 ms to 40 ms at these extemes of Eh; 2) Oxidant-induced reduction of cyt b in MXT102 was > 10-fold slower than in MT1131; 3) The EPR lineshape of the Rieske FeS center of MXT102 was insensitive to the redox state of Qpool; the g_x component of the rhombic spectrum, which changes linewidth in MT1131 from 13 mT to 4mT with Qpool reduced or oxidized was unaltered in MXT102. Antimycin sensitive cyt b reduction was unimpaired in MXT102; the rate and Eh dependence of the reaction were similiar to wild-type MT1131. Supported by USPHS GM27309.

W-Pos207 OXIDATION/REDUCTION OF CYTOCHROME cc_m FROM DESULFOVIBRIO DESULFONICANS BY PHYSIOLOGICALLY RELEVANT DONORS AND ACCEPTORS

Jeffrey F. Kramer, Daniel H. Pope, and John C. Salerno, Department of Biology and Biophysics Group, Rensselaer Polytechnic Institute, Troy, NY 12180

The redox state of cytochrome cc_m, a low potential integral membrane c-type cytochrome from Desulfovibrio desulfonicans (ATCC 7757) was monitored optically during experiments to reconstitute electron transfer with various donors and acceptors. Cytochrome cc_m is a 15 kD c-type cytochrome which shows two N=1 components in potentiometric redox titrations with midpoint potentials at -130 mV. and -270 mV. in the membrane; both were slightly lower in detergent solubilized preparations. Cytochrome cc_m was reduced by hydrogen only in the presence of soluble hydrogenase and/or cytochrome c_3. Added sulfite oxidized hydrogen reduced cytochrome cc_m. Pyruvate caused only slight reduction of cytochrome cc_m possibly due to an inability of the lactate/sulfate grown cells to transport pyruvate. Lactate reduced cytochrome cc_m to a greater extent; periplasmic components were not required. Sulfite addition caused an oxidation of the lactate reduced cytochrome cc_m. The bacterial cells appeared to be strongly coupled since the addition of CCCP caused reduction of cytochrome cc_m by endogenous substrate. The addition of sulfite to the uncoupled cells caused an increase in the reduction of cytochrome cc_m. This increased reduction may be due to the formation of internal pyruvate in the presence of ADP. These results are consistent with the participation of cytochrome cc_m in transmembrane electron transfer from hydrogen to sulfite and in the pyruvate-sulfite pathway; electron transfer from lactate to sulfite may have no vectorial component.

W-Pos208 CHARACTERIZATION OF ELECTRON TRANSFER COMPONENTS INVOLVED IN THE OXIDATION OF Mn^{+2} BY MANGANESE OXIDIZING BACTERIA

L.A. Graham, H.L. Ehrlich, J.C. Salerno, Department of Biology and Biophysics Group, Rensselaer Polytechnic Institute, Troy, NY 12180

Bacterial strain SSW_{22}, isolated from a deep sea hydrothermal vent area (Mussel Bed Vent) in the Galapagos Rift is capable of oxidizing free manganous ion (Mn^{+2}). Manganese oxidation is associated with an inducible system which is sensitive to heat and to common electron transfer inhibitors. Strain SSW_{22} is a mixotrophic, aerobic bacterium able to derive useful energy in the form of ATP from manganese oxidation [H.L. Ehrlich, Ecol. Bull. (Stockholm) 35:357-366 (1983)]. Several electron tansfer components present in both induced and uninduced bacteria have been isolated and characterized. Two soluble c cytochromes, designated Cp and Co, both with molecular weights near 10,500 Daltons, $E^{0'}$ of +265 mV and +285 mV and unusual electron paramagnetic resonance spectra (g_z near 3.3) have been purified. A cytochrome bc_1 complex has been detergent solubilized; it consists of four major polypeptides. Purified cytochrome bc_1 complex, in catalytic amounts mediates the reduction of horse heart cytochrome c by duroquinone. The more abundant of the two soluble cytochromes, cytochrome Cp, is more completely reduced by the cytochrome bc_1 complex. Antimycin A and UHDBT partially inhibit the reduction of horse heart cytochrome c by the purified complex. Manganese oxidation requires both soluble and membrane fractions (Ehrlich 1983). A cytochrome free yellow soluble fraction is capable of catalyzing cytochrome Cp reduction in the presence of membrane components. Cytochrome reduction can be inhibited by the addition of less than 1 mM EDTA and stimulated by a burst of $MnSO_4$. The soluble fraction contains flavoproteins which may be involved in manganese oxidation.

W-Pos209 COMPARISON OF PHOSPHATE METABOLISM BETWEEN METAMORPHIC STAGES OF DROSOPHILA USING NMR METHODS.

M.J. McCreery, E.M. Donatelli, R.K. Gupta, M.C. Powanda and J.S. Taylor. Letterman Army Institute of Research, Presidio, San Francisco, CA and Department of Chemistry, Beaver College, Glenside, PA 19038.

Dramatic changes in appearance during metamorphosis reflect marked internal modifications in the biochemistry and physiology of insects. We have used NMR to compare phosphate metabolism in the metamorphic stages of Drosophila melanogaster. P-31 spectra and relaxation times were collected on a Varian XL-300 using a broad-band, 16 mm probe operating at 121 MHz. Unanesthetised adult flies or pupae 24-48 hrs old were harvested from an established colony and mechanically tapped into a 16 mm NMR tube fitted with cotton plugs at bottom and top. Specimens were aerated by means of moist air passed continuously through a glass capillary tube running axially to and dispersed by the bottom plug. A second capillary tube, taped to the aeration tube, was filled with H_3PO_4 in D_2O for reference and lock. A small thermocouple placed within the sample above the rf coils was used to monitor temperature which was varied from 10° to 40° C. Under these conditions only 2% mortality occurred in adult flies at ambient temperature for 24 hrs. Spectra exhibit 5 major peaks tentatively assigned to β-ATP, α-ATP and pyridine nucleotides, γ-ATP, ArgP, and sugar phosphates. Spectral linewidths of 300-400 Hz resulted in poorly resolved peaks especially at low field. T_1's range from 0.5 s to 1.3 s whereas T_2's vary from 10 ms to 50 ms. Perchloric acid extracts exhibit narrower linewidths which are further reduced by the addition of EDTA suggesting that paramagnetic ions contribute to T_2^*. Integrals show that pupae have a lower percentage of their phosphate pool represented by ATP compared to adults. This may reflect the difference in metabolic demands between these stages.

W-Pos210 ADSORPTION OF IONIZED AND NEUTRAL PENTACHLOROPHENOL TO PHOSPHATIDYLCHOLINE MEMBRANES AND ITS EFFECT ON MEMBRANE LIPID PHASE TRANSITION. P. Smejtek, S. Wang and A. Barstad, Environmental Sciences and Resources Program and Department of Physics, Portland State University, Portland, Oregon 97207.

Bactericidal properties of pentachlorophenol (PCP) are associated with its ability to facilitate transmembrane proton transfer. We have studied adsorption of PCP on egg-phosphatidylcholine (PC) and dimyristoylphosphatidylcholine (DMPC) membranes by means of electrophoresis. Electrophoretic mobility of lipid vesicles in PCP solutions increases as they become negatively charged due to the adsorption of ionized PCP molecules. Results indicate that: (1) The dependence of zeta potential on the PCP concentration and solution pH can be understood in terms of competitive adsorption of neutral and ionized PCP, and the Langmuir-Stern-Grahame model. The following adsorption characteristics of PCP on egg PC membranes (ionic strength 0.04M) were obtained:

	Association Constant, (1/M)	Linear Partition Coefficient, (m)
Ionized PCP	9×10^4	3.5×10^{-5}
Neutral PCP	2×10^5	8.5×10^{-5}

Approximately 6 PC molecules participate in forming one adsorption site. (2) Electrophoretic mobility of DMPC vesicles in PCP solutions exhibits a step-like increase at the phase transition from the gel into liquid state. At 35 μM PCP the ionized PCP lowered the phase transition temperature whereas the neutral abolished the phase transition effect. PCP, in addition to acting in lipid membranes as a protonophore also disrupts interlipid interactions. Supported by NIH Grant No. ES00937.